

AD-A070 632

BOLT BERANEK AND NEWMAN INC CAMBRIDGE MASS

F/G 5/9

A PERFORMANCE ANALYZER FOR IDENTIFYING CHANGES IN HUMAN OPERATO--ETC(U)

MAR 79 G L ZACHARIAS, W H LEVISON

F33615-77-C-0522

UNCLASSIFIED

BBN-3910

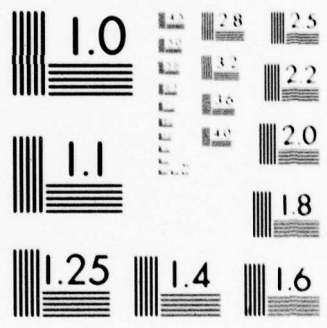
AMRL-TR-79-17

NL

1 OF 2

AD
A070632





MICROCOPY RESOLUTION TEST CHART
NATIONAL BUREAU OF STANDARDS-1963-A

AD A 070 632

AMRL-TR-79-17

LEVEL

2
B.S.



**A PERFORMANCE ANALYZER FOR
IDENTIFYING CHANGES IN
HUMAN OPERATOR TRACKING STRATEGIES**

GREG L. ZACHARIAS
WILLIAM H. LEVISON
BOLT BERANEK AND NEWMAN INC.
CAMBRIDGE, MASSACHUSETTS 02138

DDC
RECEIVED
JUN 28 1979
C

MARCH 1979

DDC FILE COPY

Approved for public release; distribution unlimited.

AEROSPACE MEDICAL RESEARCH LABORATORY
AEROSPACE MEDICAL DIVISION
AIR FORCE SYSTEMS COMMAND
WRIGHT-PATTERSON AIR FORCE BASE, OHIO 45433

70 06 21 052

NOTICES

When US Government drawings, specifications, or other data are used for any purpose other than a definitely related Government procurement operation, the Government thereby incurs no responsibility nor any obligation whatsoever, and the fact that the Government may have formulated, furnished, or in any way supplied the said drawings, specifications, or other data, is not to be regarded by implication or otherwise, as in any manner licensing the holder or any other person or corporation, or conveying any rights or permission to manufacture, use, or sell any patented invention that may in any way be related thereto.

Please do not request copies of this report from Aerospace Medical Research Laboratory. Additional copies may be purchased from:

National Technical Information Service
5285 Port Royal Road
Springfield, Virginia 22161

Federal Government agencies and their contractors registered with Defense Documentation Center should direct requests for copies of this report to:

Defense Documentation Center
Cameron Station
Alexandria, Virginia 22314

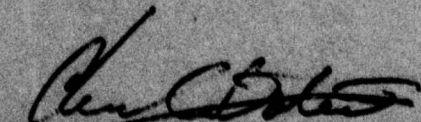
TECHNICAL REVIEW AND APPROVAL

AMRL-TR-79-17

This report has been reviewed by the Information Office (OI) and is releasable to the National Technical Information Service (NTIS). At NTIS, it will be available to the general public, including foreign nations.

This technical report has been reviewed and is approved for publication.

FOR THE COMMANDER



CHARLES BATES, JR.
Chief
Human Engineering Division
Aerospace Medical Research Laboratory

SECURITY CLASSIFICATION OF THIS PAGE (When Data Entered)

19 REPORT DOCUMENTATION PAGE		READ INSTRUCTIONS BEFORE COMPLETING FORM	
1. REPORT NUMBER	2. GOVT ACCESSION NO.	3. RECIPIENT'S CATALOG NUMBER	
AMRL TR-79-17			
4. TITLE (and Subtitle)		5. TYPE OF REPORT & PERIOD COVERED	
A PERFORMANCE ANALYZER FOR IDENTIFYING CHANGES IN HUMAN OPERATOR TRACKING STRATEGIES.		Final Rept. 11 July 77 to 13 October 78	
6. AUTHOR(s)		7. PERFORMING ORGANIZATION NUMBER	
Greg L. Zacharias William H. Levison		BBN Report No. 3910	
8. PERFORMING ORGANIZATION NAME AND ADDRESS		9. CONTRACT OR GRANT NUMBER(s)	
Bolt Beranek and Newman Inc. Cambridge MA 02138		F33615-77-C-0522	
10. CONTROLLING OFFICE NAME AND ADDRESS		11. PROGRAM ELEMENT, PROJECT, TASK AREA & WORK UNIT NUMBERS	
Aerospace Medical Research Laboratory Aerospace Medical Division, AFSC Wright-Patterson AFB OH 45433		62202F, 7184-16-03	
12. MONITORING AGENCY NAME & ADDRESS (if different from Controlling Office)		13. REPORT DATE	
12170P.		March 1979	
		14. NUMBER OF PAGES	
		169	
		15. SECURITY CLASS. (of this report)	
		Unclassified	
		15a. DECLASSIFICATION/DOWNGRADING SCHEDULE	
16. DISTRIBUTION STATEMENT (of this Report)			
Approved for public release; distribution unlimited			
17. DISTRIBUTION STATEMENT (of the abstract entered in Block 20, if different from Report)			
18. SUPPLEMENTARY NOTES			
19. KEY WORDS (Continue on reverse side if necessary and identify by block number)			
human operator modeling		human operator technology	
optimal control model		performance measurement	
visual countermeasures		compensatory tracking	
20. ABSTRACT (Continue on reverse side if necessary and identify by block number)			
An experimental and analytical study was undertaken by Bolt Beranek and Newman Inc. to develop, implement, and validate a compensatory tracking task for use as a preliminary screening task in the assessment of visual countermeasures. The optimal control model of the human operator was used to design the tracking task consisting of an unstable controlled element perturbed by a sum-of-sines disturbance function. A			

(Cont'd)

DD FORM 1 JAN 73 1473

EDITION OF 1 NOV 65 IS OBSOLETE

SECURITY CLASSIFICATION OF THIS PAGE (When Data Entered)

060100

79 06 21 052

20. Abstract

minicomputer-based system was developed to implement the task, and the resulting Performance Analyzer was used to conduct the experimental validation phase of the study. Two simulated stressors were introduced into the tracking task, and the results showed that significant differences could be detected between tracking conditions, thus validating the task's sensitivity to imposed stress. A comparison of the data trends with pre-experimental model predictions served to identify the particular stressor effects, and thus provided a means of differentiating between stressors. A follow-up quantitative model analysis provided an efficient means of compressing the tracking data made available by the Performance Analyzer, and also provided a verification of the task's utility in isolating and identifying stressor effects. ←

Accession For	
NTIS GRA&I	<input checked="" type="checkbox"/>
DDC TAB	<input type="checkbox"/>
Unannounced	<input type="checkbox"/>
Justification	
By _____	
Distribution/	
Availability Codes	
Dist	Avail and/or special
A	

PREFACE

The work reported herein was performed under Air Force Contract F33615-77-C-0522 for the Aerospace Medical Research Laboratory. The technical monitor was Lt Col Robert D. O'Donnell, Visual Display Systems Branch of the Human Engineering Division. This contract effort was performed in support of Project 7184, "Man-Machine Integration Technology," Task 16, "Perceptual Aspects of Optical Countermeasures," Work Unit 03, Tracking Task Development."

TABLE OF CONTENTS

1. Introduction	5
2. Theoretical Background	7
2.1 Human Operator Model	7
2.2 Model Validation and Application	15
3. Tracking Task Design	19
3.1 Task Dynamics	19
3.2 Loop Input Signal	25
3.3 Tracking Task Block Diagram	26
3.4 Sensitivity of Tracking Task	28
3.5 Differential Sensitivity of Tracking Task	30
4. Experiment Description	41
4.1 Task Description	41
4.2 Experimental Protocol	46
5. Experimental Results	53
5.1 Primary Data	53
5.2 Model Analysis	76
6. Conclusions and Recommendations for Future Development	90
6.1 Conclusions	90
6.2 Recommendations for Future Development	92
Appendix A: Performance Analyzer Description	95
Appendix B: Task Dynamics	153
Appendix C: Tabulated Experimental Results	158
References	165

LIST OF FIGURES

<u>Figure</u>	<u>Page</u>
2.1 Human Operator Model	8
2.2 Model for Continuous Control	11
3.1 Effect of Noise/Signal Ratio on Predicted Display Error Variance	23
3.2 Tracking Task Block Diagram	27
3.3 Score Sensitivity to Pole Location and Noise Bandwidth	29
3.4 Tracking Score and Control Sensitivity to Model Parameter Variations	32
3.5 Normalized Remnant Dependence on Model Parameters	35
3.6 Describing Function Changes with Model Parameter Changes	36
3.7 Logical Flow for Inferring Model Parameter Changes	39
4.1 Tracking Task Block Diagram	42
5.1 Tracking Score History During Initial Training	56
5.2 Tracking Score Histories as a Function of Tracking Condition	58
5.3 Tracking Scores as a Function of Tracking Condition	61
5.4a Frequency Response Measures Obtained under Normal Conditions	63
5.4b Frequency Response Measures Obtained under Diffused Conditions	64
5.4c Frequency Response Measures Obtained under Delayed Conditions	65
5.5a Frequency Response Measures Obtained under Nominal and Diffused Display Conditions	67

LIST OF FIGURES (cont.)

<u>Figure</u>		<u>Page</u>
5.5b	Frequency Response Measures Obtained under Nominal and Time Delay Conditions	68
5.5c	Frequency Response Measures Obtained under Diffused Display and Time Delay Conditions	69
5.6	Comparison of Model and Experimental Performance Scores	82
5.7a	Comparison of Model and Experimental Frequency Measures - Nominal Conditions	83
5.7b	Comparison of Model and Experimental Frequency Measures - Diffused Display Conditions	84
5.7c	Comparison of Model and Experimental Frequency Measures - Time Delay Conditions	85
A.1	Single-Axis Tracking Loop	96
A.2	Single-Axis Tracking Loop: System Breakdown	99
A.3a	Input Interface	151
A.3b	Output Interface	151
A.4	Software Interface	152
B.1	Performance Analyzer Plant Dynamics	155
B.2	Autopilot Describing Function Measurement	156

1. INTRODUCTION

The objective of the study was to develop, implement, and validate a compensatory tracking task having a wide applicability and sensitivity to a number of operator stressors present in the operator's environment. The task was to be designed for use with the type of stressors expected to be utilized in a program investigating the effects of visual countermeasures, thus serving as a preliminary screening task for countermeasure assessment. Task development was to be based on current human operator modeling theory, to allow for the isolation of the essential elements of operator performance characterizing tracking under stressed conditions.

This report summarizes the task development effort, from the initial design rationale to the experimental validation of the task's effectiveness in identifying stressor effects. Chapter 2 provides a brief description of the optimal control model of the human operator, and discusses relevant applications of the model to understanding operator performance in a variety of control and decision tasks. Chapter 3 then utilizes the model in a predictive capacity to design the tracking task, and investigate task sensitivity to simulated operator stressors. The simulation results presented in this chapter provide the rationale for the chosen task, and the detailed specifications for task implementation. An experimental program for task validation

is then discussed, with chapter 4 devoted to a description of the experimental design and protocol, and chapter 5 to a presentation and discussion of the experimental results. This chapter also describes the results of a post-experimental model analysis directed at identifying and interpreting stressor effects. Chapter 6 concludes with a summary of the major findings of the study, and recommends areas of future task development and application.

Three appendices supplement the body of the report. Appendix A provides a detailed user-oriented description of the Performance Analyzer developed and used during the course of this study. Appendix B provides some background information concerning the dynamic characteristics of the Performance Analyzer when applied to the chosen tracking task. Appendix C summarizes the experimental data in tabular format, for convenient reference.

2. THEORETICAL BACKGROUND

The basic premise underlying the tracking task development effort is that a well-trained and well-motivated human operator will perform a task in a near-optimal manner, subject to his inherent performance limitations and his understanding of the task. As we show in this section, this assumption leads to tractable mathematical models that not only have predictive capabilities but can also be used to identify the underlying causes of experimentally observed differences in operator response characteristics.

In the following discussion we describe relevant features of the human operator model and summarize some earlier validation experiments.

2.1 Human Operator Model

2.1.1 Basic Model Structure

Figure 2.1 illustrates the basic model structure for tasks which require the human to process continuous information. This conceptual model is intended to apply to a situation in which the human is required to estimate the "state" of some process, on the basis of one or more sensory informational variables.

Principal model elements are:

- (a) A linearized description of the system dynamics given by the following state equation:

$$\dot{\underline{x}}(t) = \underline{A} \underline{x}(t) + \underline{E} \underline{w}(t) \quad (2.1)$$

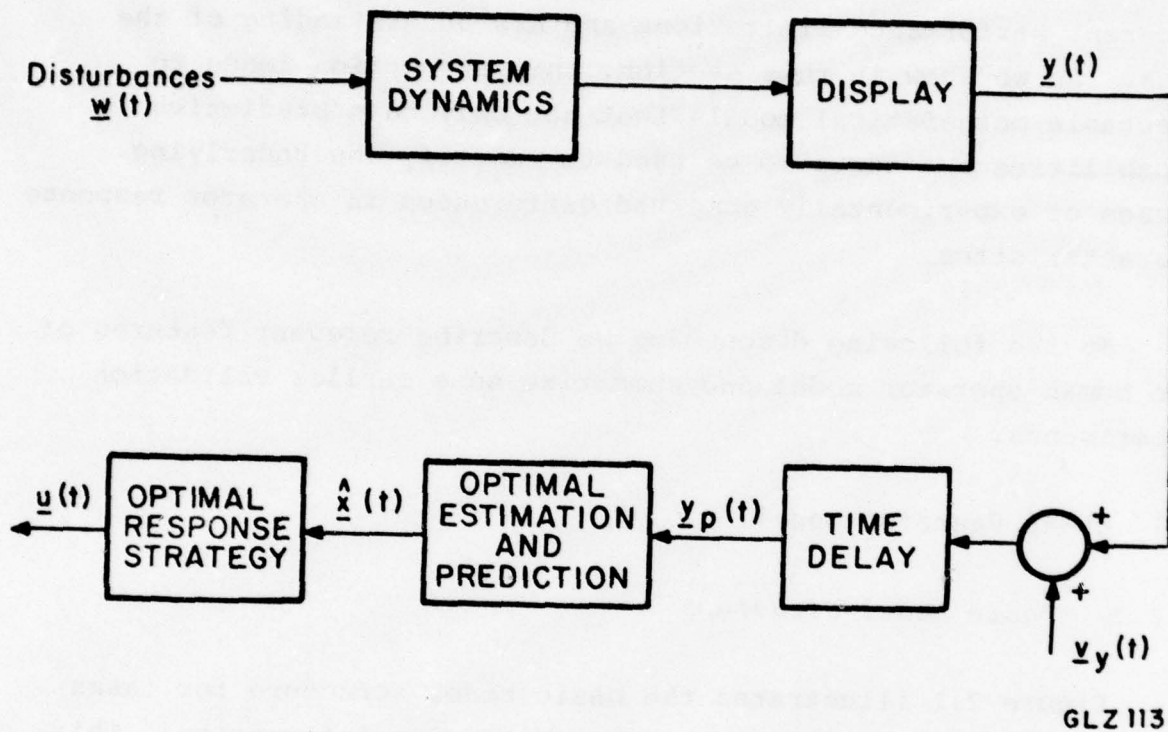


Figure 2.1: Human Operator Model

where $\underline{x}(t)$ is the vector which describes the state of the system, and $\underline{w}(t)$ a vector of white driving noise processes. (If the external forcing functions are rational noise spectra of first order or higher, the resulting "input states" are incorporated into the state vector $\underline{x}(t)$)

- (b) A "display vector" which, in general, consists of a linear transformation of the state variables and is given as

$$\underline{y}(t) = \underline{C} \underline{x}(t) \quad (2.2)$$

This vector contains the set of sensory variables used by the operator. Since both displacement and rate information are typically available from a single display element, the number of elements in the \underline{y} vector can exceed the number of physical display elements used in a specific task.

- (c) A representation of the pilot's limitations by means of an equivalent perceptual time delay τ and an equivalent observation noise vector $\underline{v}_y(t)$ to account for the various sources of "processing noise" associated with sensory, central-processing, and response activity.
- (d) A predictor and estimator to provide the "best" estimate of the current system state in a least-squared-error sense.
- (e) An optimal response strategy acting on the best estimate of the state vector, the output of which is the overt response activity $\underline{u}(t)$.

The structure of the "optimal response strategy" element will depend on the nature of the task. In the case of closed-loop continuous control, this element will consist of a set of feedback gains to generate a control (or commanded control) input to the system (Kleinman et al. (1970); Baron et al. (1970); Kleinman et al. (1971)). If the task is one of decision-making, this element may consist of a Bayesian decision process, the output of which is some action appropriate to the decision reached (Levison and Tanner (1971)).

Because we are concerned with closed-loop tracking performance, the ensuing discussion of this model is directed toward the task of continuous control.

The model of figure 2.1 becomes a model for continuous control as shown in figure 2.2, by inclusion of the following: (1) an optimal control strategy, (2) a first-order lag to account for apparent limitations on the operator's response bandwidth, and (3) a "motor noise" process to account for motor-related sources of response randomness. To account for the influence of the operator's control signal $\underline{u}(t)$ on system response, equation (2.1) is expanded as follows:

$$\dot{\underline{x}}(t) = \underline{A} \underline{x}(t) + \underline{B} \underline{u}(t) + \underline{E} \underline{w}(t) \quad (2.3)$$

The optimal predictor, optimal estimator, and optimal gain matrix represent the set of "adjustable parameters" by which the controller tries to optimize his behavior. The general expressions for these model elements depend on the system dynamics, according to well-defined mathematical rules that are described in the literature (see, for example, Kleinman et al. (1970)). The controller is assumed to adopt a response strategy which minimizes the following sum of averaged display and control variances:

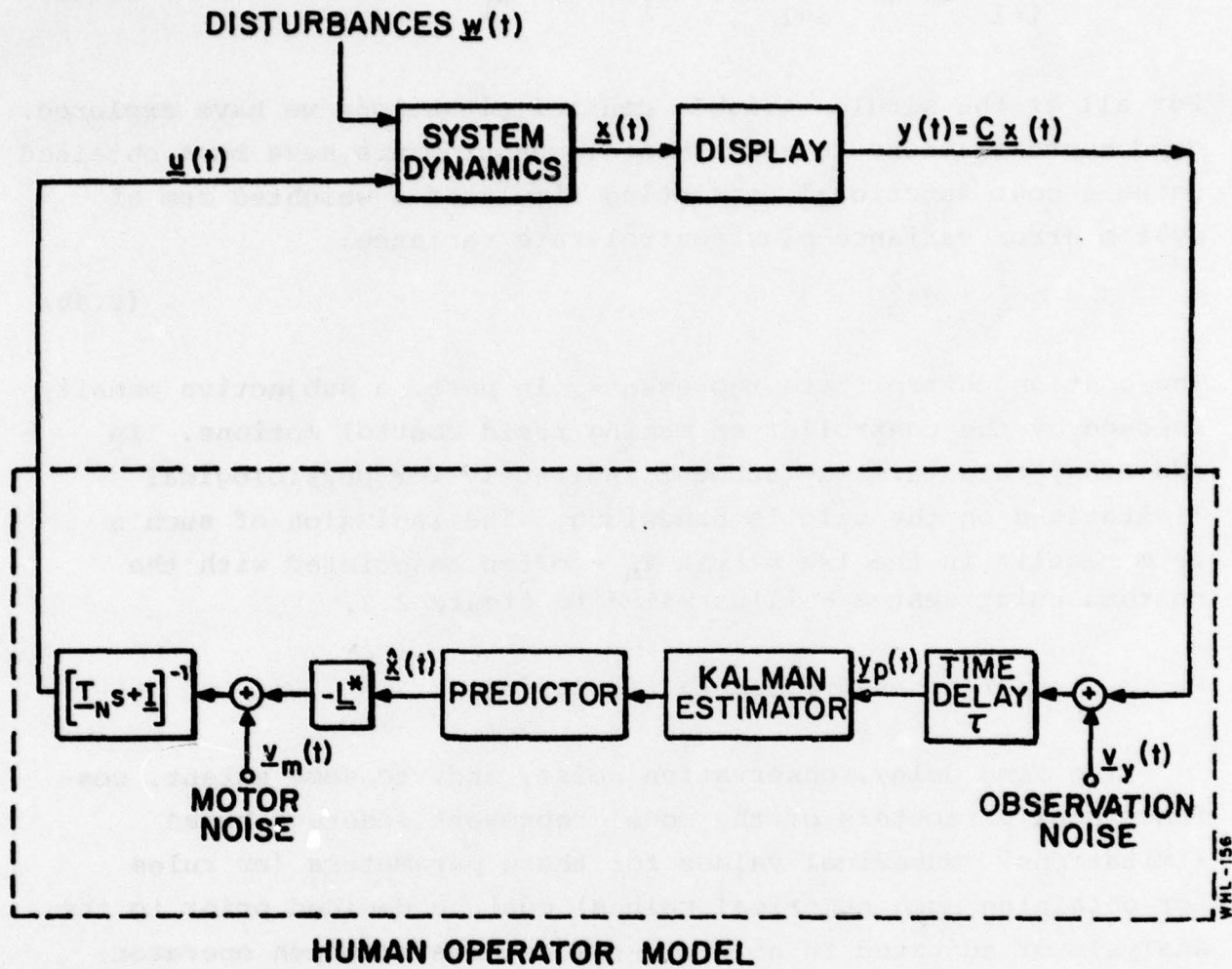


Figure 2.2: Model for Continuous Control

$$J = \sum_{i=1}^N q_i \sigma_i^2 + \sum_{i=1}^{N_u} (r_i \sigma_{u_i}^2 + g_i \dot{\sigma}_{u_i}^2) \quad (2.4a)$$

For all of the single-variable control situations we have explored, good approximations to experimental measurements have been obtained using a cost functional consisting simply of a weighted sum of system error variance plus control-rate variance:

$$J = q\sigma_e^2 + g\dot{\sigma}_u^2 \quad (2.4b)$$

The cost on control rate represents, in part, a subjective penalty imposed by the controller on making rapid control motions. In addition, this term may account indirectly for physiological limitations on the pilot's bandwidth. The inclusion of such a term results in the lag matrix T_n - often associated with the neuromuscular system - illustrated in figure 2.2.

2.1.2 Information-Processing Limitations

The time delay, observation noise, and, to some extent, cost functional parameters of the model represent inherent human limitations. Numerical values for these parameters (or rules for obtaining such numerical values) must be decided prior to the analysis or adjusted in an iterative scheme to match operator response characteristics in a particular situation.

The time delay required to match operator response behavior usually lies in the range of 0.15 to 0.22 seconds; for predictive applications of the model, a time delay of 0.2 seconds is a reasonable choice. For single-variable laboratory tracking tasks, experimental data are often well matched if the relative cost coefficient on control-rate is adjusted to yield a lag τ_n of 0.1 seconds. (Because this value is similar to values that have been used in simplified models of the human's neuromuscular system, we

refer to the lag τ_n as the "motor time constant".) For more complex, "real world" tracking tasks, reasonable values for both control-related and display-related cost coefficients can be obtained from consideration of maximum attainable (or allowable) values for these system variables.

The "observation noise" process $\underline{v}_y(t)$ is intended as a mathematical representation of the combined effects of various sources of randomness in the human's sensory, central-processing, and response mechanisms. Each perceptual variable used by the operator is considered to be corrupted by a Gaussian "white noise" process that is linearly uncorrelated with the sensory input and with other similar noise processes. The perceptual information available to the operator from the display vector \underline{y} is therefore:

$$\underline{y}_p(t) = \underline{y}(t) + \underline{v}_y(t) \quad (2.5)$$

where $\underline{y}_p(t)$ is the perceived variable, $\underline{y}(t)$ the variable presented by the display, and $\underline{v}_y(t)$ a white noise process having an autocorrelation function

$$\phi_{\underline{v}_i \underline{v}_i}(\tau) = V_{y_i} \delta(\tau) \quad (2.6)$$

or, equivalently, a uniform power spectral density function of $V_y/2\pi$ over all frequencies.* We shall refer to the quantity V_y as the "autocovariance" of the noise process.

Although not physically realizable, the notion of a white noise disturbance is a useful mathematical fiction that we adopt because it provides a representation of human operator randomness that is readily handled within the framework of modern control and

*The variable $\delta(\tau)$ is a "unit impulse" function, located at $\tau = 0$, that has zero width, infinite value, and an integral over τ of unity.

estimation theory, and because it allows us to model human control behavior with considerable accuracy. In effect, we are assuming that the bandwidth of the observation noise process is substantially greater than the response bandwidth of the man-machine system.

When the system is designed so that resolution and saturation effects in sensory and motor processes are negligible, the observation noise covariance is found to be proportional to the mean-squared value of the displayed variable (for zero-mean signals). Thus, the autocovariance of the white observation noise associated with the i th display variable may be represented as

$$V_{y_i} = \pi P_i E\{y_i^2(t)\} \quad (2.7)$$

where P_i is the "noise/signal ratio" and has units of normalized power per rad/sec. For situations in which the signal $y(t)$ is a zero-mean random process having stationary statistical properties (as in the case of most laboratory tracking experiments), the above expression may be written as

$$V_{y_i} = \pi P_i \sigma_{y_i}^2 \quad (2.8)$$

In general, when the human operator is provided with a single display variable, both displacement and rate information will be observed. Good agreement with experimental remnant data has been obtained by assuming that the "noise/signal" ratios for the position and rate variables obtained from the same display indicator are identical. Numerical values for P_i of .01 (i.e., -20 dB) have been found to be typical of single variable control situations although smaller values have been observed when operators attempt to control unstable dynamics.

The other source of human randomness is the motor noise $v_m(t)$. This noise is also assumed to be a zero-mean, Gaussian, white noise process with

$$\phi_{v_i v_i}(\tau) = v_{m_i} \delta(\tau) \quad (2.9)$$

$$v_{m_i} = \pi P_{m_i} \sigma_{\mu_i}^2$$

A motor noise/signal ratio, P_i , of about .003 (-25dB) has been found to provide a good match to experimental data.

2.1.3 Model Outputs

Once the system has been described and values assigned to operator-related model parameters, predictions can be obtained for the operator's prediction, estimation, and control strategies. Having thus completely defined the operation of the man-machine system, we can predict a variety of metrics related to overall system performance and to human response behavior.

Among the metrics that the model can predict are: (1) mean and variance of any system variable; (2) the transfer function (gain and phase) relationship between any two system variables; and (3) the power spectral density of any system variable, partitioned into a component linearly correlated with external disturbances and a "remnant-related" component associated with human operator response randomness. Thus, the model is capable of generating response metrics that can be compared with a variety of measures extracted from experimental data.

2.2 Model Validation and Application

The human operation model has been validated for a variety of control situations - mostly single-variable laboratory tracking

tasks (Levison et al. (1971); Kleinman et al. (1970); Kleinman et al. (1971)), but some complex tasks as well (Kleinman and Baron (1971); Kleinman and Killingsworth (1974); Kleinman et al. (1970)). The reader is especially directed to Kleinman et al. (1970), where it is shown that detailed response behavior (as well as mean-squared error scores) can be reproduced by the model using values for operator parameters (time delay, motor lag, and observation noise/signal ratio) that are nearly invariant across control tasks. The tasks considered in that reference span a range of operator response characteristics, indicating that the so-called "operator parameters" reflect primarily limitations of human-operator information processing that are relatively independent of the control task parameters. In particular, the notion of treating response randomness (mathematically) as an observation noise process is supported by the ability of the model to reproduce the spectrum of the stochastic portion of the operator's response across a set of tasks in which this spectrum varies substantially.

The optimal-control model has been applied extensively both as a tool for predicting continuous control behavior and as a tool for inferring changes in human response limitations resulting from changes in the nature of the control task and/or task environment. Of greatest relevance to the tracking design effort reported on here are studies in which the model has been used to account for the influence of environmental factors on tracking performance.

Generally speaking, studies of environmental factors have led to changes in model parameters that one would expect from the physical nature of the "stress". In a study of simulated anti-aircraft artillery tracking, Baron and Levison (1974) found that the presence of a visual stress was best accounted for by increases in observation noise parameters. Levison et al. (1971) also found that the observation noise/signal ratio increased when

subjects had to share attention among two or more uncorrelated tracking tasks. In the same study, Levison et al. found that the subjects would *reduce* their noise/signal ratios if the task was sufficiently difficult (i.e., if system error were particularly sensitive to operator noise).

Changes in motor-related parameters have also been found. In three separate studies of the effects of vibration on tracking performance, the presence of whole-body vibration has been accounted for largely by an increase in the motor noise parameter of the model (Levison and Houck (1975); Levison (1976); Levison (1976)). In studies involving the pilot's use of motion cues in roll-axis tracking, the presence of motion cues was accounted for by inclusion of motion-related sensory variables in the definition of the "display vector" y . Since motion did not represent a stress, values for noise/signal ratios obtained in previous laboratory tracking tasks were found adequate to match the data (Levison et al. (1976); Levison and Junker (1977)).

Gai and Curry (1976) have used the optimal control model's information processing structure to analyze failure detection in a simple laboratory task and in an experiment simulating pilot monitoring of an automatic approach. In both cases, a step or ramp was added to the observed signal at random times to simulate an instrument failure. This produced a non-zero mean value for the signal and for the "residual" (essentially, the difference between what the subject saw and what he expected to see); failure detection consisted of testing an hypothesis concerning the mean of the distribution of the residuals. The good agreement between predicted and observed detection time reported by Gai and Curry would appear to confirm the applicability of the modeling approach in these particular tasks.

The studies of Levison and Tanner and Gai and Curry provide verification of the information processing structure of the optimal control model in tasks not involving closed-loop control. These results taken in conjunction with the implicit validation provided by the tracking data, provide strong support for this model of human information processing.

3. TRACKING TASK DESIGN

The initial phase of this study was devoted to the choice of the tracking task to be used in measuring changes in human operator performance. Two specific design objectives were called for:

- a. Overall sensitivity of the task to changes in operator behavior induced by environmental stressors
- b. Differential sensitivity of the task to qualitatively different stressors

The first objective was chosen to ensure detection of a change in operator performance in response to only slight changes in the tracking task environment. The second was chosen to provide the capability of identifying changes in operator strategy associated with specific changes in the task environment.

To minimize the amount of trial-and-error task design associated with an empirically-based effort, the human operator model of the previous chapter was used in a predictive mode, to simulate tracking performance in a variety of conditions. This allowed for a rapid evaluation of a number of different task designs, and for a detailed examination of task sensitivity to simulated stressors. This chapter describes the results of this sensitivity study, and provides a rationale for the particular tracking task chosen for experimental validation.

3.1 Task Dynamics

One of the fundamental determinants of operator tracking

performance is the set of dynamics used in the tracking loop. If the dynamics are particularly easy to control, then performance tends to be an insensitive function of task stress; conversely, dynamics which are controlled only with great difficulty are associated with performance changes which are highly sensitive to task stressors. A particular example which demonstrates this is the study of hypoxia on tracking, conducted by Replogle, et al (1970).

In their study, they required the subjects to perform two control tasks, singly and in combination. An unstable set of dynamics was used for one of the tasks, and had the following form:

$$P(s) = \frac{\lambda}{s-\lambda} \quad (3.1)$$

The critical frequency λ was adjusted continuously according to the operator's ability to reduce system error: the smaller the error score, the more unstable the dynamics became. No loop input signal was used in this task, since the subject tended to track his own remnant. This type of unstable task, with a variable critical frequency, has been the subject of some study in the past, and has been named the "critical tracking task" by Jex et al (1966).

The second control task used in this experiment was control of third-order dynamics typical of aircraft pitch dynamics. A loop input was applied directly to the display to simulate a pitch command, and thus this second task simulated one of pitch regulation.

Replogle et al. found that the levels of hypoxia which they studied produced a significant performance degradation for the task involving the unstable dynamics, but had no measurable effect on performance in the pitch-regulation task. In order to explain these results, we used the human operator model, described in the previous chapter, in a simulation of operator performance under different stressed conditions.

Details relating to the pitch dynamics and input signal were not available at the time this analysis was performed. Accordingly, we selected a set of dynamics from the literature in order to have a basis for modeling this task. The dynamics were:

$$P(s) = \frac{13.4 (1 + 2.3s)}{s[1 + 0.316s + 0.085 s^2]} \quad (3.2)$$

which were those used by Sadoff and Dolkas (1967) in their study of the effects of sustained acceleration on a simulated pitch-regulation task. A second-order forcing function was assumed, and the input bandwidth was adjusted to give approximately the same system error scores that Sadoff and Dolkas obtained in the absence of acceleration stress.

In our simulation of operator performance under different stressed conditions, we chose to identify changes in stress with changes in the operator's noise/signal ratio. This model parameter was chosen because it is the parameter that we identify most closely with the operator's ability to process information, as discussed in the previous chapter. We represented the effects of hypoxia, then, by an increase in the noise/signal ratio.

A white-noise forcing function was introduced in our representation of the unstable dynamics task to simulate the effects of system noise and pilot tremor. The pole location λ was held fixed, and the relation between error variance and noise ratio was determined. Figure 3.1 shows a set of curves obtained for pole frequencies ranging from 1.5 to 3.0 radian/second. Also shown on the same log-log plot is the relationship between system error and noise/signal ratio for the stable pitch-regulation task. The error scores are given in arbitrary units; it is the percentage changes with noise ratio that are of interest.

One can readily see from the figure why stress has a much greater effect on performance with the unstable task. Consider, for example, the task of controlling a vehicle with an unstable pole at 3 rad/sec. If the pilot allows his noise/signal ratio to increase from -26 dB to -24 dB, error variance increases nearly three-fold; an additional increase of 1 dB in noise/signal appears to make the task uncontrollable. Thus, the pilot must work very hard at this task to keep the error within reasonable bounds. Anything that diminishes his information-processing capability will cause him to relax his error criterion so that the task difficulty is reduced to a more manageable level.

The error score is much less strongly dependent on the pilot's noise characteristics for the stable pitch task. Figure 3.1 shows that a 2 dB increase, say from -22 to -20 dB, raises the error score by less than 10 percent. Even an increase as large as 6 dB raises the score only by about 45 percent. Thus, if the levels of hypoxia investigated by Replogle et al. correspond to an increase in the pilot's noise/signal ratio of 2 or 3 dB, then we would expect to observe a significant performance degradation on the unstable task and no significant change on stable-task performance.

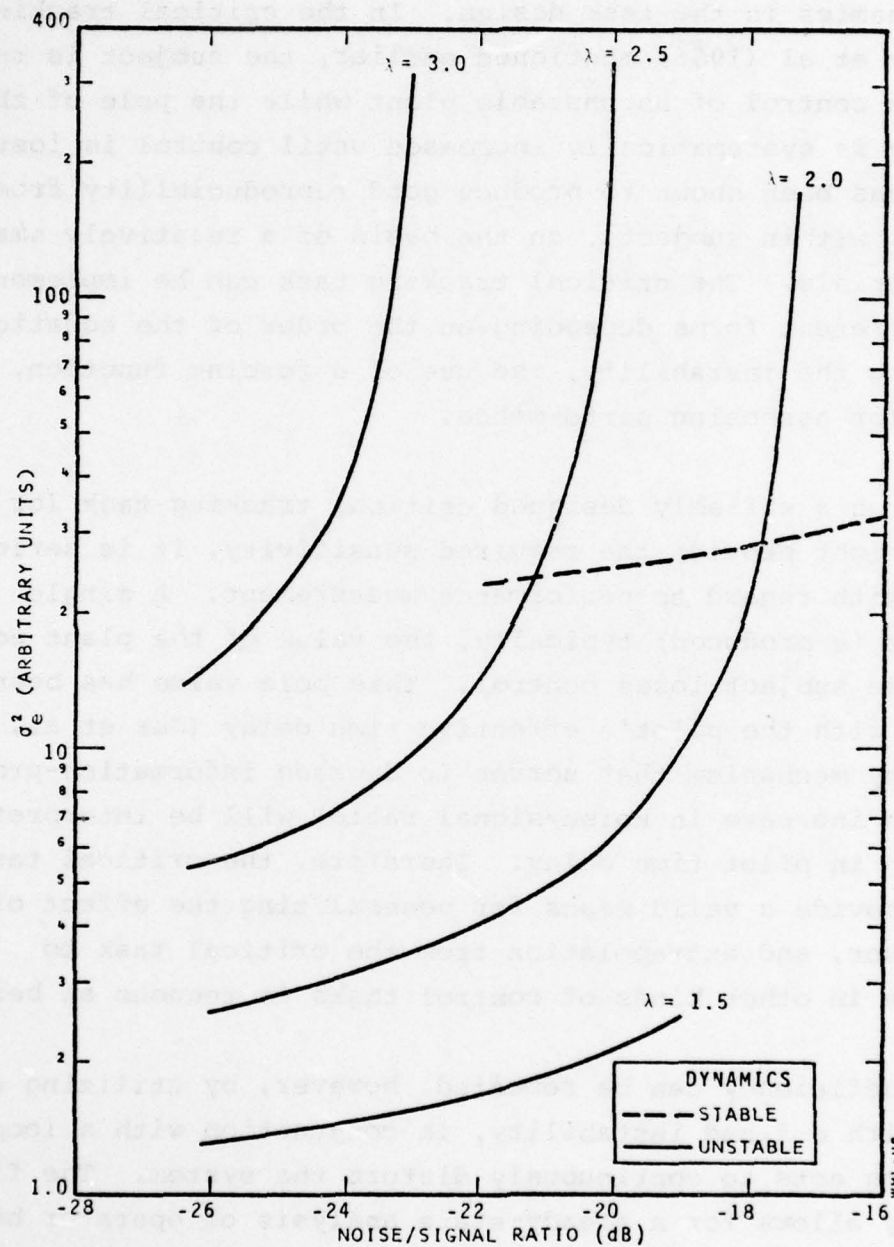


Figure 3.1: Effect of Noise/Signal Ratio on Predicted Display Error Variance

This sensitivity of error score seen in the unstable tracking task thus argues for the incorporation of unstable controlled element dynamics in the task design. In the critical tracking task of Jex et al (1966) mentioned earlier, the subject is required to maintain control of an unstable plant while the pole of the instability is systematically increased until control is lost. This task has been shown to produce good reproducibility from day to day, within subjects, on the basis of a relatively small sample of trials. The critical tracking task can be implemented in many different forms depending on the order of the equation representing the instability, the use of a forcing function, and the logic for assessing performance.

Although a suitably designed critical tracking task (or set of tasks) might provide the required sensitivity, it is seriously deficient with regard to performance measurement. A single measurement is produced; typically, the value of the plant pole at which the subject loses control. This pole value has been associated with the pilot's effective time delay (Jex et al, 1966). However, any mechanism that serves to degrade information-processing (such as an increase in noise/signal ratio) will be interpreted as an increase in pilot time delay. Therefore, the critical task does not provide a valid means for generalizing the effect of a task stressor, and extrapolation from the critical task to performance in other kinds of control tasks is tenuous at best.

This deficiency can be remedied, however, by utilizing unstable dynamics with a fixed instability, in conjunction with a loop input signal which acts to continuously disturb the system. The fixed instability allows for a steady-state analysis of operator behavior, and the input signal can be chosen for efficient off-line frequency analysis of operator performance. Such steady-state frequency domain information provides an abundance of performance metrics,

when compared with the single critical frequency available from the time-varying no-input critical tracking task.

3.2 Loop Input Signal

A loop input signal which continuously disturbs the plant necessitates continuous compensatory control actions by the human operator. To avoid "pre-programmed" control actions, it is important that the input signal be "random-appearing" to the operator; by this we mean that the operator is unable to predict the time history of the input signal. Such a signal may be obtained from a random-noise generator, or it may be constructed from a sufficient number of deterministic signals (e.g., sinusoids) so that the subject is not able to memorize the time pattern of the input; otherwise, he may attempt a "precognitive" mode of tracking which may differ considerably from the strategy adopted when the input appears to be random.

Even with a stable set of plant dynamics, tracking becomes especially difficult when the loop input is a wide bandwidth signal. For this reason, most experimenters choose to limit the high frequency content by either choosing a step-down "shelf" spectrum (for example, see Jex et al. (1966)), or by choosing a spectrum which continuously decreases in power at the higher frequencies (see Levison, et al. (1971)). The latter approach can be realized by choosing the power spectral density (PSD) of the input to be a rational polynomial function of frequency, with the number of poles exceeding the number of zeroes. The simplest such function is a first-order PSD function given by

$$\Phi(s) = \left| \frac{K}{s+a} \right|^2 \quad (3.3a)$$

The break frequency a specifies where the signal power begins to roll-off, and the parameter K specifies the signal's RMS level. Substituting $j\omega$ for s , the equivalent frequency domain PSD function representation is

$$\Phi(\omega) = \frac{K^2}{\omega^2 + a^2} \quad (3.3b)$$

Of course, higher order PSD functions can be used to provide more rapid attenuation of the high frequency power, if deemed necessary for the particular experiment at hand.

3.3 Tracking Task Block Diagram

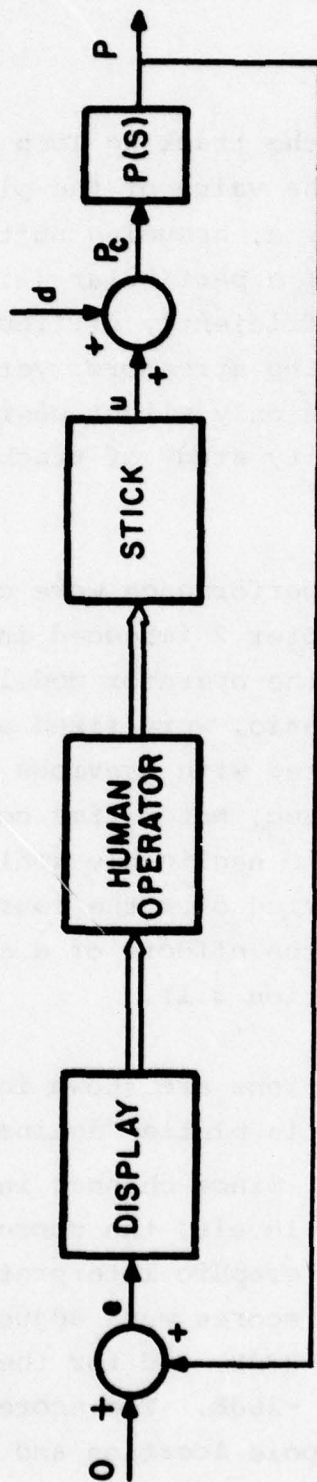
A block diagram of the tracking task is shown in figure 3.2. A compensatory tracking display provides the subject with a measure of system error e , which he attempts to minimize by appropriately manipulating the control stick. The stick signal u is summed with the loop input disturbance signal d , to yield the plant dynamics command p_c . The plant output p is then fed back to become the display signal e . This positive feedback results in an "outside-in" display, necessitating negative feedback compensation by the human operator.

As noted in section 3.1, the plant dynamics $P(s)$ are given by

$$P(s) = \frac{\lambda}{s - \lambda} \quad (3.4)$$

where the plant pole λ remains fixed throughout the course of a tracking run. The PSD function of the loop input d is chosen to be first-order, scaled so as to ensure that the RMS level is unity:

$$\Phi_{dd}(\omega) = \frac{2a}{\omega^2 + a^2} \quad (3.5)$$



$$P(S) = \frac{\lambda}{S - \lambda} \quad \Phi_{dd}(\omega) = \frac{2a}{\omega^2 + a^2} ; d^2 = 1$$

GLZ106

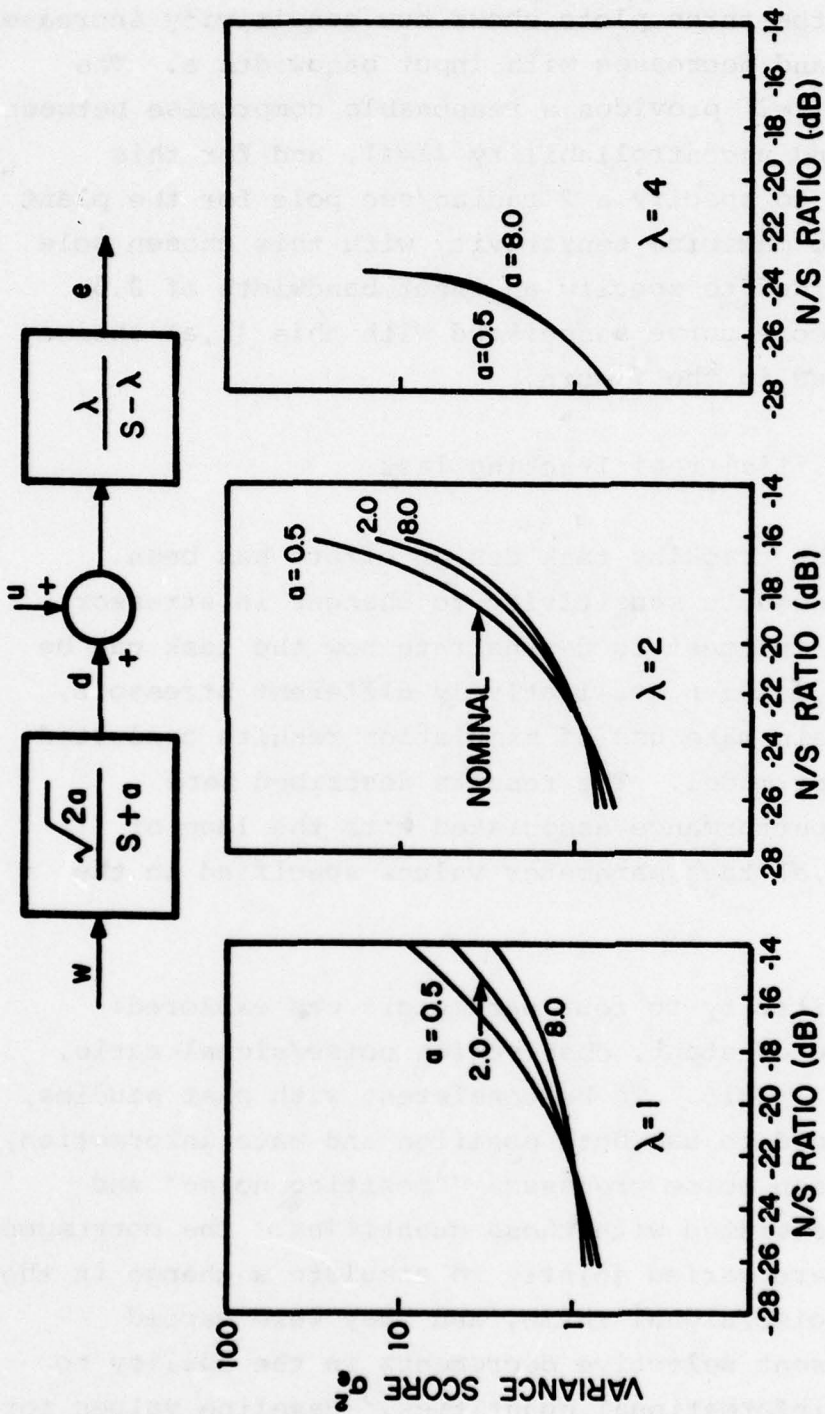
Figure 3.2: Tracking Task Block Diagram

3.4 Sensitivity of Tracking Task

For a complete specification of the tracking loop illustrated in figure 3.2, we need only specify the value of the plant pole λ and the input signal break frequency a , assuming unity gains for both display and stick. The choice of a particular (λ, a) pair should be such as to make the task sufficiently difficult to ensure adequate sensitivity to imposed tracking stressors, yet not result in a task which is uncontrollable with only slight degradations in the tracking environment. A sensitivity study of tracking performance is thus called for.

Several simulations of tracking performance were conducted, using the human operator model of chapter 2 imbedded in the tracking loop of figure 3.2. All of the operator model parameters, except for observation noise/signal ratio, were fixed at "nominal" values consistent with levels associated with previous human operator research: time delay = 0.2 sec, motor time constant = 0.1 sec, and motor noise/signal ratio negligibly small. The observation noise/signal ratio was varied over the course of the model runs, in an effort to simulate the effects of a stressed environment (recall discussion of section 3.1).

The main results of these simulations are shown in figure 3.3, in which tracking error score σ_e^2 is plotted against the observation noise/signal ratio (N/S). Since changes in score are of greater interest than absolute levels, the scores have been normalized for a more convenient graphic interpretation of the results; for the first two plots, scores were adjusted to yield unity error at an N/S level of -23dB, and for the third plot adjusted to yield unity error at -26dB. The score curves themselves are parameterized against pole location and input bandwidth a .



GLZ107

Figure 3.3: Score Sensitivity to Pole Location and Noise Bandwidth

A comparison of the three plots shows how sensitivity increases with pole location λ and decreases with input bandwidth a . The moderate instability ($\lambda=2$) provides a reasonable compromise between insensitivity ($\lambda=1$) and uncontrollability ($\lambda=4$), and for this reason it was decided to specify a 2 radian/sec pole for the plant dynamics. In order to maximize sensitivity with this chosen pole value it was also decided to specify an input bandwidth of 0.5 radian/second. The score curve associated with this (λ, a) choice of (2, 0.5) is labelled in the figure.

3.5 Differential Sensitivity of Tracking Task

To this point, the tracking task design effort has been devoted to ensuring adequate sensitivity to changes in stressor levels. It is now of interest to demonstrate how the task can be used to differentiate between qualitatively different stressors, and to do this, we again make use of simulation results conducted with the human operator model. The results described here investigate tracking performance associated with the loop of figure 3.2 and the (λ, a) task parameter values specified in the previous section.

Performance sensitivity to four parameters was explored: time delay, motor time constant, observation noise/signal ratio, and motor noise/signal ratio. To be consistent with past studies, the operator was assumed to use both position and rate information, and separate observation noise processes ("position noise" and "rate noise") were associated with these quantities. The corresponding noise/signal ratios were varied jointly to simulate a change in the overall observation noise/signal ratio, and they were varied individually to represent selective decrements in the ability to obtain and use these informational quantities. Baseline values for

operator-related parameters were as before: time delay = 0.2 sec, motor time constant = 0.1 sec, observation noise/signal ratio = -23 dB, and motor noise/signal ratio negligibly small.*

Figure 3.4 shows the dependence of the tracking error variance σ_e^2 and the variance of the rate-of-change of control input σ_u^2 to changes in the various model parameters. In each plot, the left-most arrow on the abscissa indicates the assumed nominal value for that particular parameter; the next arrow indicates the parameter value associated with a doubling of the nominal score; the right-most arrow indicates the parameter value associated with a quintupling of the nominal score. Thus, for example, a change in observation noise from -23dB to -20dB cannot be differentiated from a change in time delay from 0.2 sec to 0.27 sec when only σ_e^2 is measured; this is because both parameter changes result in an identical doubled score.

At least one of the parameters, however, can be differentiated from the others by considering measures other than tracking score. As shown in figure 3.4, all of the control rate scores increase with increasing tracking scores except for the case due to changes in the motor time constant τ_N . Here σ_u^2 actually decreases, reflecting the lower bandwidth of the human operator. Thus, confronted with an increase in tracking score σ_e^2 , the experimenter can decide whether or not there has been a change in the motor time constant by simply examining the associated change in the control rate score σ_u^2 .

*The nominal value for observation noise/signal ratio was lower than generally found in most laboratory tracking tasks, but was consistent with values found in a study employing unstable system dynamics (Levison et al. (1971)).

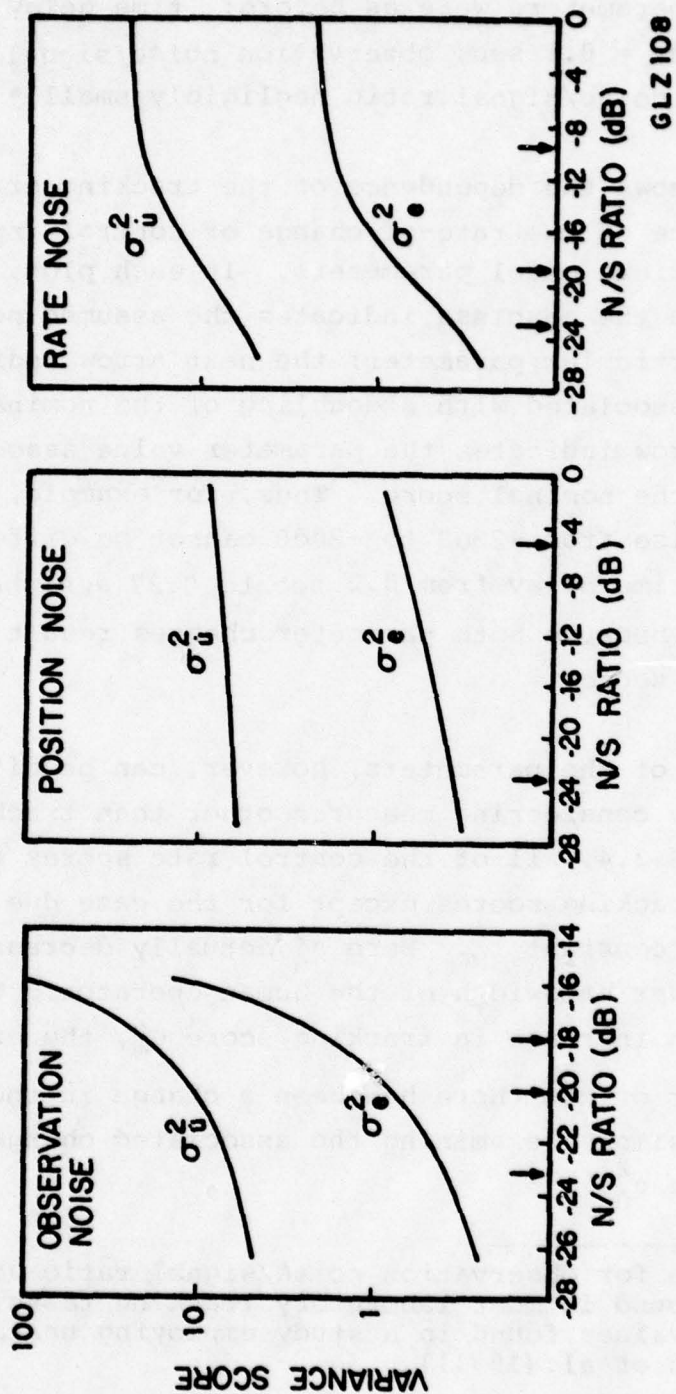


Figure 3.4: Tracking Score and Control Sensitivity to Model Parameter Variations

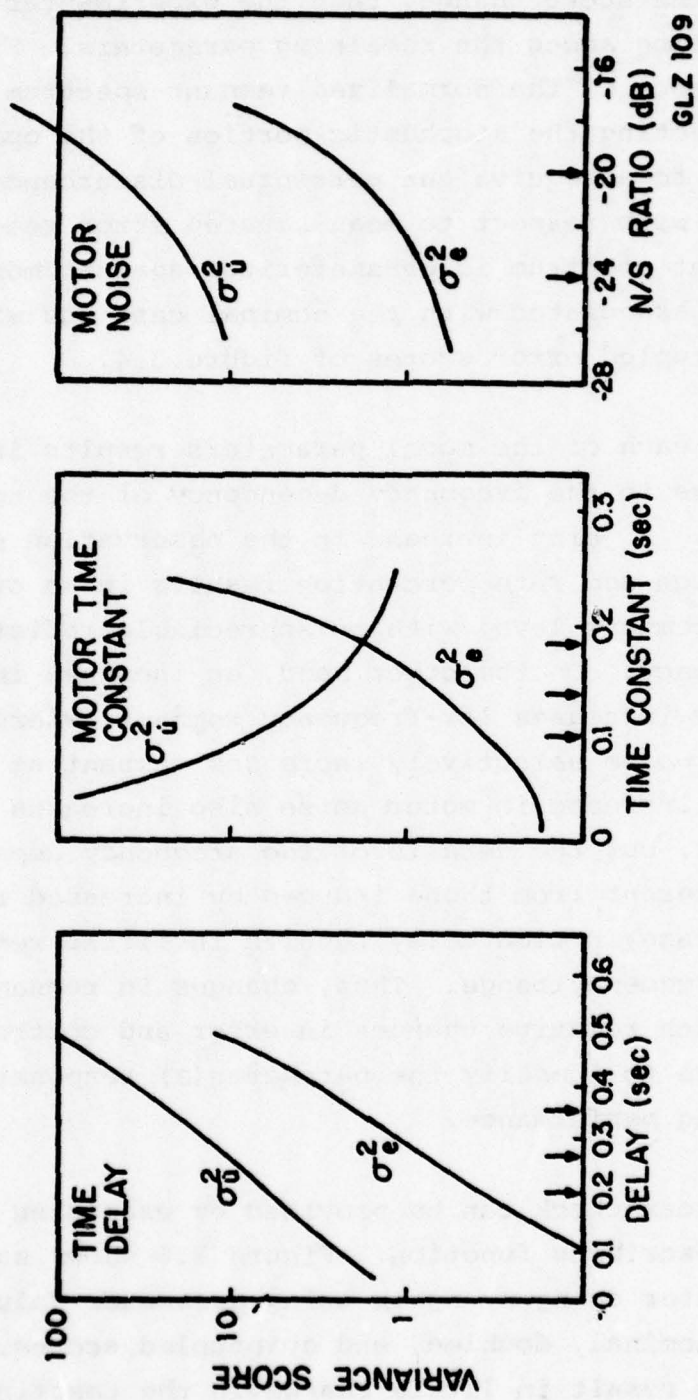
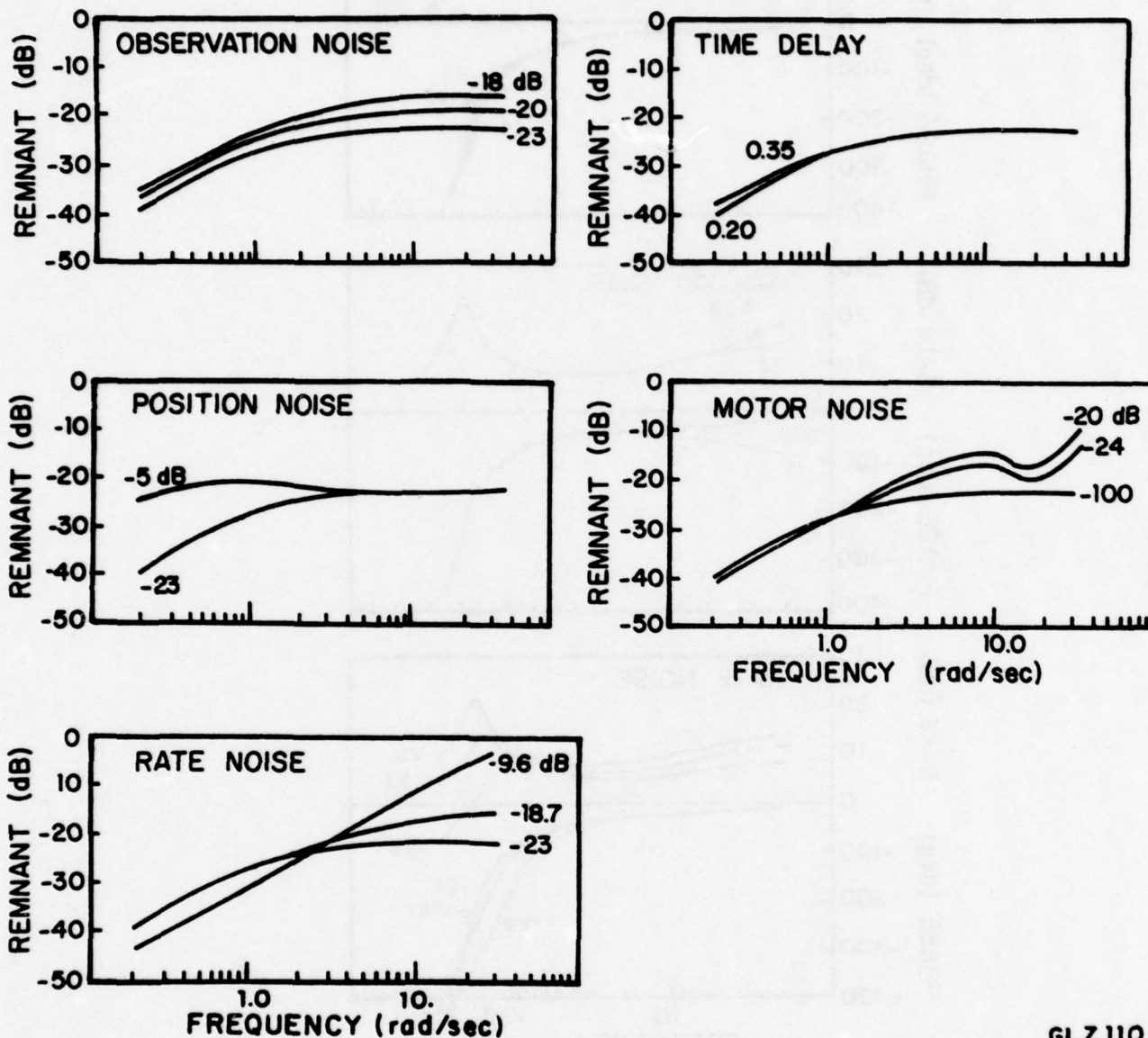


Figure 3.4 (cont.): Tracking Score and Control Sensitivity to Model Parameter Variations

If it is determined that a change in the parameter τ_N is not responsible for the score change, then the experimenter is faced with differentiating among the remaining parameters. Figure 3.5 shows the dependence of the normalized remnant spectrum which is obtained by reflecting the stochastic portion of the operator's control response to an equivalent perceptual disturbance on error rate, normalized with respect to mean-squared error rate. The normalized remnant spectrum is parameterized against model parameter values associated with the nominal case and with the doubled and quintupled error scores of figure 3.4.

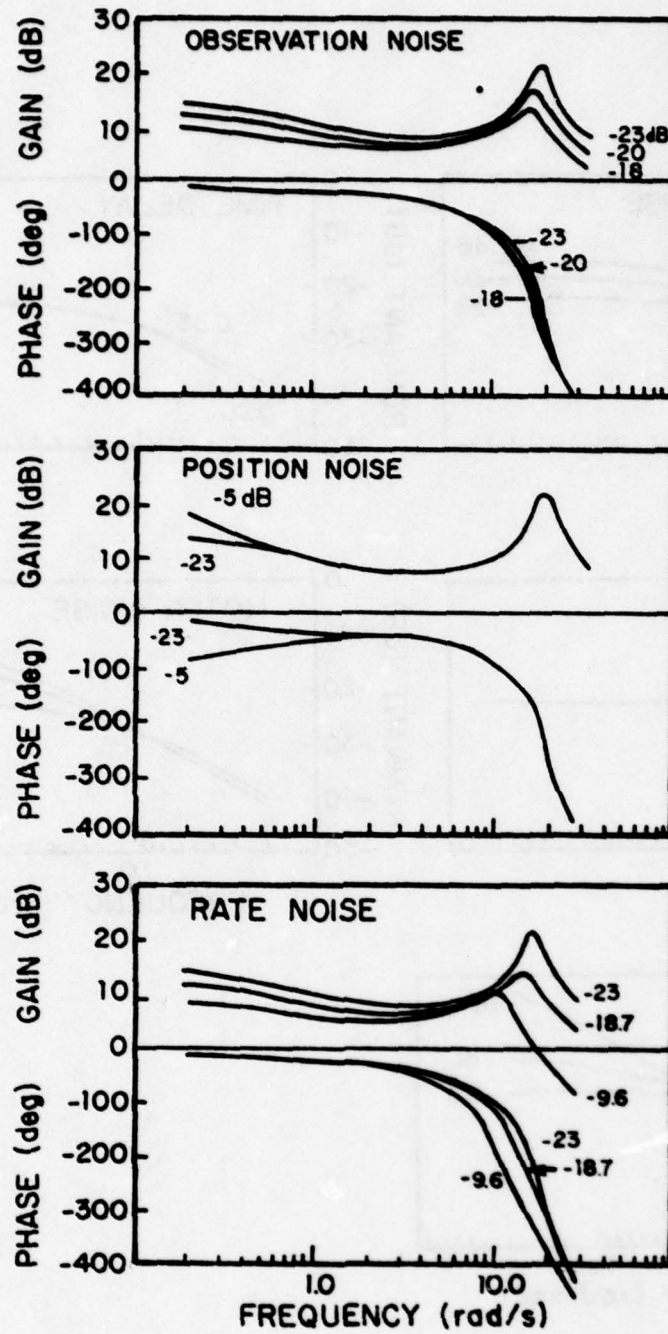
A change in each of the model parameters results in a distinctive change in the frequency dependency of the normalized remnant spectrum. A joint increase in the observation noise/signal ratios for position and rate perception results in an overall increase in the remnant level with no appreciable redistribution of power with frequency. On the other hand, an increase in position noise selectively increases low-frequency remnant, whereas an increase in rate noise selectively increases remnant at high frequencies. An increase in motor noise also increases high-frequency remnant, but the details of the frequency dependency are somewhat different from those induced by increased rate noise. Finally, an increase in time delay results in little remnant change, throughout the frequency range. Thus, changes in remnant behavior, in conjunction with relative changes in error and control-rate scores, allows one to identify the parameter(s) responsible for the change in tracking performance.

A partial cross-check can be provided by examining changes in the operator's describing function. Figure 3.6 shows such changes with model parameter changes, again using parameter values associated with nominal, doubled, and quintupled scores. Changes in position noise result in little change in the describing function and thus this measure serves to isolate the position noise



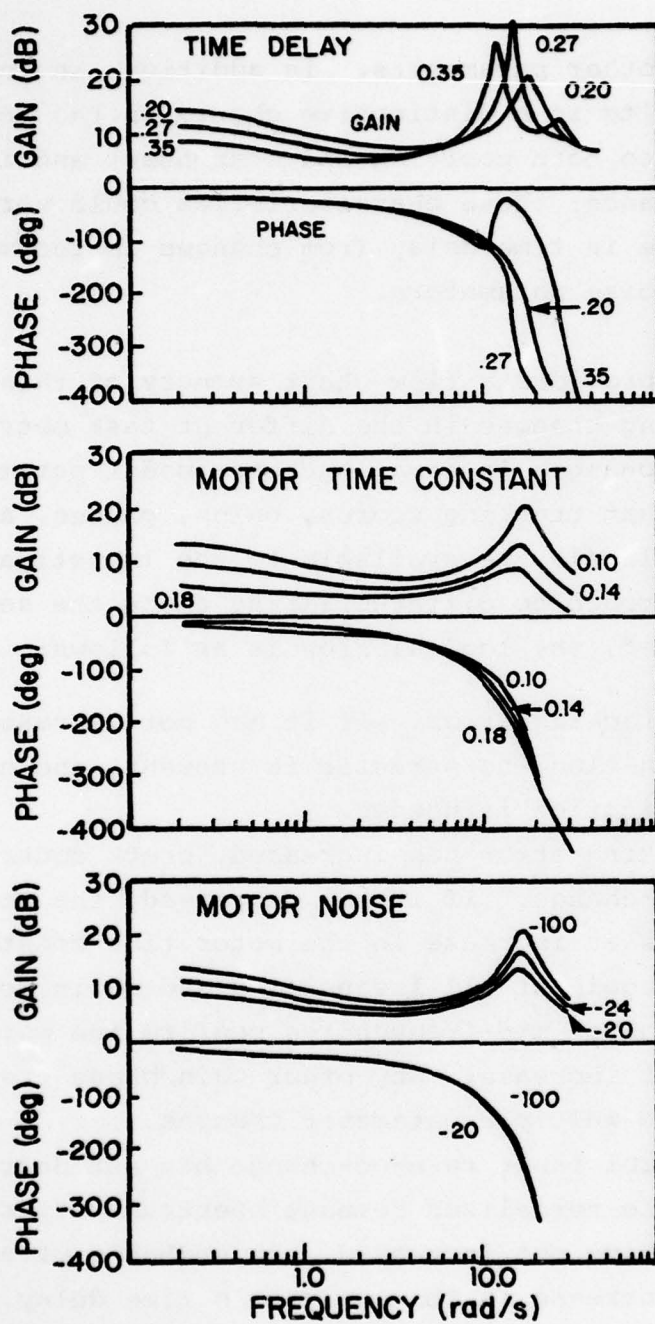
GLZ 110

Figure 3.5: Normalized Remnant Dependence on Model Parameters
(normalized with respect to display error rate)



GLZ 111

Figure 3.6: Describing Function Changes with Model Parameter Changes



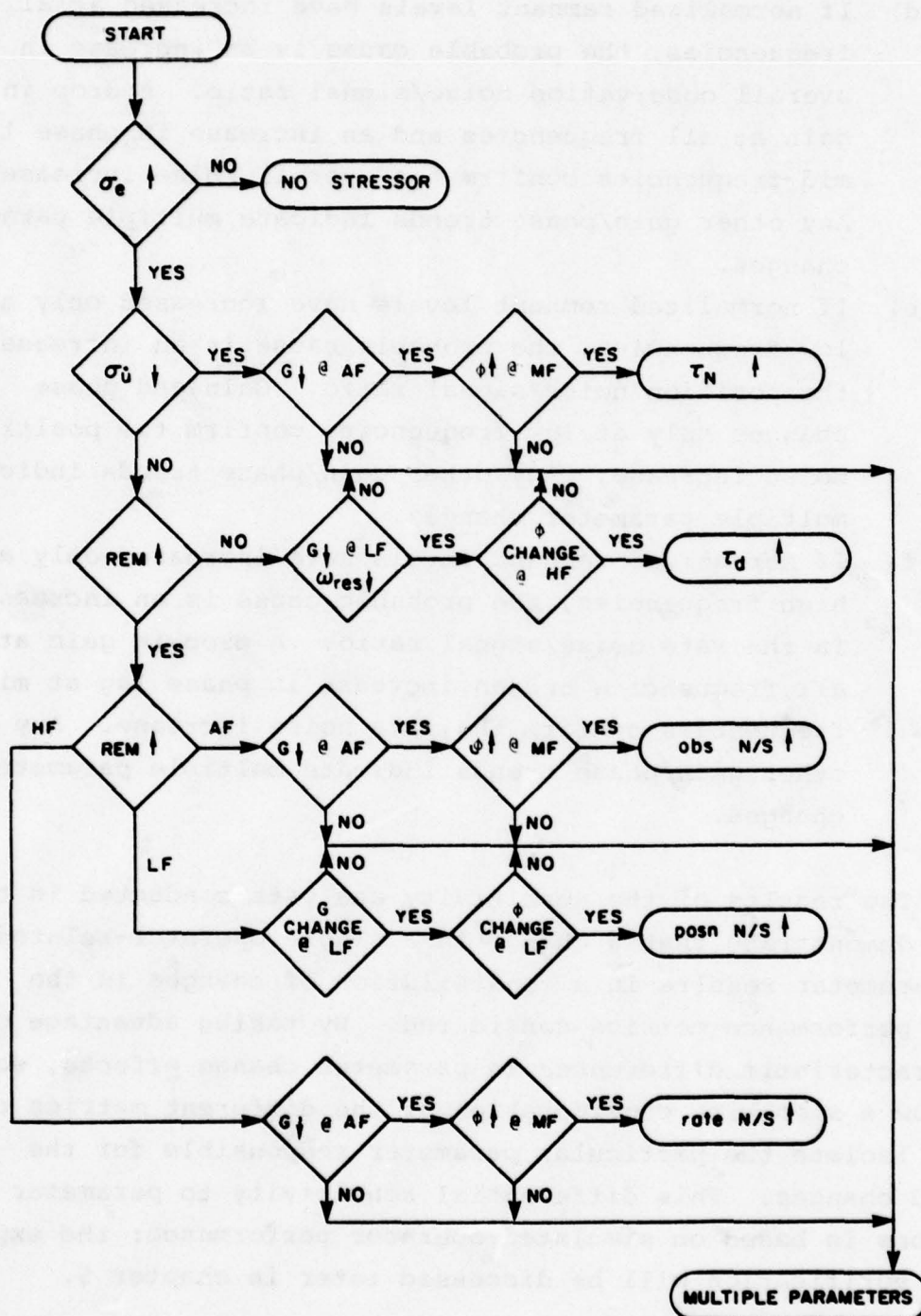
GLZ 112

Figure 3.6 (cont.): Describing Function Changes with Model Parameter Changes

parameter from the other parameters. In addition, an increase in the time delay results in a distinctive change in the resonance peak (with respect to both position and sharpness) and in the behavior near resonance; these characteristics could serve to distinguish a change in time delay from changes in the motor time constant and noise parameters.

Figure 3.7 provides a flow chart summary of this step-wise approach to assessing changes in the different task metrics and inferring probable changes in human operator model parameters. The chart assumes that tracking scores, gains, phases, and normalized remnant levels are available to the investigator, and illustrates one approach to differentiating among the several parameters. In brief, the logical flow is as follows:

- a) Check tracking error. If it has not increased, then, by definition, no stressor is present, and no parameter identification is needed.
- b) If tracking error has increased, check control input rate-of-change. If it has decreased, the probable cause is an increase in the motor time constant. A drop in gain at all frequencies and an increase in phase lag at mid-frequencies confirm the motor time constant increase. Any other gain/phase trends indicate multiple parameter changes.
- c) If control input rate-of-change has not decreased, check the normalized remnant spectrum. If remnant levels have not increased, the probable parameter change is an increase in the operator's time delay. A drop in gain at low frequencies, a drop in the resonant frequency, and a change in the phase lag at high frequencies confirm the time delay increase. Any other gain/phase trends indicate multiple parameter changes.



GLZ 130

Figure 3.7: Logical Flow for Inferring Model Parameter Changes

- d) If normalized remnant levels have increased at all frequencies, the probable cause is an increase in the overall observation noise/signal ratio. A drop in gain at all frequencies and an increase in phase lag at mid-frequencies confirm the overall noise increase. Any other gain/phase trends indicate multiple parameter changes.
- e) If normalized remnant levels have increased only at low frequencies, the probable cause is an increase in the position noise/signal ratio. Gain and phase changes only at low frequencies confirm the position noise increase. Any other gain/phase trends indicate multiple parameter changes.
- f) If normalized remnant levels have increased only at high frequencies, the probable cause is an increase in the rate noise/signal ratio. A drop in gain at all frequencies and an increase in phase lag at mid-frequencies confirm the rate noise increase. Any other gain/phase trends indicate multiple parameter changes.

The results of the sensitivity analysis conducted in this chapter demonstrate that a change in a single operator-related model parameter results in a constellation of changes in the several performance metrics considered. By taking advantage of the characteristic differences in parameter change effects, we have shown how a step-wise consideration of the different metrics can be used to isolate the particular parameter responsible for the observed changes. This differential sensitivity to parameter variations is based on simulated operator performance; the experimental verification will be discussed later in chapter 5.

4. EXPERIMENT DESCRIPTION

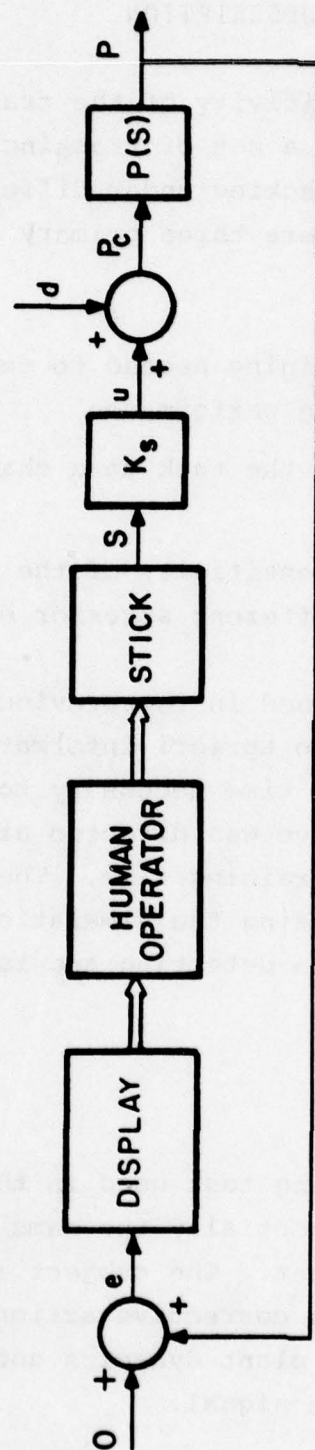
In order to validate the sensitivity of the tracking task described in the previous chapter, a set of tracking experiments was conducted at BBN to compare tracking under different environmental conditions. There were three primary objectives of the experimental study:

- a) Determine the amount of training needed to ensure consistent operator tracking performance
- b) Validate the sensitivity of the task to a change in the operator environment
- c) Validate the differential sensitivity of the task and its utility in isolating different stressor effects

Since the model simulations described in the previous chapter assumed a fully-trained subject, no apriori information was available concerning the amount of time necessary to train on the task. Thus, the first objective was directed at determining an empirically based estimate of training time. The second two objectives were directed at validating the simulation results, and verifying the task's utility in detecting and isolating stressor effects.

4.1 Task Description

A block diagram of the tracking task used in the experiments is given in figure 4.1, and is essentially the same task which was analyzed in the previous chapter. The subject is provided an error display on which to base his corrective actions needed both for stabilizing the unstable plant dynamics and for compensating against the loop input disturbance signal.



GLZ117

Figure 4.1: Tracking Task Block Diagram

The tracking error was displayed on a 10 cm wide by 6 cm high oscilloscope face, with 1 cm horizontal and vertical grid lines providing a stationary reference. The outside-in display consisted of a vertical bar 2.6 cm long, which was deflected laterally according to the value taken on by the display signal e . The display was centered in azimuth a distance of approximately 60 cm from the subject's eyes, so that one centimeter of display displacement resulted in approximately one degree of angular displacement. Subjects' sitting heights were such that the display elevation angle was within 10 degrees of eye level of each subject.

The subjects used a left-right force control stick located approximately 35 cm to the right and 25 cm in front of the subject; an arm rest at a comfortable sitting height provided support for the subject's arm and hand. Since only 5 cm of the stick were available for grasping, subjects used a combination of finger and thumb grips for manipulating the stick. The stick stiffness was such that one pound of force applied to the top end of the stick resulted in approximately 1 mm of lateral displacement of the stick. The stick gain K_s , shown in the figure and used to convert from pounds of stick force to centimeters of plant command, was set at 5 cm/pound, a level which provided adequate controllability without being overly sensitive.

The loop input disturbance signal, d shown in the figure, was constructed from 13 sinusoids whose amplitudes were selected so that the input signal power spectral density (PSD) approximated the following continuous PSD function:

$$\phi_{dd}(\omega) = \frac{2a}{\omega^2 + a^2} \quad (4.1a)$$

The first-order form of this PSD function was chosen on the basis of the simulation results of the previous chapter, as was the break frequency:

$$a = 0.5 \text{ rad/sec} \quad (4.1b)$$

The input signal amplitudes were all scaled to provide an RMS input signal level of one cm. In order to prevent subjects from learning the input waveforms during the course of the experiment, a random number generator was used to vary the phase relationships of the input signal sinusoids from one tracking run to the next. Thus, the input was "random-appearing" as previously discussed in section 3.1.

The plant dynamics used in the experiment were

$$P(s) = \frac{\lambda}{s-\lambda} e^{-\tau_0 s} \quad (4.2a)$$

The first order instability was chosen on the basis of the simulation results of the previous chapter, as was the pole value:

$$\lambda = 2 \text{ rad/sec} \quad (4.2b)$$

The plant dead-time τ_0 was not explicitly specified to be a part of the nominal set of dynamics, but rather was due to the digital implementation of the tracking loop. Its value was determined by an input-output system measurement described in appendix B, and was found to be

$$\tau_0 = 32 \text{ msec} \quad (4.2c)$$

As just noted, the tracking loop was implemented on a digital computer, with the display and stick providing the analog interfaces to the human operator. The programmable digital system, developed specifically for human operator tracking experiments, is named the Performance Analyzer, and is described in detail in appendix A. In brief, it provides the investigator with a

simplified means for defining the desired tracking task, automated calibration of the interface hardware, real-time control of the tracking experiment, storage of the tracking time histories, and post-experimental analysis of tracking performance.

For this set of experiments, the Performance Analyzer software was implemented on a Digital Equipment Corp. PDP-11/34, located on site at BBN. The experimenter controlled the program via a teletype terminal, and monitored the display error during tracking via a slave scope. Subjects were located in an adjoining sound-proof room, containing the scope display, control stick, and an intercom for communicating with the experimenter. Room lighting and display intensity were adjusted to comfortable levels, and remained fixed throughout the set of experiments.

To investigate the sensitivity of the tracking task to changes in the task environment, two simulated stressors were utilized during the course of the experiment. One was directed at simulating "visual noise" imposed on the tracking display, and consisted of a diffused display error bar presented on the scope. By inserting a translucent sheet between the display grid lines and the face of the display, the vertical bar could be diffused over a width of approximately one cm, without affecting the display reference provided by the grid lines. The second stressed condition was directed at simulating any stressor which would act to increase the operator's central processing time (e.g., confusion, ambiguity, etc.), and was implemented by adding a time delay to the plant dynamics controlled by the operator. The time delay chosen was 40 milliseconds, and was in addition to the dynamic delay of 32 milliseconds already mentioned above.

4.2 Experimental Protocol

Six male college students between the ages of 18 and 29 years of age were used for the experiment. All were right-handed and had normal visual acuity, although some wore corrective lenses.

A tracking run lasted for 185 seconds, and tracking score was computed from the standard deviation of the display error, σ_e . This was computed over an interval equal to the period of the imposed disturbance signal, which was 163.8 seconds. Since the scoring interval was shorter than the duration of the tracking run, scoring did not begin until 10.6 seconds after run commencement, to allow for subject "warm-up".

Three such tracking runs, interspersed with one minute rest intervals, comprised a block of runs. Four such blocks, interspersed with 15-minute rest intervals outside of the subject room, comprised a normal day's tracking session for each subject. The overall experiment was conducted over a month's time.

The experiment was conducted in three phases, consisting of an initial training phase, an intermediate training phase on the stressed conditions, and a control phase for comparing performance under the different conditions.

4.2.1 Initial Training Phase

At the outset, each subject was instructed as to the task dynamics involved, and the objective of minimizing the tracking score. The subject was then made familiar with the task dynamics by being given the opportunity to stabilize and control the display bar displacement, with no loop input disturbing his

control actions. This two-minute practice run was then followed by two tracking runs with the disturbance signal present, at a half cm RMS level (half its nominal value). If the subject managed to control the bar displacement for the entire length of both runs, the next run was conducted at the nominal one cm RMS input level, as were subsequent runs. If however, the subject lost control of the task at this lower level, he was rerun at the same level until able to successfully complete two such runs in a row; at that point, the input level was raised to the nominal one cm RMS value.

During the first day of tracking, high and low input signal levels were chosen according to the subject's ability to successfully complete a tracking run. Thus, if a subject failed to complete a run at the one cm RMS input level, subsequent runs were conducted with the half cm RMS input, until two in a row were successfully completed, whereupon the subject was returned to the one cm RMS input level. After the first day of tracking, this training protocol was no longer followed; instead, if a subject failed to complete a run at the nominal one cm RMS input level, he was simply rerun at the same level.

Each day of training was begun with a 30-second "warm-up" run, to allow the subject to adjust mentally and physically to the task. This was followed by four three-run blocks, to yield 12 runs per day. The initial training phase consisted of four such days, to yield 48 completed tracking runs per subject.

Throughout the first training phase, tracking score was reported to the subject at the end of each run, and the subject was encouraged to modify his handgrip, gaze, and tracking strategy in any manner he felt which would help minimize his tracking score. Each subject was also allowed to view a plot of

his run-to-run score history, to assess his progress in learning the task. To maintain motivation, subjects were also made aware of each other's scores.

Because of early implementation difficulties with the Performance Analyzer, the phases of the loop input signal were not varied from run-to-run for this initial training phase. Thus, the same input signal was used for all tracking runs, and the subjects had the opportunity of "learning" the input over the course of training. However, this was not felt to be a significant factor in determining task proficiency, since comparable scores were later obtained when subjects tracked randomized inputs. This issue will be discussed later in chapter 5.

4.2.2 Intermediate Training Phase

All of the subjects participated in a second training phase directed at training them in the three task conditions which would eventually be used for stressor comparisons. To avoid the input signal "learning" problem just mentioned, all runs conducted during this intermediate training phase utilized an input signal which was randomized from run to run. One of the conditions was designated the nominal condition and, except for the input signal randomization, was identical to that used in the initial training phase just described. A second condition was designated the diffused condition and consisted of the diffused error bar display described in section 4.1. The third condition was designated the delay condition, and involved the plant dynamics time delay also described in section 4.1. Again, all conditions utilized a randomized input signal during this intermediate training phase.

Each subject participated in three training sessions, with each day's session devoted exclusively to one of the three conditions. As before, each session consisted of four three-run blocks, to yield 12 training runs per condition per subject. To provide some balance for sequential learning effects, subjects were exposed to the different conditions in a balanced order, according to table 4.1. Note that this is not a full-factorial design, since subjects were trained as a pair, on a given condition.

Table 4.1: Presentation Order for Intermediate Training Phase

Session	Subject					
	KDH	SAH	TMV	DMI	KJW	LEK
1	A	A	B	B	C	C
2	B	B	C	C	A	A
3	C	C	A	A	B	B

A: nominal

B: time delay

C: diffuse display

As before, the subject was instructed to minimize his tracking error by any means he felt appropriate. If the condition was nominal, the subject was informed that the task was the same as what he had previously trained on. If the condition was the delay case, the subject was informed that he might notice some response lag, but that he should attempt to do his best at minimizing his tracking score. If the condition was the diffused display case, the subject was immediately aware of the condition under which he would be tracking; again, he was simply told to do his best at minimizing his tracking score.

Each session began with a 30-second "warm-up" run on the condition which would be used throughout that day's session. After each full 185-second tracking run, the subject was informed of his tracking score; as before, the subject was periodically shown his run-to-run score history, so that he could assess his progress. If a subject failed to complete a tracking run, he was given a short rest period and then simply restarted on the same run.

4.2.3 Control Phase

All of the subjects participated in the third phase of the experiment, directed at comparing tracking performance under the three conditions on which they had trained. The tracking task and the three conditions were identical to those used in the previous training phase, and only the order of presentation and number of replications were varied. This phase was completed in a single session of tracking, consisting of four three-run blocks. The overall design is given in table 4.2, and was chosen to provide a balance for ordering effects within a given block, for the first three blocks; the fourth block is simply a replication of the first.

Experimental protocol was similar to that used in the earlier phases, except for the initial "warm-up" period. For the control sessions, the subject was allowed to "warm-up" with a 30-second run on each of the three conditions, before starting the first block of runs. As before, if a subject failed to complete a run, he was given a short rest period, and simply restarted on the same run.

Table 4.2: Presentation Order for Control Phase

Block	Run	Subject					
		DMI	KJW	TMV	SAH	LEK	KDH
1	1	A	B	C	A	B	C
	2	B	A	B	C	C	A
	3	C	C	A	B	A	B
2	4	B	C	A	B	C	A
	5	A	B	B	C	A	C
	6	C	A	C	A	B	B
3	7	C	A	B	C	A	B
	8	B	B	A	A	C	C
	9	A	C	C	B	B	A
4	10	A	B	C	A	B	C
	11	B	A	B	C	C	A
	12	C	C	A	B	A	B

A: nominal

B: diffuse display

C: time delay

5. EXPERIMENTAL RESULTS

The major results of the various tracking experiments are described in this chapter. Since most of the results presented here are displayed graphically, appendix C provides the reader with a more detailed tabulated summary of the tracking data. The primary data obtained from the experiments are presented and discussed in section 5.1, and the results of a model analysis effort are discussed in section 5.2.

5.1 Primary Data

The primary data obtained from the tracking runs consisted of tracking scores (error, stick, and stick rate), describing functions (gain and phase), and normalized remnant.

Tracking scores were calculated for each individual run included in the data analysis. These scores consisted of the variance of the display error, equivalent stick, and equivalent stick rate. To obtain the latter two scores, the stick signal was first converted from the recording units (lbf) to equivalent units of plant command (cm), via the stick gain K_S . The variance of this converted stick signal was then computed to yield the equivalent stick score. Since the stick rate signal was not saved during a tracking run, the equivalent stick rate score was also computed from the converted stick signal. This was done by first calculating the power spectrum of the converted stick signal, multiplying each component by the square of the associated frequency, and integrating over frequency, to yield an estimate of the stick rate variance. Details of this and other score computation procedures are given in the Performance Analyzer description of Appendix A.

Describing functions were calculated for each individual run conducted during the control phase of the experiment, after the

subjects had been trained on the three experimental conditions. Describing function gain and phase values for the human operator were calculated at each frequency contained in the loop input, by dividing the Fourier transform of the equivalent stick signal by the transform at the display error. Since the Performance Analyzer introduced a phase shift in the measurements (see Appendix B), all human operator describing functions were corrected for this shift.

Estimates of normalized remnant were obtained by partitioning the equivalent stick spectrum into input-correlated and remnant-related components, and, at each loop input frequency, calculating the equivalent remnant power referred to display error rate, and normalizing by the variance of the display error rate. The mathematical details are discussed in Levison et al (1969), and some implementation details are given in the Performance Analyzer description of appendix A.

The input-correlated and remnant-related components of the stick spectrum were also used to calculate the correlated-to-remnant power ratio (C/R) at each loop input frequency. If a C/R ratio was found to be less than 6dB, this indicated that more than 20% of the response power at that frequency was uncorrelated with the loop input. Accordingly, the corresponding describing function gain and phase values were flagged, to assure that they would not be included in the data base, because of their low reliability.

Additional data processing procedures are to be found in the following sections describing the results of the three experimental phases.

5.1.1 Results of Initial Training Phase

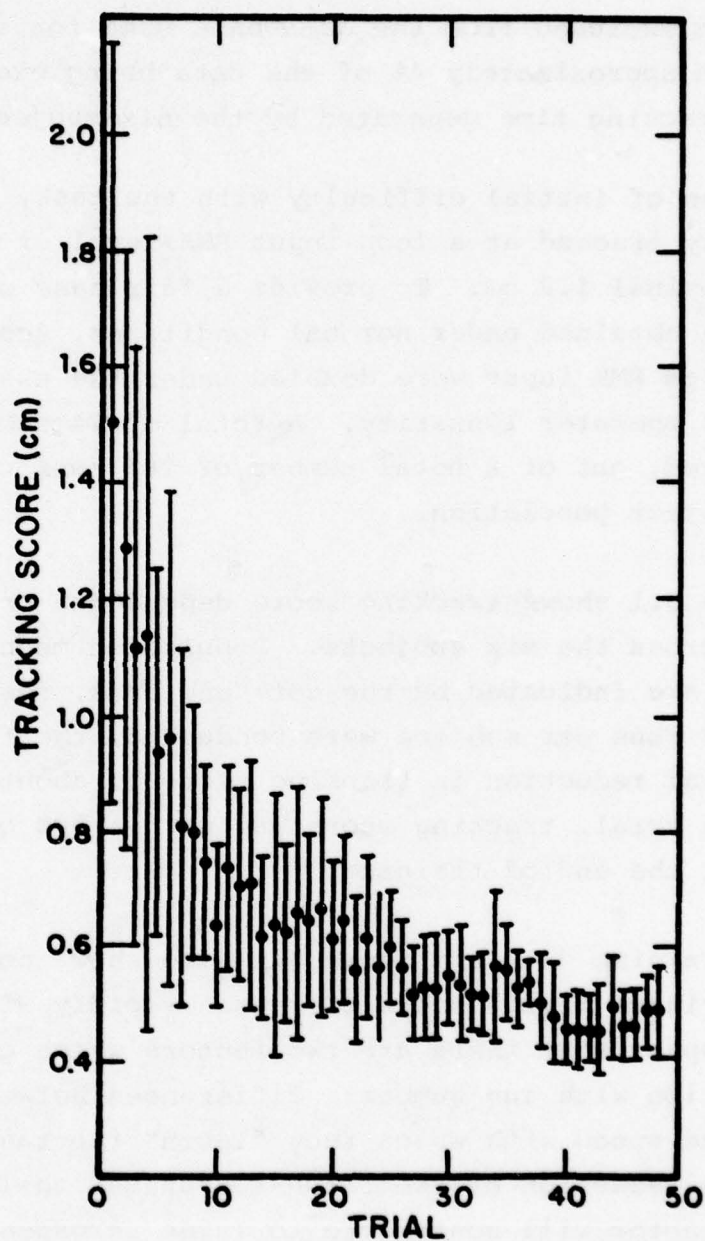
As noted in the previous chapter, each subject successfully completed 48 training runs. On the occasion when a subject lost

control of the task, he was simply rerun, and the data of the aborted run excluded from the data base used for analysis. This resulted in approximately 4% of the data being excluded, in terms of total tracking time generated by the six-subject population.

Because of initial difficulty with the task, subjects occasionally tracked at a loop input RMS level of 0.5 cm, rather than the nominal 1.0 cm. To provide a fair base of comparison with scores obtained under nominal conditions, scores obtained with a 0.5 cm RMS input were doubled under the assumption of approximate operator linearity. A total of 24 such run scores were adjusted, out of a total number of 288 runs completed by the six-subject population.

Figure 5.1 shows tracking score dependence on run number, averaged across the six subjects. Population means and standard deviations are indicated by the dots and bars, respectively. Although 48 runs per subject were conducted, the figure shows a substantial reduction in tracking score by about the 15th trial; by the 30th trial, tracking score was within 20% of the scores obtained at the end of training.

The training data of figure 5.1 also show how the across-subject variance in the score decreases rapidly with run number. It would appear that there are two factors which contribute to this reduction with run number: differences between subjects in terms of the speed with which they "learn" the task, and, within subjects, a reduction of their run-to-run variability with training. The first factor will contribute to large across-subject variance at the beginning of training, since this is where individual learning curves show the greatest difference. The second factor will similarly contribute to the observed reduction in across-subject variance with run number, since each subject becomes progressively less variable from run-to-run.



GLZ 114

Figure 5.1: Tracking Score History During Initial Training (six subject average)

5.1.2 Results of Intermediate Training Phase

As noted in the previous chapter, each subject completed 36 intermediate training runs, 12 on each condition. When a subject lost control during a run, the same procedure was used as during the initial training phase: the subject was simply rerun and the data of the aborted run excluded from the data base. This resulted in less than 2% of the data being excluded, in terms of total tracking time generated by the six-subject population.

It was anticipated that training times under all three conditions would be considerably shorter than that seen during initial training. This is confirmed by the tracking score histories shown in figure 5.2, illustrating average behavior for the six subjects with run number, under the three conditions. The nominal training data, in fact, show no evidence of a "learning" curve, and would appear to be a simple continuation of the asymptotic training behavior already illustrated in figure 5.1, associated with the initial training phase. Since the data of figure 5.1 were obtained with a loop input signal which was never changed from run-to-run, and the data of figure 5.2 were obtained with a signal which was randomized from run-to-run, it would appear that "learning" of the input signal plays at most a minor role in determining performance, at least for this task.

Figure 5.2 also shows the tracking score histories for training under the two stressed conditions: diffused display and time delay. In contrast with the nominal case, the diffused and delayed conditions show a definite learning period, although it appears to be quite short, on the order of 5 runs. Also evident are the higher scores obtained under the diffused and delayed conditions, when compared with the nominal. Statistical

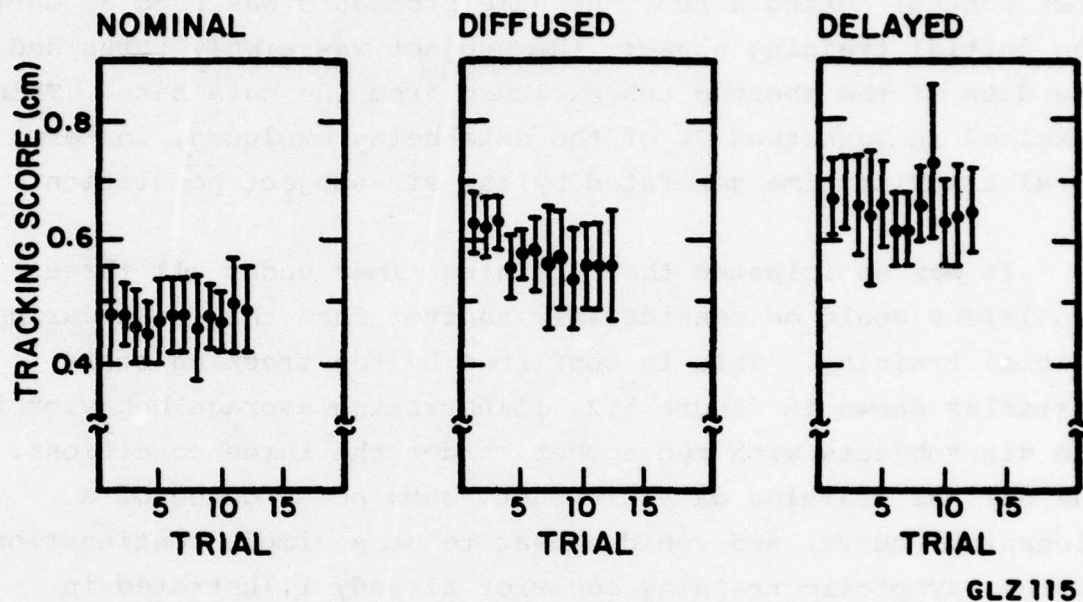


Figure 5.2: Tracking Score Histories as a Function of Tracking Condition (six subject average)

tests of significance will be made in the next section, but the apparent score increases shown in the figure suggest that the diffused and delayed conditions can indeed be labelled as "stressed" conditions.

5.1.3 *Results of Control Phase*

As noted in the previous chapter, each subject completed 12 control runs, four on each condition. When a subject lost control during a run, the same procedure was used as during the previous two experiment phases: the subject was simply rerun and the data of the aborted run excluded from the data base. This resulted in less than 2% of the data being excluded, in terms of total tracking time generated by the six-subject population.

Tracking scores and frequency domain measures were calculated for each tracking run. These measures were then averaged across the four replications completed by each subject under each condition,* to yield the means and standard deviations of the various measures, associated with each subject tracking under a particular condition. With six subjects and three conditions, this resulted in 18 sets of statistics. The means were then averaged across subjects, to obtain overall statistical measures of performance with condition. To test for significant differences between conditions, paired differences were formed from corresponding subject means; these differences were then subjected to a two-tailed t-test of significance.

*Low reliability gain and phase measurements were excluded from each subject's average if the corresponding C/R ratio was found to be less than 6 dB.

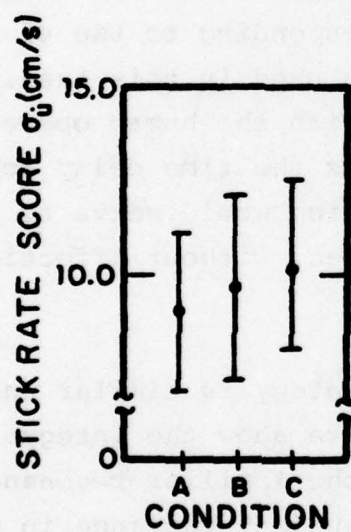
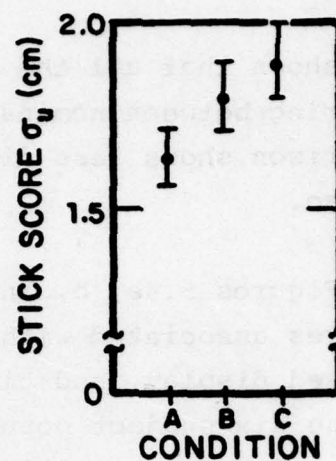
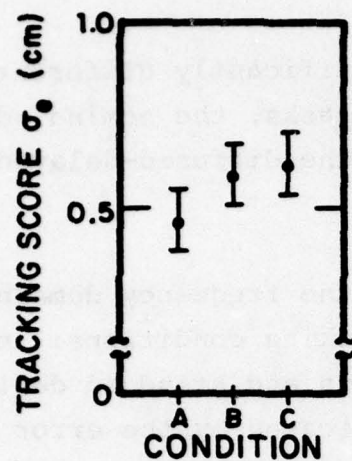
Figure 5.3 shows score variations due to the differing task conditions: across-subject means and standard deviations are given for display error (σ_e), stick (σ_u), and stick rate ($\sigma_{\dot{u}}$) scores, the latter two given in the equivalent plant command units of cm and cm/sec, respectively. Although the standard deviations are comparable across conditions, the score means show a definite dependence on condition. Tracking score is raised by about 30% over nominal, when subjects track under the diffused or delayed conditions. A similar trend is seen with the stick score, indicating more operator effort under the stressed conditions. The stick rate score shows a similar trend, but is not as definitive because of the larger variances associated with it.

To test for significant differences between conditions, paired differences were calculated from the corresponding individual subject means. The results of a two-tailed t-test across conditions are given in table 5.1. Significance levels are shown for the three condition comparisons; a level above 0.05 was considered not significant (N.S.).

Table 5.1: Significance Levels between Conditions

score \ condition pair			
	<u>nominal</u> <u>diffused</u>	<u>nominal</u> <u>delayed</u>	<u>diffused</u> <u>delayed</u>
σ_e	.001	.001	.05
σ_u	.001	.001	.01
$\sigma_{\dot{u}}$	N.S.	.001	N.S.

The table confirms the conclusions to be made from the bar plots of figure 5.3. The display score is significantly different across conditions, as is the stick score; the stick rate score, however indicates a significant difference only when nominal tracking is compared with delayed tracking. The table



A: NOMINAL
B: DIFFUSE DISPLAY
C: TIME DELAY

GLZ 116

Figure 5.3: Tracking Scores as a Function of Tracking Condition (six subject average)

also shows that all the scores are significantly different when comparing between nominal and delayed tasks; the nominal-diffused comparison shows less difference, and the diffused-delayed even less so.

Figures 5.4a, b, and c summarize the frequency domain measures associated with the three tracking conditions: nominal, diffused display, and time delay. Means and standard deviations for the six-subject population are indicated by the error bars at each frequency. All phase measurements were corrected by the addition of a 32 msec lead, to compensate for the 32 msec lag introduced by the measurements made by the Performance Analyzer (see appendix B). In addition, the phase measurements associated with the time delay case (figure 5.4c) were adjusted by the addition of a 40 msec lag, corresponding to the 40 msec dead-time present in the plant dynamics used in this case. In this way the time delay is associated with the human operator rather than the plant dynamics, and thus the time delay condition simulates the effect of any stressor which would serve to increase the operator's processing time by 40 msec, without affecting any other aspect of operator behavior.

The figures show that operator strategy is similar under all three tracking conditions. The gain data show the integrator-like response at low frequencies, and the familiar resonance at approximately 20 rad/sec. The across-subject variance in gain is least in the midband, with larger deviations at both ends of the measurement spectrum. The phase data show a nearly constant lag in the neighborhood of 40 deg, at the low- and mid-frequencies, and then drop off rapidly in the neighborhood of the resonant frequency. Except for the three highest measurement frequencies, the phase data are characterized by very small across-subject

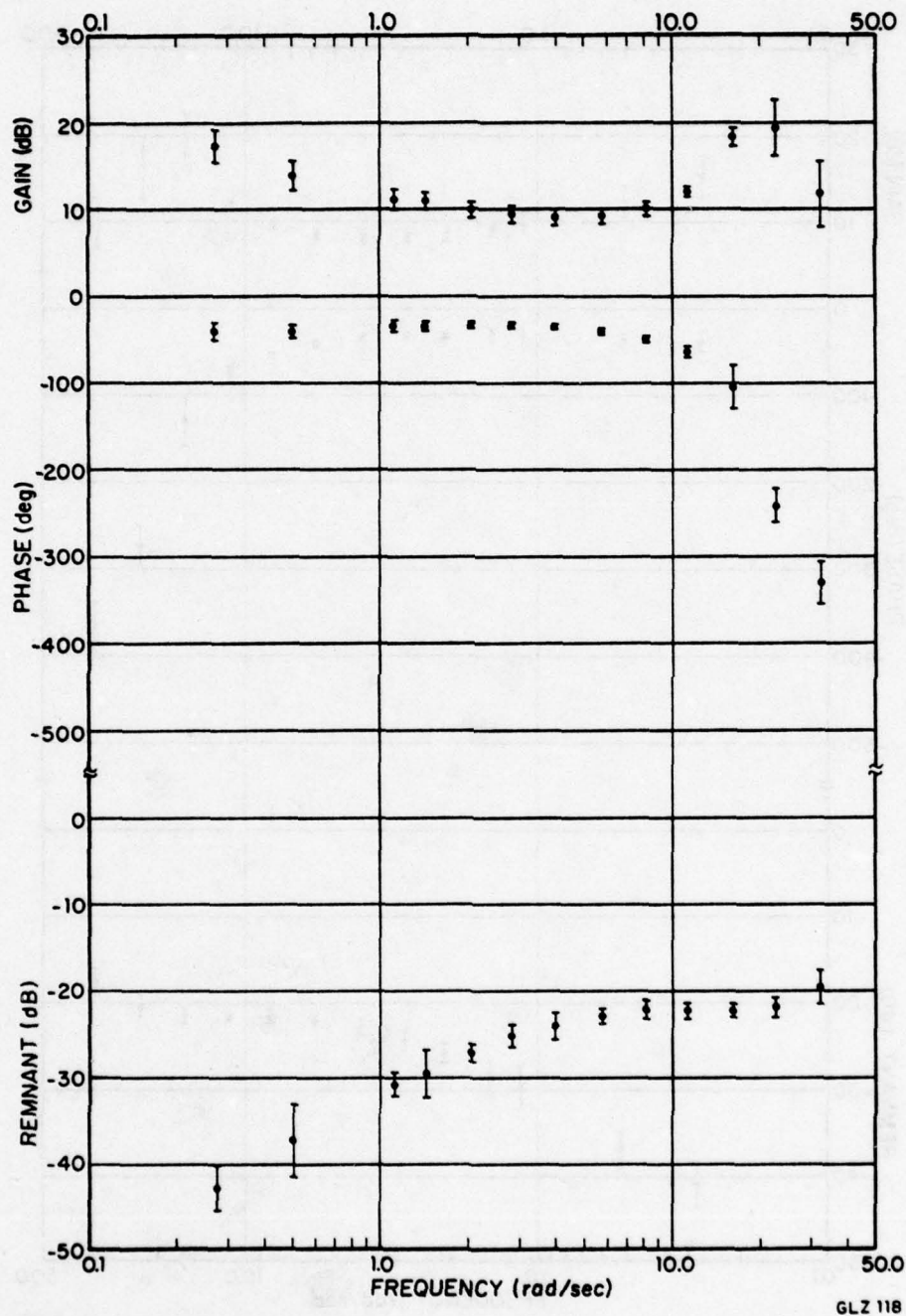
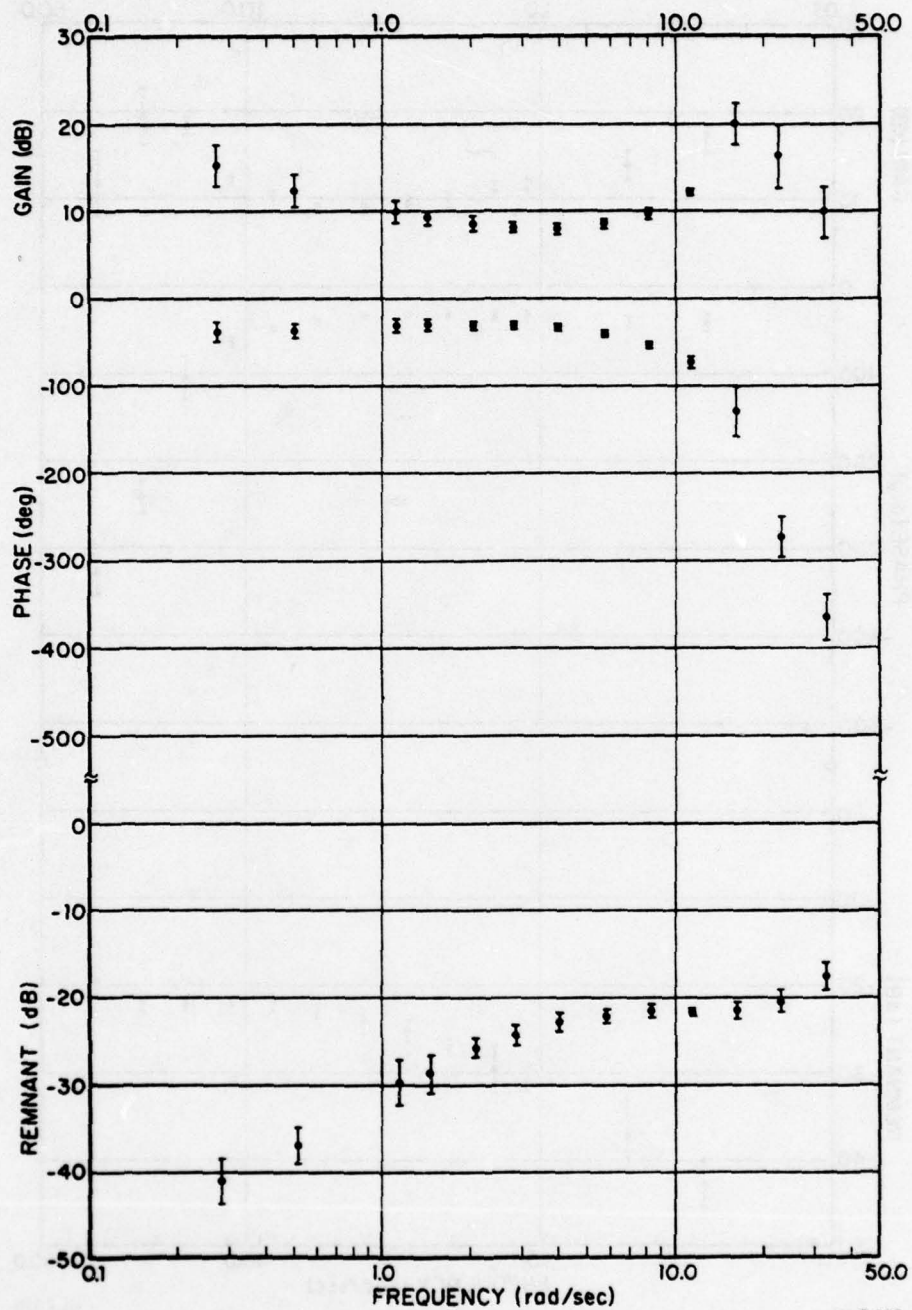


Figure 5.4a: Frequency Response Measures Obtained under Nominal Conditions



GLZ 119

Figure 5.4b: Frequency Response Measures Obtained under Diffused Conditions

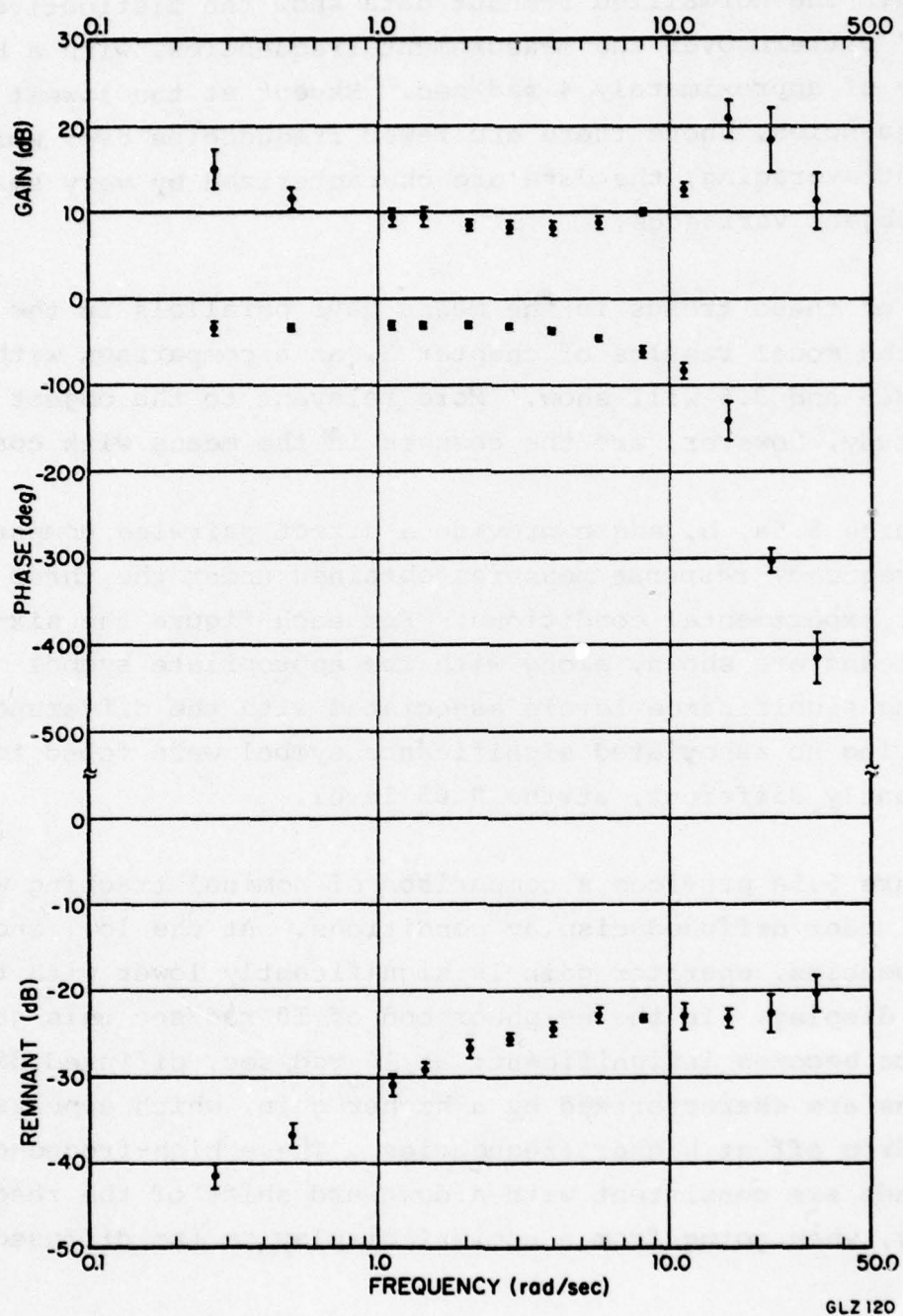


Figure 5.4c: Frequency Response Measures Obtained under Delayed Conditions

variances. The normalized remnant data show the distinctive "washout" pattern over the measurement frequencies, with a break frequency of approximately 4 rad/sec. Except at the lowest measurement frequencies, where there are fewer frequencies over which to do remnant averaging, the data are characterized by very small across-subject variances.

All of these trends in the means have parallels in the illustrated model results of chapter 3, as a comparison with figures 3.5 and 3.6 will show. More relevant to the object of the study, however, are the changes in the means with condition.

Figures 5.5a, b, and c provide a direct pairwise comparison of the frequency response measures obtained under the three different experimental conditions. For each figure the six-subject means are shown, along with the appropriate symbol indicating significance levels associated with the differences. Means having no associated significance symbol were found to be not significantly different, at the 0.05 level.

Figure 5.5a provides a comparison of nominal tracking with tracking under diffused display conditions. At the low- and mid-frequencies, operator gain is significantly lower with the diffused display. In the neighborhood of 10 rad/sec this gain difference becomes insignificant; at 16 rad/sec, diffused display conditions are characterized by a higher gain, which appears to rapidly drop off at higher frequencies. These high-frequency gain trends are consistent with a downward shift of the resonant frequency, when going from a nominal display to the diffused display.

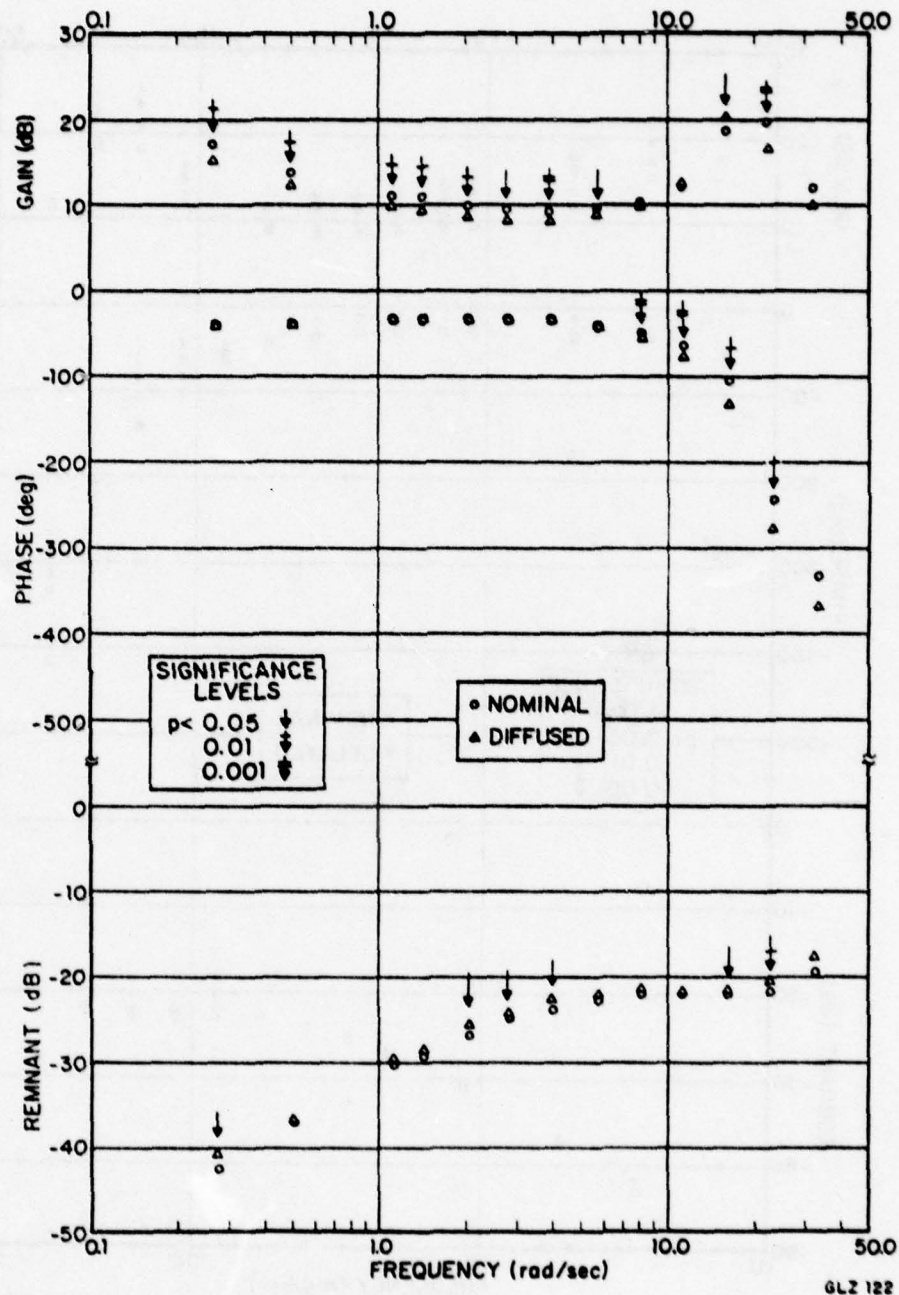


Figure 5.5a: Frequency Response Measures Obtained under Nominal and Diffused Display Conditions

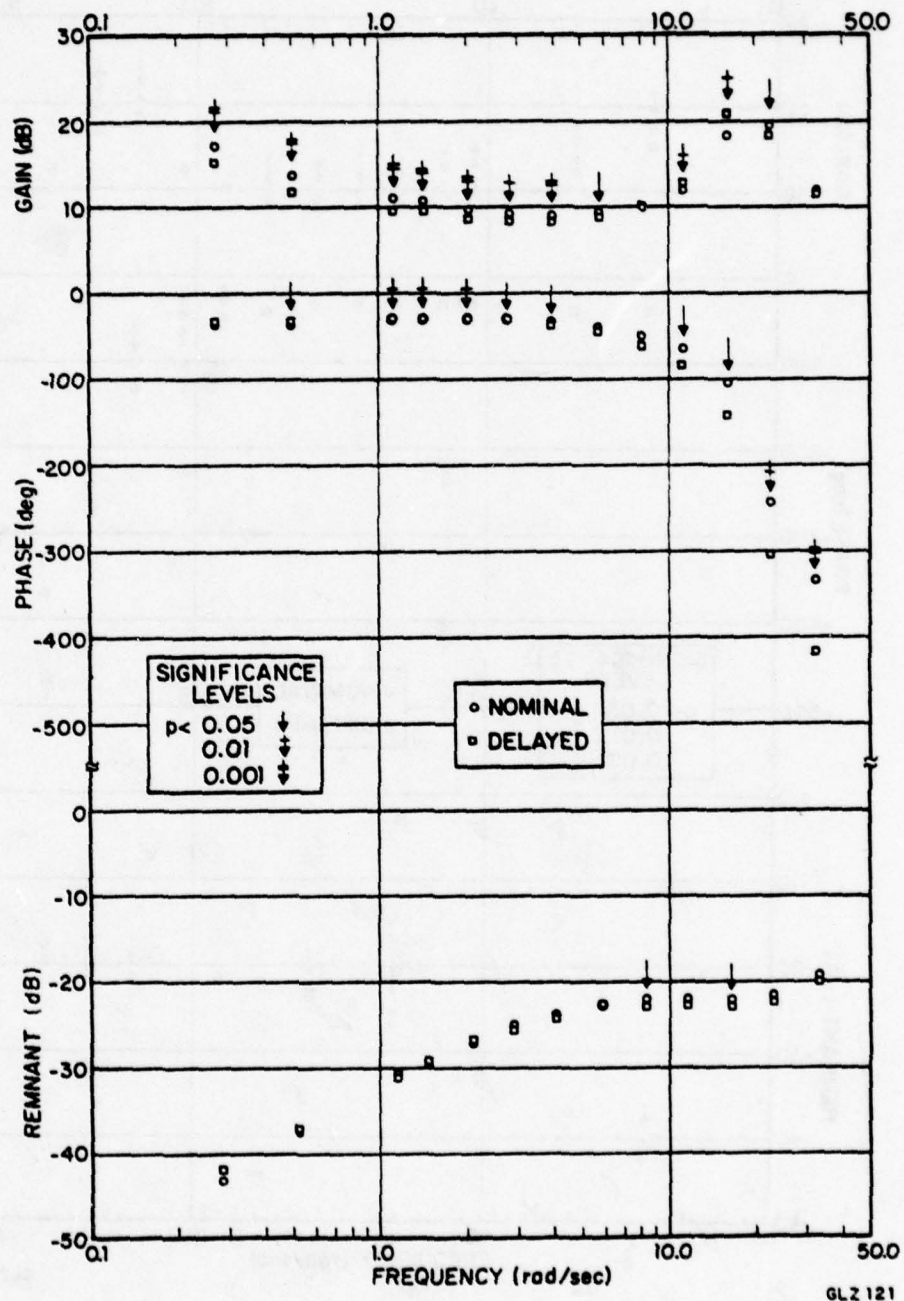


Figure 5.5b: Frequency Response Measures Obtained under Nominal and Time Delay Conditions

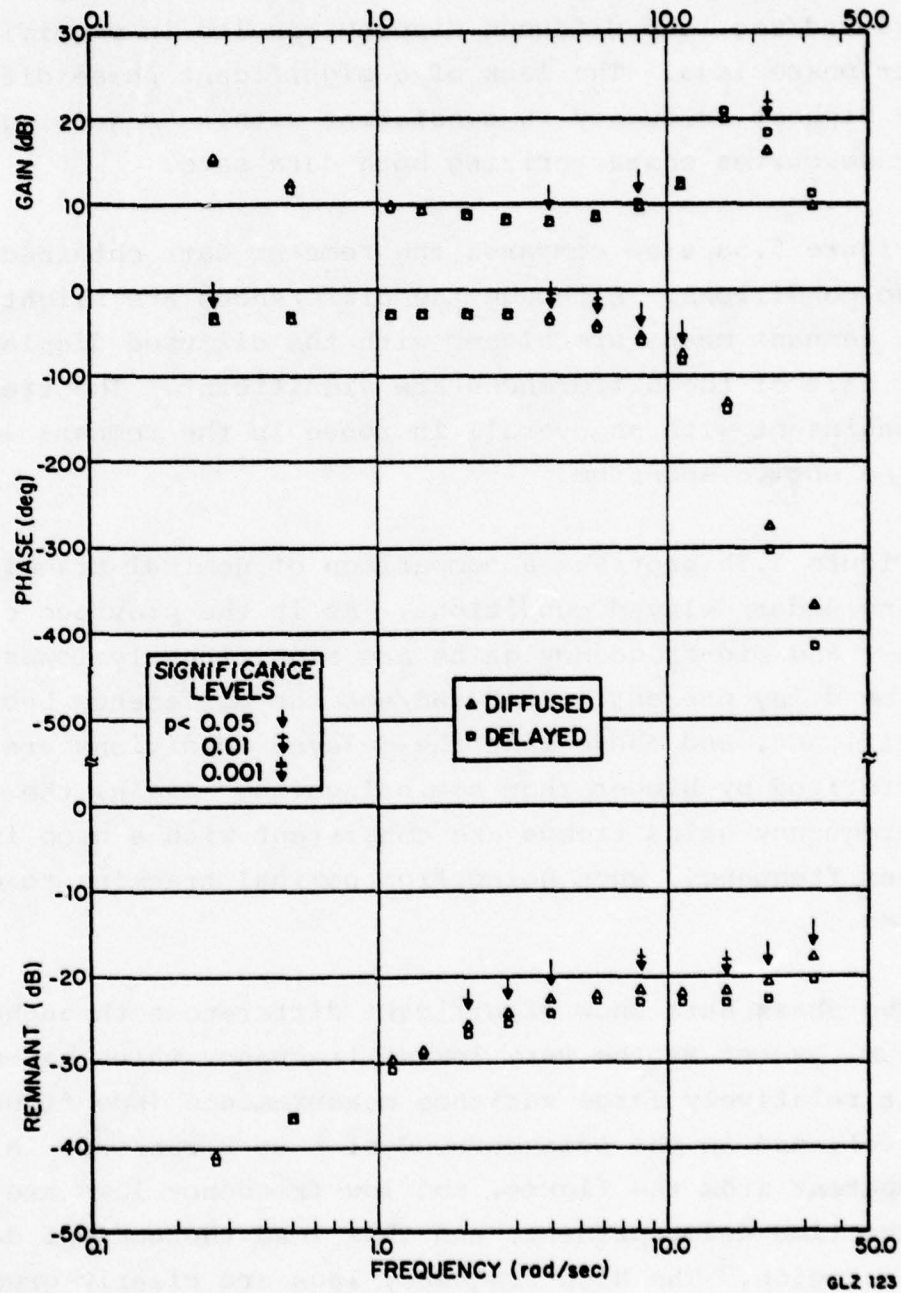


Figure 5.5c: Frequency Response Measures Obtained under Diffused Display and Time Delay Conditions

The corresponding phase data show no significant differences at the low- and mid-frequencies. However, in the region from 8 to 20 rad/sec, the diffused display results in significantly greater phase lags. The lack of a significant phase difference at the highest frequency is consistent with a "rejoining" of the phase curves characterizing both data sets.

Figure 5.5a also compares the remnant data obtained under the two conditions. Although the differences are slight, all of the remnant means are higher with the diffused display, and almost half of the differences are significant. The trends seen are consistent with an overall increase in the remnant level, over the entire spectrum.

Figure 5.5b provides a comparison of nominal tracking with tracking under delayed conditions. As in the previous case, the low- and mid-frequency gains are significantly lower with the time delay present. At 8 rad/sec the difference becomes insignificant, and above that the delayed conditions are characterized by higher than nominal gains. Again, the high-frequency gains trends are consistent with a drop in the resonant frequency, when going from nominal tracking to delayed tracking.

The phase data show significant differences throughout the spectrum, except at the very lowest frequency which has associated with it relatively large variance measurements (see figures 5.4a and 5.4c), and in the neighborhood of 5 to 8 rad/sec. Although not apparent from the figure, the low-frequency lags are less with the time delay present, and thus lead the nominal data in this region. The high-frequency lags are clearly greater with the delay present, and thus the relative phase relations are reversed from that seen at the low frequencies. The 5 to 8 rad/sec neighborhood in which no significant differences are seen is the lead-lag transition region.

Figure 5.5b also compares the remnant data obtained under the two conditions. At the low- and mid-frequencies no obvious trends are apparent; at the high frequencies, the delayed tracking condition is characterized by lower than nominal remnant levels. The fact that only two of the means are (marginally) significantly different suggests that the time delay has little effect on the measured remnant levels.

Figure 5.5c provides a comparison of the effects of the diffused display with those of the time delay. The low- and mid-frequency gains show little difference, although the high-frequency trends suggest a more sharply-defined resonant peak associated with delayed tracking. The phase data show little difference up to about 4 rad/sec, at which point the increased lag associated with the time delay becomes apparent. Although the phase differences at the highest three measurement frequencies are not statistically significant (because of the larger variances characterizing these measurements), the increasing lag with delayed tracking becomes substantial.

Figure 5.5c also compares remnant data obtained under the two conditions. Except for the measurement at 0.5 rad/sec, all of the remnant means are higher with the diffused display. Since more than half of the differences are significant, the remnant trends are consistent with the notion of higher overall remnant levels associated with the diffused display, when compared with the time delay.

5.1.4 *Summary of Primary Data*

This section summarizes the major findings of the three experimental phases: initial training phase, intermediate training phase, and control phase.

The initial training phase showed that the most significant reduction in tracking score occurred within the first 15 trials, and that by the 30th trial, scores were within 20% of their asymptotic levels. Across subject variance showed a similar reduction with run number, due to both across-subject differences in learning time needed for the task, and due to a reduction of individual run-to-run variability with run number.

The intermediate training phase confirmed the asymptotic performance of the subjects on the nominal task, and was characterized by considerably shorter training times on the two stressed tracking tasks. Asymptotic performance on the two stressed conditions was reached in approximately five runs, with tracking scores for both the diffused display and time delay conditions considerably higher than that achieved under nominal conditions. The use of a randomized loop input signal showed little or no difference when compared with the use of a signal which was repeated from run-to-run, based on the similar scores achieved during this phase and those achieved at the end of the initial training phase.

The control phase provided additional measures of tracking performance, including tracking scores, describing functions, and remnant levels. Tracking error and stick displacement scores obtained under the two stressed conditions were found to be significantly higher than the corresponding nominal scores, with differences on the order of 30%. Stick rate score differences were not significantly different, except when comparing nominal with delayed tracking.

The operator describing functions obtained during the control phase all showed the same basic trends with frequency, for the three different tracking conditions. Within subject t-tests showed, however, that the stressed conditions resulted in a significant lowering of the low- and mid-frequency gains; the high-frequency gain changes were consistent with a reduction of the operator's resonant peak frequency, combined with a sharpening of the gain resonance. Significant phase differences were also found when comparing the two stressed conditions with nominal tracking, the primary effect being an increase in the high-frequency lag. Tracking with a time delay also resulted in a small but significant lead at the low frequencies, when compared with the phase data obtained under nominal conditions.

The normalized remnant measures obtained during the control phase provided an additional differentiation between the effects of the three tracking conditions. The diffused display resulted in consistently higher than nominal remnant levels throughout the measurement spectrum, with almost half of the differences significant. In contrast, the effects of the time delay showed no consistent pattern in the remnant measurements, when compared with the nominal measurements, and only two of the 13 measures were found to be significantly changed due to the delay.

5.1.5 *Discussion of Primary Data*

The findings just summarized serve to verify the human operator model predictions made earlier in chapter 3, and, when interpreted in terms of model parameter variations, they verify the utility of the task for differentiating between qualitatively different task stressors.

A comparison of the measured frequency response given in figures 5.4a, b, and c with the model predictions of figures 3.5 and 3.6, shows that the model predicts the basic describing function and remnant trends with frequency, with a "nominal" operator parameter set. Since the measured response under the stressed conditions differs only slightly from that made under nominal conditions (compare figures 5.4b and c with figure 5.4a), the implication is that the model parameters need only be changed slightly from their "nominal" values, to account for the effects of either stressor. That this is indeed the case will be seen in the next section; for now, however, it suffices to note that we should expect only slight changes from nominal, with no extensive parameter variations needed to account for the stressor effects.

Four basic features characterize the changes in the frequency response measures when going from the nominal tracking condition to the diffused display condition (see figure 5.5a): a) a lowering of the low- and mid-frequency gain; b) a decrease in the resonant peak frequency; c) an increase in the high-frequency phase lag; and d) an overall increase in the remnant level. A review of the model's predicted frequency response, given in figures 3.5 and 3.6 of chapter 3, shows that these changes can be interpreted as simply an increase in the overall observation noise/signal ratio. Although variations in other parameters

might account for the describing function changes (figure 3.6), none of them produce the observed overall increase in the remnant level (figure 3.5). Thus, if one parameter were to be identified with the changes observed with the diffused display condition, the best candidate would be the overall observation noise/signal ratio.* The fact that an increase in this noise level parameter can qualitatively account for the changes seen with diffused display tracking is intuitively satisfying, since one might very well expect a diffuse display to introduce visual "noise" into the tracking loop.

A similar argument can be made for the observed changes in the frequency response measures when going from the nominal tracking condition to the time delay condition (figure 5.5b). Here, changes similar to the diffused display case are seen in the gain and phase data, although one might argue for an additional sharpening of the resonant peak with the time delay case (figure 5.5c). More significant, however, is the fact that the remnant level is effectively unchanged from its nominal level; thus, one can eliminate from consideration an increase in the observation noise/signal ratio. The model's predicted frequency response (figures 3.5 and 3.6) instead argues for a change in the operator's time delay, the only parameter which accounts for the observed describing function changes and the lack of change observed in the remnant level. The fact that this parameter is effectively identified from the measurements made under the time delay conditions clearly serves to verify this comparative approach based on model predictions.

*This does not preclude the involvement of additional parameter changes, of course, and this possibility is discussed further in the next section.

Although the discussion has been somewhat qualitative, based on general "features" of the data, one can conclude that the tracking task is capable of differentiating between the effects of two different stressors. The approach requires only a brief comparison of the frequency response measures with the human operator model predictions, and serves to isolate the model parameter change most likely responsible for the measured change under the stressed tracking condition. It is anticipated that such an approach would be quite satisfactory for a screening evaluation of tracking stressors; however, it is the intent here to provide a more rigorous justification for this approach, and the next section addresses the problem in a more quantitative manner.

5.2 Model Analysis

To interpret stressor effects on tracking, a model analysis effort was conducted using the optimal control model of the human operator. The primary objective was to express stressor effects in terms of model parameter changes, so as to provide a quantitative basis for the arguments made in the previous section. A secondary objective was to demonstrate the model's utility in reducing the amount of data needed to characterize tracking performance, by condensing a large-dimension data vector to a small-dimension model parameter vector.

5.2.1 *Analysis Procedure*

The method for identifying model parameters was similar to that used in earlier study programs and described by Levison et al (1976). Parameter values were sought which would match the various metrics of the model to the corresponding experimentally derived metrics, which consisted of: 1) performance scores;

2) describing function gain; 3) describing function phase; and 4) remnant level. The matching was accomplished by minimizing a scalar cost function J which was defined as the mean component value of a four-dimensional vector of matching errors:

$$J = (J_1 + J_2 + J_3 + J_4)/4 \quad (5.1a)$$

where

$$\underline{J} = (J_1, J_2, J_3, J_4)^T \quad (5.1b)$$

Each component J_i of the matching error vector corresponded to one of the metric groups mentioned above. Each component was computed from the sum of the normalized squared differences between model metric and experiment mean; normalization was accomplished by dividing the difference by the associated experimental standard deviation. To illustrate, the second component J_2 was computed from the describing function gain errors according to:

$$J_2 = \frac{1}{N} \sum_{i=1}^N \left[\frac{G_i - G_i^m}{\sigma_i} \right]^2 \quad (5.2)$$

where G_i is the mean experimental gain at the i th frequency, σ_i is the associated standard deviation, and G_i^m is the corresponding model prediction; for this experiment, N was set to 13 to correspond to the number of test frequencies used. A similar procedure was used for the other components of the matching error vector \underline{J} .

This type of error function provided for a simultaneous matching of the various metrics. The normalization procedure just described, combined with the averaging of (5.1), assured that an error score of unity was obtained whenever model predictions differed, on the average, from experimental measurements by one standard deviation. Thus, the error function also provides some qualitative indication of "goodness-of-fit".

The model matching effort was conducted for each of the three data sets obtained under the three conditions tested in the experimental control phase: a) nominal task; b) diffused display; and c) time delay. No attempt was made to hold particular parameter values constant across conditions; instead, a global search of model parameter values was made for each of the data sets, to arrive at three separate parameter sets, one for each condition. In this way the effect of a stressor could be directly interpreted in terms of its effect on the model parameters.

The optimal control human operator model used in this analysis was essentially that described in chapter 2, with two modifications to account for low-frequency phase trends: a) motor noise was added to control rate, rather than to commanded control as described earlier in chapter 2; and b), the concept of "pseudo motor noise" was introduced to allow a differentiation between the actual motor noise driving the system and the pilot's internal estimate of this noise. A detailed description of this revised model is given by Levison et al (1976). The model was used in a simulation of the tracking task described in the previous chapter, with the loop input disturbance signal power spectral density function given by (4.1). The modelled plant dynamics were those described earlier, and defined by (4.2); the plant dead-time was simulated with a first-order Pade approximation. The model analysis provided performance scores, describing functions, and normalized remnant estimates, in addition to the model matching errors described above.

5.2.2 Analysis Results

Table 5.2 presents the parameter values obtained from the model matching effort, for the three experimental conditions. The last row of the table gives the resulting normalized matching score (computed according to (5.1)), and indicates that the matching errors are not unreasonable, being between 0.5 and 0.7 standard deviations.

An increase in the time delay is one of the primary effects seen with either of the two stressed conditions: the diffused display results in an 11% increase over the nominal condition delay, and the time delay results in a 23% increase. Relevant to the stressor identification problem is the fact that the delay condition results in an increase of 35 milliseconds in operator delay, which corresponds to more than 85% of the simulated 40 millisecond delay used in the actual tracking experiment. The model matching effort has thus effectively identified the time delay stressor.

Table 5.2: Operator Model Parameters for Three Experimental Conditions

Parameter	Dimension	Nominal	Diffused	Delayed
Time delay	sec	0.154	0.171	0.189
Observation noise (position)	dB	-25.0	-24.0	-25.0
Observation noise (rate)	dB	-23.0	-22.0	-23.0
Observation noise (overall)	dB	-27.1	-26.1	-27.1
Motor time constant	sec	0.080	0.080	0.080
Motor noise	dB	*	*	*
Pseudo motor noise	dB	-30	-30	-28
Matching score	-	0.52	0.50	0.67

* negligible

The observation noise/signal ratios show that a best fit is obtained when rate information is considered to be a noisier variable than position information, by a consistent 2 dB across conditions. If this is translated into allocation of attention between the two information channels, then the matching is closest when position is "attended to" 61% of the time and rate is "attended to" 39% of the time. The overall observation noise/signal ratio corresponding to this attention allocation is also shown, and indicates that very low levels are achieved (-26 to -27 dB), indicative of the task difficulty and subject proficiency. Of direct relevance to the stressor identification problem is the fact that the delay condition is characterized by an observation noise/signal ratio identical to that obtained under nominal conditions. In contrast, the diffused condition results in a noise level 1 dB higher, entirely consistent with the intuitive notion that the diffused display introduces visual "noise" into the tracking task. In this sense, the model matching effort has identified the diffused display stressor.

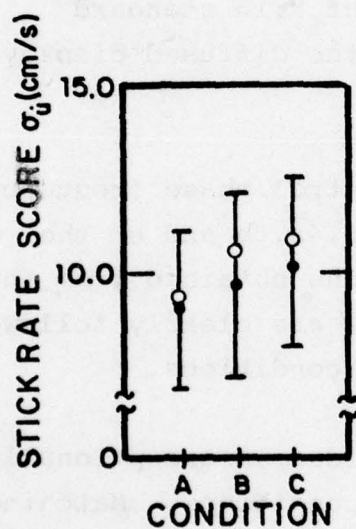
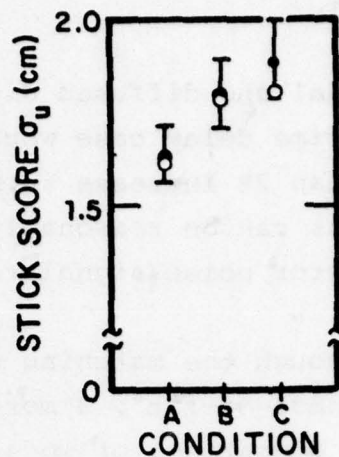
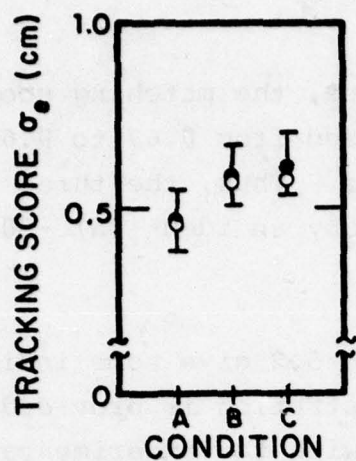
The parameters related to the "motor" functions of the operator model show little or no change with experimental condition, as might be expected from the nature of the stressors. The motor time constant maintains a fixed value of 0.08 seconds across conditions, and the motor noise is best chosen to be negligibly small (-100 dB) for all conditions. The pseudo motor noise parameter was introduced as the result of an earlier model development effort (Levison et al. (1976)), and primarily affects the accuracy with which the low frequency phase data are matched. Although the parameter values shown indicate that the delayed condition is best characterized by a 2 dB increase in the pseudo motor noise/signal ratio, the model matching score is relatively insensitive to a change in this parameter. In fact, if the noise/signal ratio were lowered to the -30 dB level characterizing

the nominal and diffused display conditions, the matching score for the time delay case would only be raised from 0.67 to 0.68, a less than 2% increase in modelling error. Thus, the three conditions can be reasonably well matched by an identical -30 dB pseudo motor noise/signal ratio.

Although the matching scores of table 5.2 give some indication of "goodness-of-fit", a more graphic illustration is provided by a direct comparison of model predictions with the experimental data. Figure 5.6 repeats the control phase performance scores of figure 5.3; the superimposed open circles indicate the model predictions obtained from the matching procedure just described. All of the trends with condition are closely followed, with small matching errors: an average error of 0.13 standard deviation for the nominal case, 0.32 for the diffused display, and 0.57 for the time delay.

Figures 5.7a, b, and c repeat the control phase frequency domain data presented earlier in figures 5.4a, b and c; the smooth curves indicate the model predictions obtained from the matching effort. Again, all of the trends are clearly followed, both with respect to frequency and across conditions.

The figures show that the model provides an exceptionally good fit to the gain data, for all three conditions. Matching errors were an average 0.40 standard deviation for the nominal case, 0.22 for the diffused display, and 0.63 for the time delay. The model duplicated the low- and mid-frequency gain drops seen with the stressed tracking conditions, and also followed the high-frequency shift in the gain data. Although the data are sparse at the highest frequencies, the model indicates a definite trend toward a reduction in the resonant frequency, and an increase



A: NOMINAL
 B: DIFFUSE
 DISPLAY
 C: TIME
 DELAY

GLZ129

Figure 5.6: Comparison of Model and Experimental Performance Scores (model = open circles)

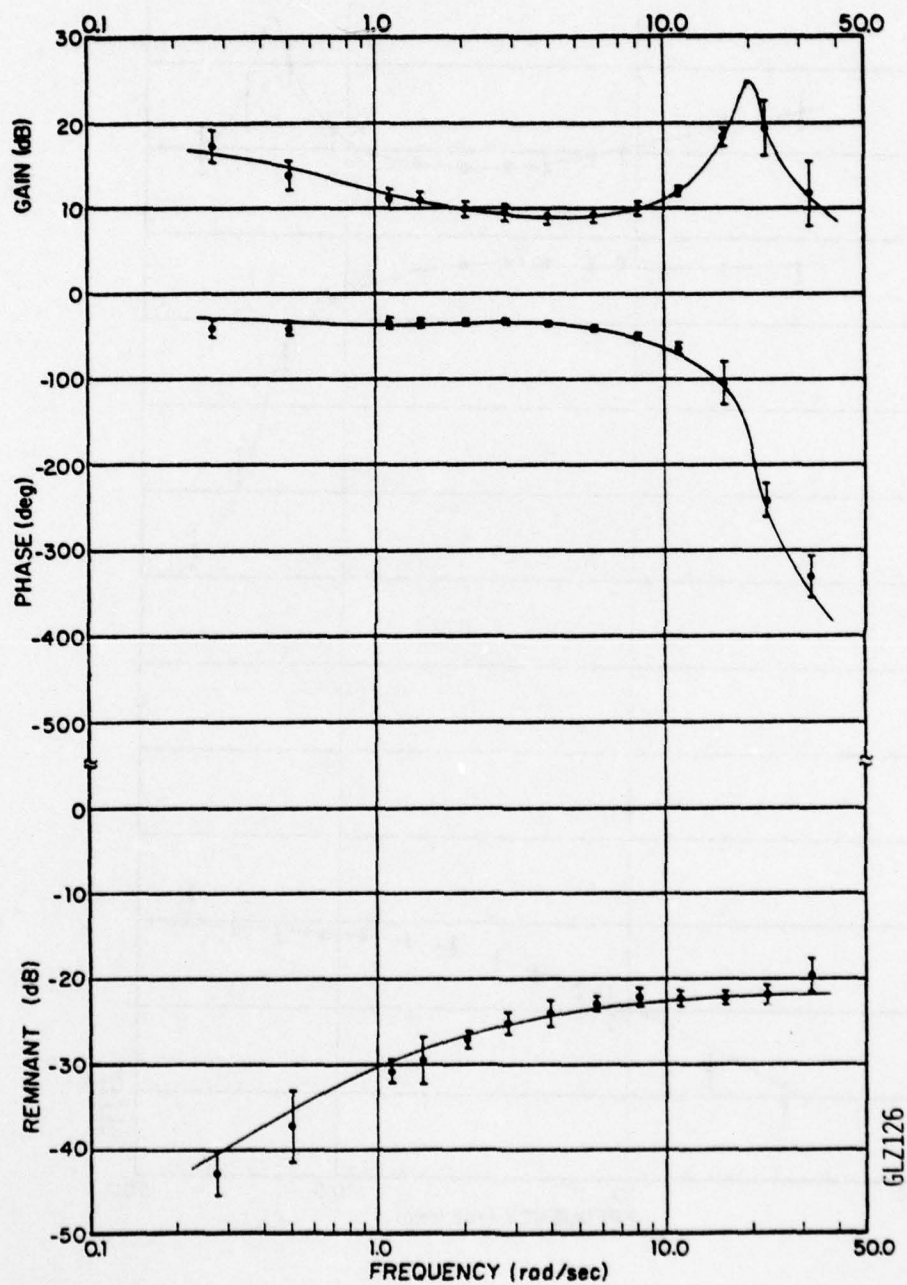


Figure 5.7a: Comparison of Model and Experimental Frequency Measures - Nominal Conditions

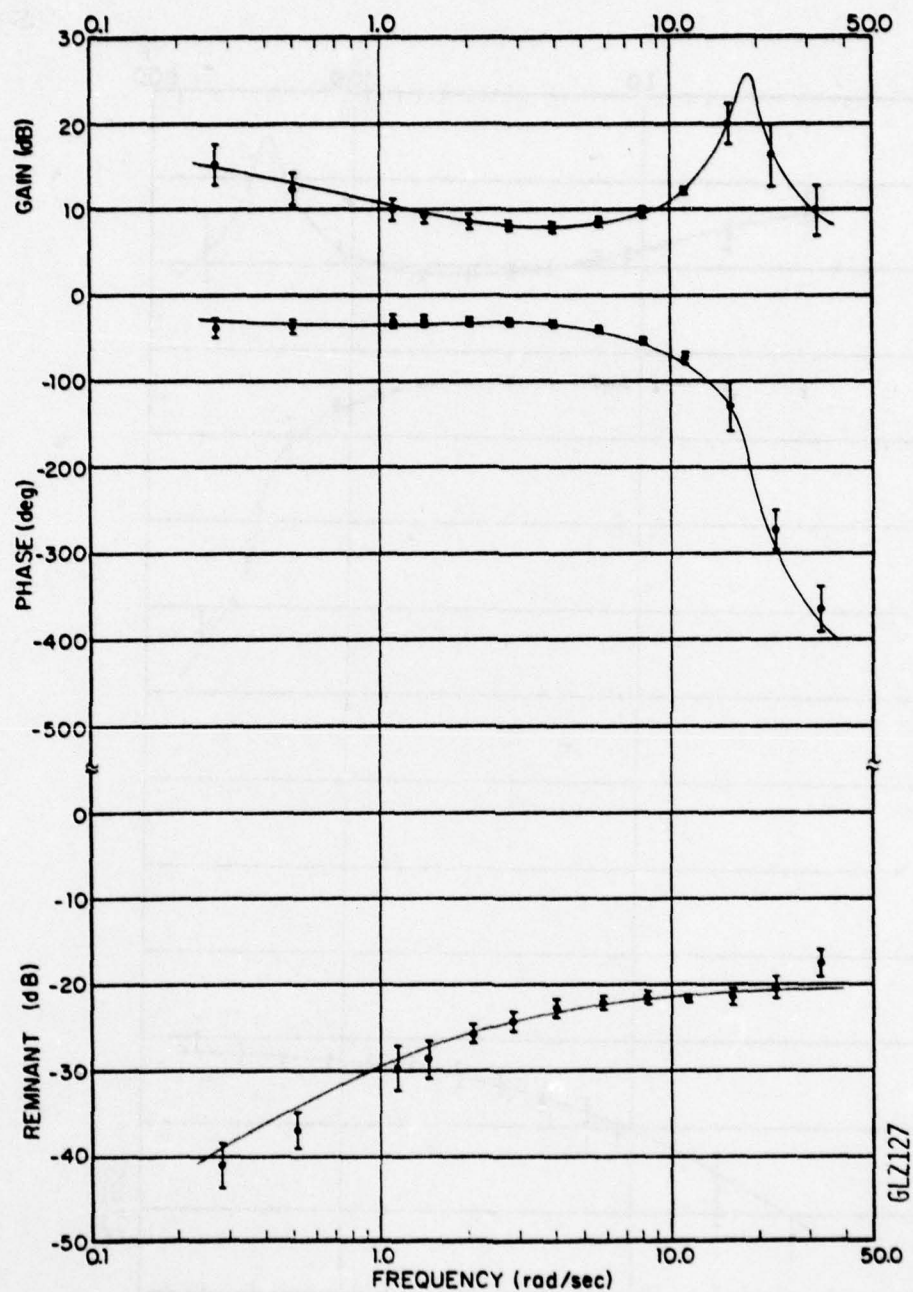


Figure 5.7b: Comparison of Model and Experimental Frequency Measures - Diffused Display Conditions

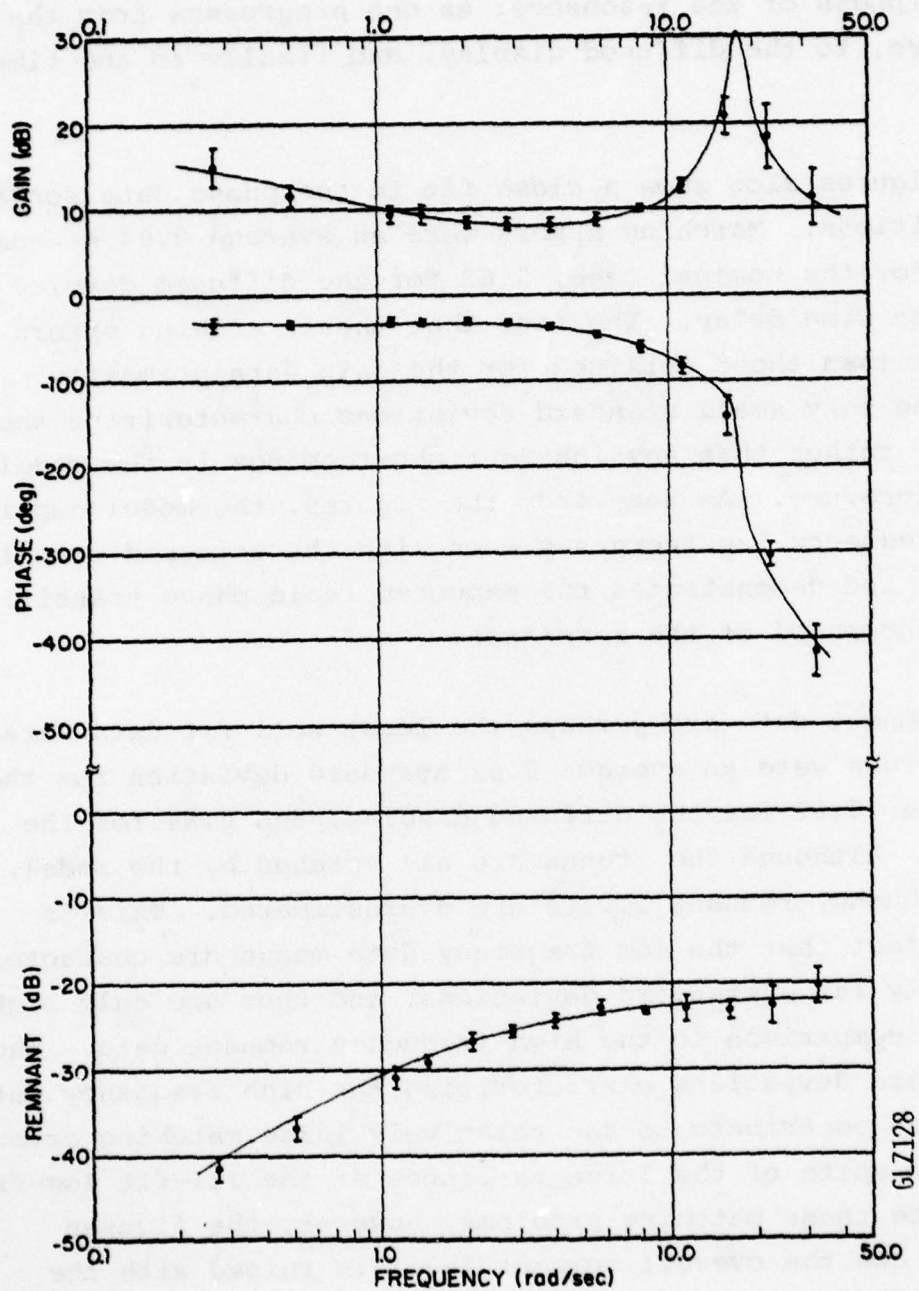


Figure 5.7c: Comparison of Model and Experimental Frequency Measures - Time Delay Conditions

in the sharpness of the resonance, as one progresses from the nominal case, to the diffused display, and finally to the time delay.

The figures also show a close fit to the phase data for all three conditions. Matching errors were an average 0.94 standard deviation for the nominal case, 0.63 for the diffused display and 0.63 for the time delay. The fact that these matching errors were larger than those obtained for the gain data primarily reflects the very small standard deviations characterizing the phase data, rather than any inherent shortcomings in the model matching procedure. As seen from the figures, the model duplicates the high-frequency lag increases seen with the stressed tracking conditions, and demonstrates the expected rapid phase transition in the neighborhood of the resonance.

The remnant data are perhaps the least well fit data sets. Matching errors were an average 0.62 standard deviation for the nominal case, 0.82 for the diffused display, and 0.84 for the time delay. Although the trends are all matched by the model, the low-frequency remnant levels are overestimated. This is due to the fact that the low frequency data means are characterized by relatively large standard deviations, and thus are only lightly weighted in comparison to the high frequency remnant data. The small standard deviations characterizing the high frequency data also serve to contribute to the relatively large matching errors obtained, in spite of the large variances at the ill-fit low-frequency end. Despite these matching problems, however, the figures demonstrate how the overall remnant level is raised with the diffused display condition, while remaining effectively unchanged with the time delay condition. Such behavior is entirely consistent with the earlier observations made concerning the observation noise/signal ratio values obtained from the fitting procedure.

5.2.3 *Discussion of Analysis Results*

The model analysis results demonstrate that a considerable amount of data compression can be achieved by suitably adjusting the human operator model parameters to fit the data. Since each data set consisted of three scores in addition to gain, phase and remnant measurements at 13 frequencies, each data set consisted of 42 means and 42 standard deviations. By using a weighted fitting procedure which takes into account the standard deviations, the human operator model effectively reduced these 84 measurements to 5 specified model parameters, and managed to fit the data within approximately 0.5 standard deviations, on the average. Of course, some accuracy is lost with this less-than-perfect fit, and some information is lost since the model only predicts means and not variances; however, the data reduction is substantial and the model provides a very efficient means of data compression.

More important to the stressor identification effort, however, is the task's demonstrated ability to provide the experimenter with a means of differentiating between stressors. The discussion of the previous section concerned model parameter variations most likely responsible for the observed changes in operator behavior; here, the model analysis provided quantitative support for the conclusions made earlier concerning the effects of the two stressors studied in this program: a diffused display and a time delay.

Reference to table 5.2 shows that the diffused display had two effects: a) a 1.0 dB increase in the operator's overall noise/signal ratio; and b) a 17 msec increase in his time delay. All the other parameters were unchanged from the parameter set associated with nominal tracking conditions. The implication is

that the diffused display not only added "visual" noise to the tracking loop, but also was responsible for increasing the operator's time delay. The first effect is entirely consistent with the characteristics of the diffuser, and thus serves to validate the utility of both the tracking task and the model analysis in identifying stressor characteristics. The second effect, however, was not expected, since an increase in a signal's noise level need not imply a requirement for additional processing time. The model analysis results, however, indicate that additional processing time was indeed associated with the stressor, and that it is inappropriate to assume a one-for-one correspondence between a stressor characteristic (e.g., "noisiness") and a change in a single human operator model parameter (e.g., observation noise/signal ratio).

Table 5.2 also shows that the time delay had two effects on the operator: a) a 35 msec increase in the operator's time delay; and b) a 2 dB increase in his pseudo motor noise/signal ratio. All the other parameters were unchanged from the parameter set associated with nominal tracking conditions. As argued earlier, the 2 dB noise increase is of questionable significance, since it only served to reduce the matching error by less than 2%. Thus, it is not unreasonable to ascribe this apparent increase to the variance of the data, rather than to any significant change in operator behavior. The 35 msec increase in the operator's time delay, however, is sizeable, and corresponds quite closely to the 40 msec delay added to the loop. Since the data analysis procedure associated the loop delay with the operator's response (recall discussion given in section 5.1.3), the delayed tracking condition effectively simulated any tracking stressor which would serve to increase the operator's time delay, without affecting any other aspect of operator behavior. The fact that the model analysis

5

accounted for 35 of the 40 milliseconds, with no call for a readjustment of any other operator parameters, again validates the task's ability in identifying stressor effects.

Because the model fitting procedure is highly non-linear, no variance estimates were available for the derived model parameters. Thus, parameter value confidence intervals could not be generated, and statistical tests of parameter differences between conditions could not be performed. The conclusions made above are thus subject to a more rigorous statistical verification; however, one can argue for their validity based on some of the earlier results presented in this chapter. First, the primary data comparisons made in table 5.1 and figures 5.5a, b, and c show a large number of significant differences between conditions, throughout the range of the many measurements available. Second, these differences do not appear randomly through the data, but rather follow trends which are consistent with particular model parameter changes, as argued in section 5.1.5, and demonstrated numerically in the previous subsection. Thus, it is not unreasonable to expect that the significant differences present in the primary data measurements would be reflected as significant differences between the inferred model parameters, if the model parameter variances were comparable. That they are comparable is supported by the similarity of the primary data spread seen in all three experimental conditions (figures 5.4a, b, and c), and by the comparable fit errors obtained from the model analysis (table 5.2). Thus, although the parameter variances are not available for firm statistical tests of significance, one can make a fair argument for the significance of the observed parameter differences discussed above.

6. CONCLUSIONS AND RECOMMENDATIONS FOR FUTURE DEVELOPMENT

6.1 Conclusions

The principal results of this study may be summarized as follows:

1. Pre-experimental analysis using the optimal control model of the human operator provides a rapid means of tracking task design, and allows the experimenter to investigate the effects of various task structures and parameter choices without the need for an extensive experimental pilot study.
2. The use of an unstable controlled element provides the desired task sensitivity to environmental stress, and the incorporation of a sum-of-sines disturbance signal allows for the calculation of important operator frequency domain measures required for the interpretation of stressor effects. The combination of an instability with a disturbance signal ensures task sensitivity and stressor identifiability.
3. The minicomputer-based Performance Analyzer developed to implement the tracking task provides the experimenter with a simplified means for defining the task parameters, automated calibration of the interface hardware, real-time control of the tracking experiment, storage of the tracking time histories, and post-experimental analysis of tracking performance.

4. Subjects learn the basic tracking task relatively rapidly, and in 15 tracking runs are relatively close to their final asymptotic scores. After learning the basic task, subjects require on the order of 5 additional runs to reach approximate asymptotic performance under the stressed conditions.
5. The task demonstrates sensitivity to both stressors used in this study: a display diffuser which degraded the target image, and a 40 millisecond dead-time which adds a delay to the operator's response. Tracking scores under both stressed conditions are significantly higher than that obtained without the stressors, thus validating the sensitivity of the task.
6. The describing function and remnant measures obtained from the tracking data show significant differences between experimental conditions, and verify the trends predicted by the pre-experimental model simulations. A direct comparison between the data and the model simulations shows that the diffuse display acts to increase the operator's observation noise/signal ratio; in contrast, the dead-time acts to increase the operator's time delay. Thus, the task demonstrates a differential sensitivity to the two stressors, and the various measures provided by the Performance Analyzer serve to isolate the particular qualities of the stressor.

7. The results of the quantitative model analysis validate the qualitative conclusions regarding stress effects, based on predicted operator trends. A best fit to the diffused display tracking data was obtained by a 1.0 dB higher than nominal observation noise/signal ratio, and a 17 millisecond longer than nominal operator time delay. These results are consistent with a "noisy" visual image generated by the diffuse display. The dead-time tracking data was best fit with a 35 millisecond longer than nominal operator time delay, again an effect consistent with the quality of the stressor. This quantitative analysis again confirms the task's capability for differentiating between stressors.

6.2 Recommendations for Future Development

The principal recommendations for future development are as follows:

1. The capabilities of the Performance Analyzer should be extended to include testing of multi-axis single-display tracking behavior. This would allow for the simulation of a more realistic display of the target and provide the operator with the additional visual cues which typify aircraft tracking situations. Due to its modular design, the extension of the Performance Analyzer capabilities would involve a straight-forward programming effort; it is anticipated that the primary development would be devoted to display generation.

2. To further simplify operation of the Performance Analyzer, development should proceed on a "hardwired" version having a fewer number of user options, and with less user input required for specification of the task parameters. A microprocessor-based instrument could be directly developed from a simplified version of the current software, thus minimizing the amount of software development. By integrating the real-time hardware (clock, A-to-D converter, D-to-A converter) with the analog interface hardware (control stick and display), a self-contained microprocessor-based instrument could be developed to provide all of the important capabilities currently available from the Performance Analyzer. By reducing the number of task specification options, a smaller software development effort would be needed, and the completed instrument would provide for a minimum of operational demands placed on the user.
3. Development should proceed on a method for rapid automated identification of human operator model parameters. Since parameter identification allows for a substantial reduction in the amount of data needed to characterize operator behavior, a capability for the rapid analysis of individual tracking runs would be highly desirable. Parameter changes between single runs could be used directly in identifying stressor effects on individual runs. Individual run processing would also allow for the generation of model parameter statistics, a capability

AD-A070 632

BOLT BERANEK AND NEWMAN INC CAMBRIDGE MASS
A PERFORMANCE ANALYZER FOR IDENTIFYING CHANGES IN HUMAN OPERATO--ETC(U)
MAR 79 G L ZACHARIAS, W H LEVISON

F33615-77-C-0522

UNCLASSIFIED

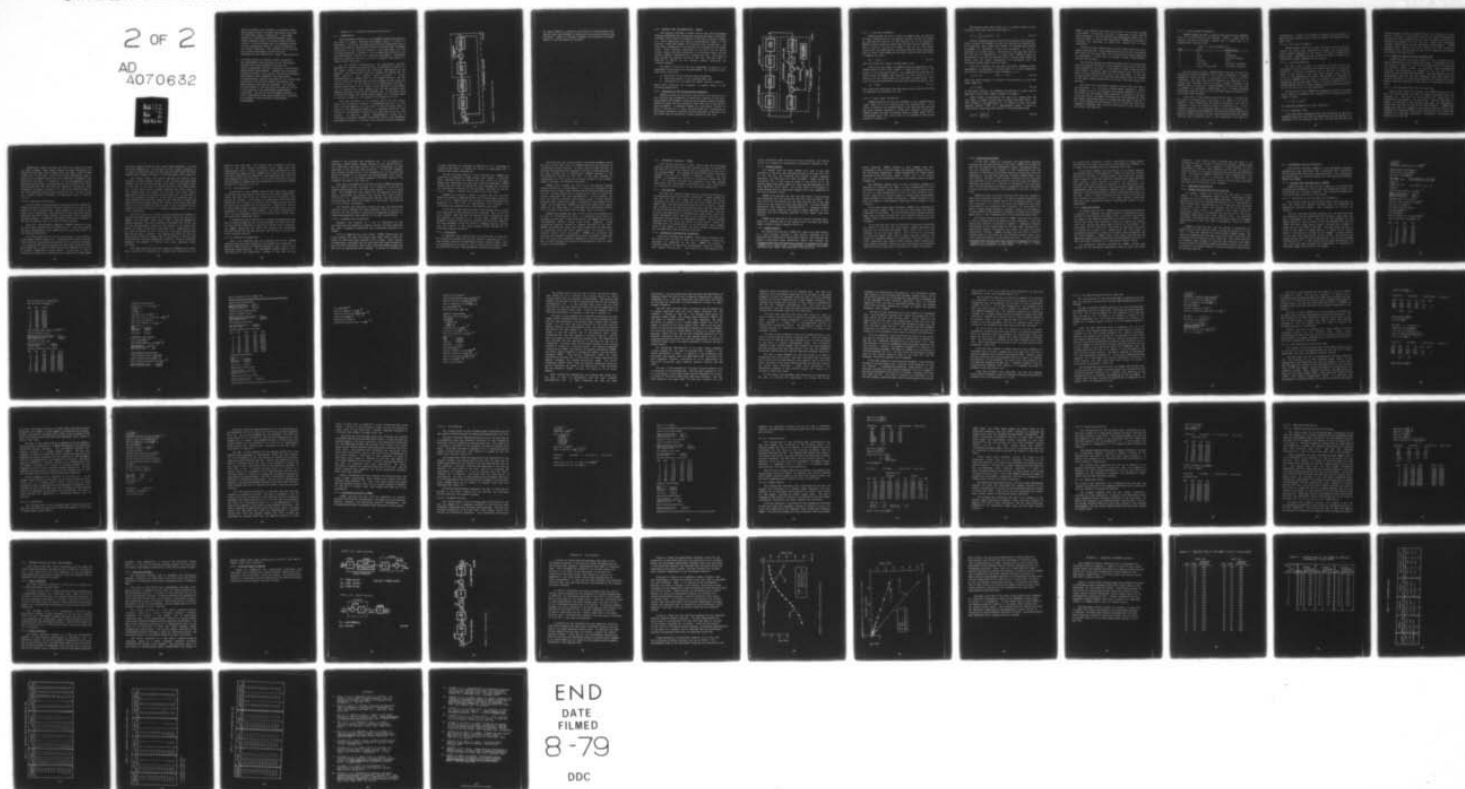
BBN-3910

AMRL-TR-79-17

NL

2 OF 2

AD
A070632



which is likely to be required in situations where the stressor effects are small and within the range of individual subject differences. Since model analysis is currently conducted manually using a direct parameter search to minimize model matching errors, it is anticipated that an automated identification capability would be a direct extension of the current technique. This approach would minimize the software development effort and take advantage of past experience in model identification.

4. An effort should be directed toward correlating the measurements made available by the Performance Analyzer with other measures obtained from typical laboratory tracking situations, in particular, physiological measurements. Because the Performance Analyzer provides a rich array of tracking performance measurements which complement the large array of physiological indicies available to the investigator, significant correlations between performance and physiological state may be uncovered. The failure of such efforts in the past may have been due solely to the paucity of the performance measurements considered. The use of the Performance Analyzer in such a correlative study could remedy this situation, by providing a wide spectrum of performance measurements.

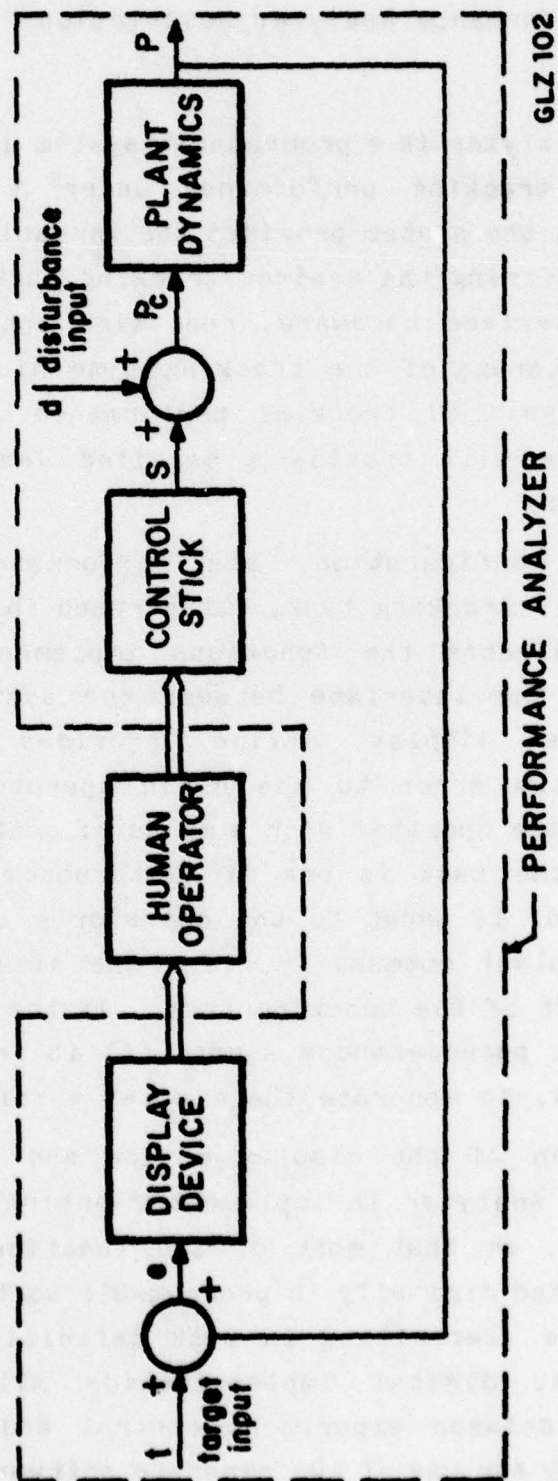
Appendix A: Performance Analyzer Description

A.1. INTRODUCTION

The Performance Analyzer is a programable system developed for the study of manual tracking performance under a variety of conditions. Currently, the system provides the investigator with a simplified means for defining the desired tracking task, automated calibration of the interface hardware, real-time control of the tracking experiment, storage of the tracking time histories, and post-experimental analysis of tracking performance. Subsequent sections presented here will provide a detailed description of these various functions.

In its present configuration, the Performance Analyzer implements a single-axis tracking task, illustrated in figure A.1. The dashed region indicates the functions implemented by the Analyzer, and defines the interface between the system and the human operator. The display device provides a visual representation of system error to the human operator, and the control stick provides the operator with a means of controlling the displayed error. If the task is one of disturbance nulling, a pseudo-random signal (d) is added to the operator's stick signal (s), to generate the plant command (p_c) for the simulated plant dynamics defined as part of the tracking task. If the task is one of target tracking, the pseudo-random signal (t) is instead added to the plant signal (p), to generate the display error (e).

With the exclusion of the display device and the control stick, the Performance Analyzer is implemented entirely on a DEC PDP-11/34 minicomputer, so that most of the functions shown in figure A.1 are implemented digitally in programable software. This allows for considerable flexibility in task definition and loop control. In addition, digital implementation allows for a convenient separation between experiment control and subsequent performance analysis, by the use of two separate software packages:



GLZ 102

PERFORMANCE ANALYZER

Figure A.1: Single-Axis Tracking Loop

A.2. TRACKING TASK IMPLEMENTATION: OCMRUN

This section provides a closer look at how the Performance Analyzer implements the closed-loop tracking task just illustrated. A slightly more detailed breakdown of the loop is given in figure A.2, which emphasizes the hybrid analog/digital nature of the Analyzer (digitized signals are indicated with an asterisk). The three major components of the Analyzer are indicated by the dashed lines: input interface consisting of the stick and an analog filter; output interface consisting of the display scope; and the digital computer responsible for closing the loop. This section will discuss the digital portion of the loop, and the reader is referred to section A.5 for further details concerning the interface modules.

The digital portion of the loop diagrammed in figure A.2 is implemented by the use of the program OCMRUN. The program provides three major functions:

- a) definition of the tracking task parameters;
- b) real-time control of the tracking task; and
- c) calibration of the input and output interface modules.

These three functions are discussed in greater detail in the following subsections.

A.2.1 Definition of the Tracking Task Parameters

OCMRUN provides an interactive facility for the definition of the tracking task parameters of particular interest to the user. Using appropriate prompts, branching and parameter legality checks, OCMRUN can guide the user through a rapid "set-up" of the desired task parameters. A detailed example of a particular "set-up" is given in section A.4.1. Here, the discussion will concentrate on the general parameter selection options available to the user, and the checks made on particular values selected by the user.

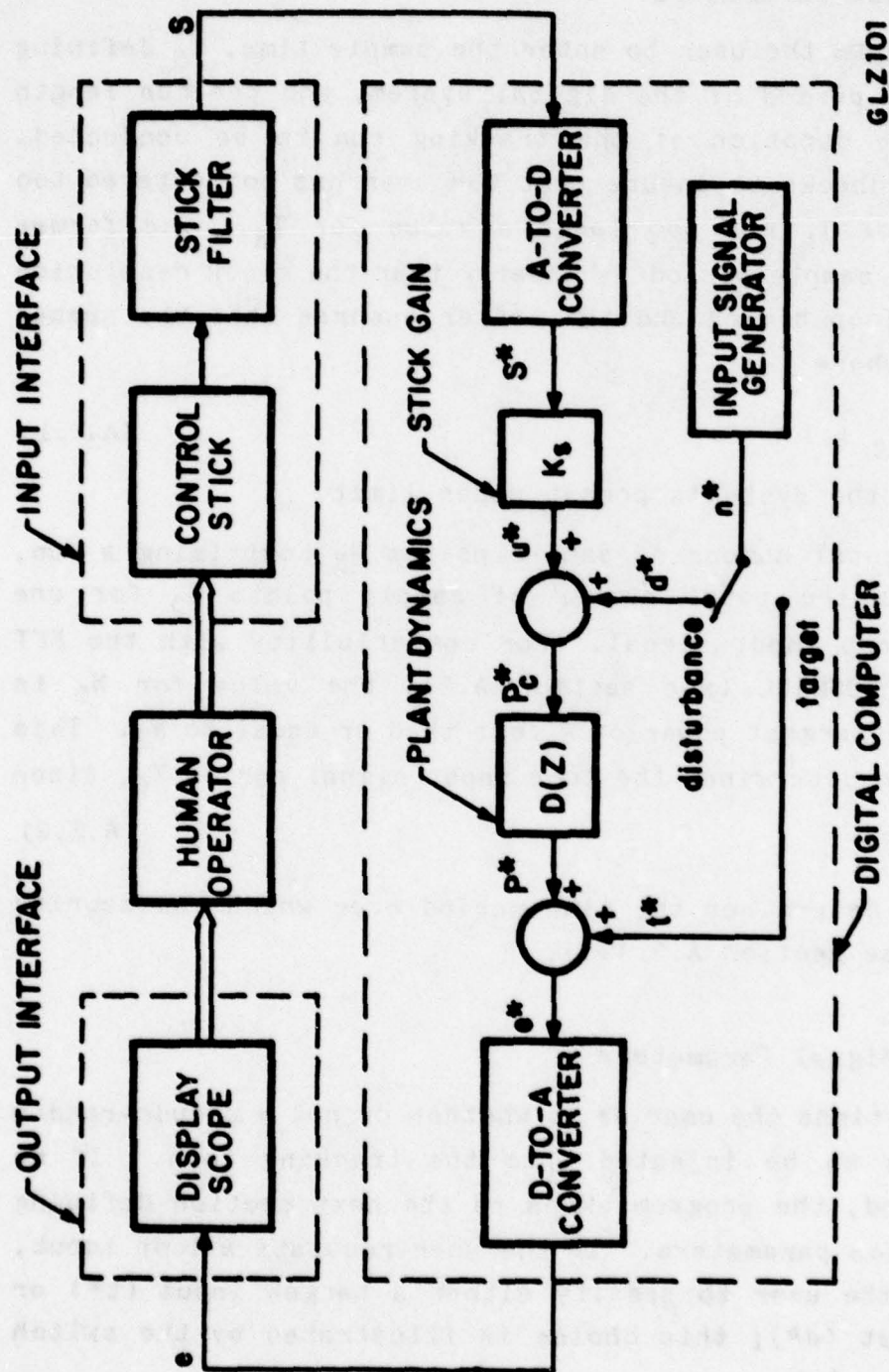


Figure A.2: Single-Axis Tracking Loop: System Breakdown

A.2.1.1 Time Base Parameters

OCMRUN prompts the user to enter the sample time, T_S defining the basic sample period of the digital system, and the run length T_R , defining the duration of the tracking run to be conducted. OCMRUN provides checks to ensure that the user has not entered too small a value for T_S nor too large a value for T_R . The former ensures that the sample period is greater than the clock resolution used for basic loop timing and the latter ensures that the number of samples N_S , where

$$N_S = T_R/T_S + 1 \quad (\text{A.2.1})$$

does not exceed the system's preset upper limit.

Given the total number of sample points N_S comprising a run, OCMRUN specifies the total number of sample points N_0 for one period of the loop input signal. For compatibility with the FFT routine used by OCMANL (see section A.3), the value for N_0 is chosen to be the largest power of 2 less than or equal to N_S . This value for N_0 then determines the loop input signal period T_0 , since

$$T_0 = N_0 T_S \quad (\text{A.2.2})$$

This value also determines the time period over which run scoring is conducted (see section A.2.1.5).

A.2.1.2 Input Signal Parameters

OCMRUN questions the user as to whether or not a pseudo-random input signal is to be injected into the tracking loop. If no signal is desired, the program skips to the next section defining the plant dynamics parameters. If the user requests a loop input, OCMRUN prompts the user to specify either a target input (t^*) or disturbance input (d^*); this choice is illustrated by the switch setting of figure A.2.

The pseudo-random input signal n^* is a digital version of the following continuous sum-of-sines signal n :

$$n(t) = \sum_{j=1}^N A_j \sin(\omega_j t + \phi_j) \quad (\text{A.2.3})$$

Several parameters must be specified to define this function. After a prompt from OCMRUN, the user can request the "nominal" set of frequencies, which means that OCMRUN will automatically define the number of components N and each frequency ω_j ($j=1, N$), according to a preset table. Alternatively, the user can type in his own set of frequencies; in this case, OCMRUN allows for corrections to be made during data entry, and provides checks to ensure that the chosen frequencies are consistent with the previously chosen sample and run times.

Once the frequency set has been specified, OCMRUN provides adjustments, as necessary, to ensure that all of the frequencies are integral multiples of a base frequency ω_0 , or

$$\omega_j = h_j \omega_0 \quad (j=1, \dots, N) \quad (\text{A.2.4})$$

where the base frequency is related to the period T_0 of the loop input signal by:

$$\omega_0 = 2\pi/T_0 \quad (\text{A.2.5})$$

At the user's option, the harmonic multipliers h_j above can be specified to be either simple integers or primes.

Under normal circumstances, the user will request that the loop input n consist of more than a single sine wave ($N>1$). In this situation, the amplitudes A_j are chosen so that the power spectral density (PSD) of n approximates either a first or second-order continuous PSD function of the following form:

$$\phi_{nn}(\omega) = \left(\frac{K}{a^2 + \omega^2} \right)^\lambda \quad (\text{A.2.6})$$

where λ is chosen by the user to be either 1 or 2, after a prompt from OCMRUN. In addition, the user is requested to enter the PSD break frequency a and the desired root-mean-square (RMS) value of the loop input n . Given these parameters, OCMRUN then proceeds to calculate the individual A_j which will satisfy all of these conditions.

Should the user request that the loop input consist of only a single sinusoid ($N=1$), then OCMRUN prompts the user for the desired RMS value for the loop input, and calculates the single amplitude A , accordingly. In this case, no attempt is made to approximate a desired PSD function.

The relation between the specified RMS value of the loop input and the resultant RMS display error depends on the type of tracking task requested by the user. If the task is target tracking and no stick signal is present, then the RMS display error (in cm) will equal the user-specified RMS value of the loop input. If the task is disturbance nulling, the resultant RMS display error will depend on the plant dynamics specified by the user (see next section for options).

The final set of parameters needed to define the loop input n are the phases ϕ_j . By using a random number generator, values are chosen so as to be uniformly distributed between 0 and 2π . The "seed" for the random number generator is chosen on the basis of the particular run number associated with the upcoming run, thus providing a consistent means of randomizing the phases from run to run. This ensures that the subject will not "learn" the input over a number of repeated runs, since the time history of the loop input will differ for each run.

A.2.1.3 Plant Dynamics Parameters

OCMRUN prompts the user to specify the type of plant dynamics $P(s)$ to be controlled by the subject. Table 1 lists the six options currently available, ranging from a simple gain to a second-order low-pass filter.

Table 1: Plant Dynamics $P(s)$

Type	$P(s)$	description
1	K	gain
2	K/s	integrator
3	K/s^2	double integrator
4	$K/(s+a)$	lag
5	$K/s (s+a)$	lag plus integrator
6	$K\omega_n^2/(s^2+2\xi_n\omega_n s+\omega_n^2)$	2nd order low-pass

Once the type is chosen, OCMRUN prompts the user to enter the appropriate plant parameters. For a gain, integrator, or double integrator, only the gain is required; for a lag or lag plus integrator, the gain and break frequency are required; for a second-order low-pass filter, the gain, natural frequency, and damping ratio are required. These parameter values are later used by OCMRUN to calculate coefficients for a general-purpose difference equation used for the real-time digital simulation of the chosen plant dynamics.

In addition to the dynamics specified in table 1, the user has the option of specifying a dead-time to be added to the plant dynamics. After specifying the dynamic parameters, the user is prompted to enter the desired amount of dead-time, T_D . A zero response results in no dead-time added to the plant dynamics. A non-zero response causes OCMRUN to recalculate the dead-time as the nearest integer multiple of half the previously-specified sample time T_S ; this calculated value is then displayed to the user for

confirmation. A check is also made to ensure that the number of dead-time wait counts, T_D/T_S , does not exceed the system's preset upper limit.

A.2.1.4 Stick Gain Parameter

OCMRUN prompts the user to enter the stick gain K_S , used to convert the stick value, expressed in pounds, to an equivalent plant command, expressed in cm, cm/sec, or cm/sec², depending on plant order. Adjusting this gain allows the user to adjust stick sensitivity without changing the plant gain.

A.2.1.5 Scoring Parameters

For each loop variable of interest, tracking scores are calculated to yield estimates of the mean, RMS value, and standard deviation. Scoring is conducted over an interval of length T_0 , equal to the period of the loop input signal (recall section A.2.1.2), and commences at a time T_I during the run. Normally, T_I is set by OCMRUN, but the user is provided the opportunity of specifying the scoring start time; if the user chooses to do so, OCMRUN ensures that T_I is small enough so that the scoring interval T_0 will be over prior to run termination.

At the end of a run, OCMRUN also computes the overall tracking score, based on a weighted sum of display error variance and stick signal variance:

$$J = (\sigma_e^2 + W \sigma_u^2)^{1/2} \quad (\text{A.2.7})$$

The weighting parameter W is user specified.

A.2.1.6 Parameter Files

Once the above parameters have been specified by the user, OCMRUN provides the user with the opportunity of storing them in a parameter file, for possible later use. In this way the user can

create several different parameter files for different tracking tasks of interest. By doing this prior to the actual tracking run, the user can then minimize "set-up" time by simply reading in the appropriate parameter file at run time, rather than proceeding through a specification of each individual task parameter. OCMRUN supports both reading from and writing into user specified parameter files, and provides the user with the appropriate prompts for guidance during file I/O.

A.2.2 Real-Time Control of the Tracking Task

OCMRUN provides real-time control of the tracking task by proper sequencing of the computations needed to implement the loop illustrated in figure A.2, and by the timing facility afforded by the system's digital clock. In addition, some housekeeping functions are maintained by OCMRUN, to aid the user in run identification and data file labelling. Detailed examples of these housekeeping functions and the subsequent real-time output are given in section A.4.1; here, the discussion will concentrate on the general features available to the user for conducting a tracking task.

A.2.2.1 Run Identification and File Labelling

Prior to the start of an actual run, OCMRUN displays to the user the current date and the run number associated with the upcoming run. The user is then provided the opportunity of changing the run number, if he so desires. Both the data and run number, in addition to the current clock time, are subsequently stored with the data, to aid in run identification. OCMRUN then prompts the user for comments to be stored with the data of the upcoming run; these partially fulfill the function of a laboratory notebook in providing additional information concerning the particulars of the run.

OCMRUN then prompts the user for a disc file name to be used for data storage. Some simple checks are made concerning the legality of the name, and if found valid, the name is used to open a data file on the disc. This file is then immediately used to store the run identification and file labelling information just entered by the user. In addition, all of the parameter values defining the particular tracking task are also saved in the file. This provides the user with the later option of listing all those parameters discussed in section A.2.1, for a firm identification of the task parameters used during a particular run. It also allows for a simple restart procedure, as described later in section A.2.2.4.

A.2.2.2 Real-Time Task Control

Once the above file maintenance functions have been completed, OCMRUN proceeds to initialize various routines to be used in the conduct of the tracking task. This results in a zeroing of the plant initial conditions, initialization of the loop input signal generator and data filing routine, and zeroing of the cumulative scoring counters. In addition, the output D-to-A line is zeroed to provide the subject with an initially zeroed display.

With this initialization completed, OCMRUN prompts the user for the proper terminal entry to begin the run. This entry begins the basic computational loop responsible for real-time control of the tracking experiment.

The loop begins with an A-to-D conversion of the subject's stick signal (recall figure A.2). Using the scale factors obtained from an earlier calibration (see section A.2.3), the stick voltage, s , is converted to units of pounds force and then, using the stick gain factor K_s , to units of equivalent plant command (cm, cm/sec, or cm/sec², depending on plant order). If the task is one of disturbance nulling, this equivalent stick signal u^* is then summed

with the signal d^* from the loop input signal generator, to yield the plant command p_c^* . If the task is one of target tracking, or if user has specified that no loop input be used, then the plant command p_c^* is simply set equal to the equivalent stick signal u^* .

The digital filter $D(z)$ which simulates the desired plant dynamics is then updated, based on the current and past plant commands, and the current and past plant state. The updated state is then used to calculate an updated version of the plant output p^* . If the task is one of target tracking, the plant output is then summed with the signal t^* from the loop input signal generator, to yield the display error signal e^* . If the task is one of disturbance nulling, or if the user has specified that no loop input be used, then the display error signal e^* is simply set equal to the plant output signal p^* . Using a scale factor obtained from an earlier calibration (see section A.2.3), the display error signal e^* is then converted to a display voltage signal, e , via a D-to-A conversion.

Once the display error signal has been generated by OCMRUN, no further real-time operations are necessary until the next stick sample is to be made. This "wait" time is used by OCMRUN for several purposes. The loop variables of interest (n^* , s^* , p^* , and e^*) are appropriately scaled and then stored in an output data buffer for later filing on the disc data file. Cumulative scores for these variables are also calculated, to maintain running sums and running sums of squares. The appropriate value for the loop input signal at the next sample time is calculated, in anticipation of its use over the next computation interval. Finally, the plant dynamics are updated to reflect the newly generated state variables.

Once these functions have been completed, OCMRUN enters a wait loop, periodically checking the elapsed time indicated by the

system's real time clock. The elapsed time is measured from the time of the last A-to-D conversion which began the loop computations; once it reaches a pre-set value determined by the user-specified sample period, OCMRUN exits from its wait loop and initiates another A-to-D conversion, thus restarting the real-time loop computations just described. This looping continues until the desired number of samples have been obtained, at which point OCMRUN proceeds to "close-out" the run.

A.2.2.3 Run Termination

At the end of a run, OCMRUN stops the real-time clock, outputs to the disc any tracking data left over in the output data buffer, closes the disc data file, and zeroes the D-to-A channel, thus zeroing the display. In addition, the cumulative scores obtained during the run are used to calculate the tracking scores for the pertinent loop variables (n^* , s^* , p^* and e^*). These scores consist of each signal's mean, standard deviation, and RMS value, and are displayed to the user via the terminal. The total tracking error score is also displayed, based on the display score, stick score, and stick score weighting factor.

A summary printout of any stick or display overloads which may have occurred during the run is also provided, to notify the user of over-voltage conditions at the A-to D and/or D-to-A converter. The summary specifies, for stick and display, the percentage overload during the scoring interval, and the point at which the first overload occurred.

A.2.2.4 Multiple Tracking Runs

With a run completed and the tracking data filed, OCMRUN questions the user as to whether or not another run is desired. A negative answer results in program termination and a return to the operating system monitor. An affirmative answer results in a continuation of the program and a prompt to the user for any

changes in the tracking task parameter set. If no changes are requested, OCMRUN begins another sequence of run identification, file labelling, real-time control, and run termination, as just described in the previous three sections. If the user requests that changes be made prior to the upcoming run, he is given the option of reading in an entirely new data/parameter file (recall section A.2.1.6), or of simply changing individual values of the parameter set used in the last run.

Once the new parameter set has been defined, OCMRUN increments the run number by one, and uses it to generate a new set of pseudo-random phases for the loop input signal, if one is being used. This changes the time history of the upcoming loop input signal, preventing the subject from learning the input (recall section A.2.1.3). OCMRUN also provides the user with the option of recalibrating the stick and display at this point (see section A.2.3 for further discussion).

The options just mentioned provide the user with sufficient flexibility for changing the task parameters from run to run, if desired, and yet provide a relatively streamlined procedure for conducting sequential replications of the same tracking task.

A.2.2.5 Premature Run Termination

Normally, the duration of a run is determined by the user-specified run length T_R ; however, certain run-time conditions can cause a premature termination and a shortened effective run length.

Prior to sampling the stick signal, OCMRUN checks that the A-to-D buffer has been previously read from, before using the buffer to store the newly sampled stick voltage. Under unusual circumstances, the buffer may not have been read from following an earlier A-to-D conversion, and in this situation OCMRUN prompts the user with an appropriate error message. A normal run termination

is then initiated, as described in section A.2.2.3, resulting in tracking data which is saved, but which is associated with a shorter than normal tracking run.

During real-time control of the tracking run, OCMRUN also checks for an abnormally large display error signal, a condition which indicates that the subject has lost control of the task. Rather than continuing the task under these circumstances, OCMRUN prompts the user with an appropriate error message and initiates run termination according to the procedure described in section A.2.2.3. Again, a shorter than normal run is the result.

OCMRUN also provides a check to ensure that the real-time signal processing is completed within the allotted sample interval. If it is not, OCMRUN avoids the problem of desynchronization by prompting the user with an appropriate error message, and initiating run termination as in the previous two cases.

In the three cases just described, the tracking data is saved up to the point of the detected error condition. This is not the case, however, when the user initiates an early termination from the terminal, by typing in a \hat{C} . In this case, neither the task parameter values nor the data are saved on the disc file; however, the task parameter values are saved in computer memory, and the user can restart a run using normal system procedures for restarting program execution.

A.2.3 Calibration

To implement the tracking loop, provisions must be made for the conversion between the internal digital representation of a loop variable and the corresponding external analog voltage. This is accomplished by the use of a set of scale factors whose values are specified during a semi-automated calibration procedure.

Following the user specification of the task parameter values and prior to the start of a run, OCMRUN checks for the presence of a valid set of scale factors. If such a set is found, the user is provided the opportunity to generate a new set by recalibrating; if the user decides not to recalibrate, OCMRUN proceeds to the initialization portion of the run. If the user decides to recalibrate, or if a valid set of scale factors is not present, OCMRUN initiates a calibration procedure.

OCMRUN first prompts the user as to the desired maximum display deflection, in centimeters. To take full advantage of the maximum D-to-A voltage range, OCMRUN then provides minimum, maximum and zero voltage signals while prompting the user to adjust the display scope gain and zero appropriately. In this manner, the user can quickly calibrate the display scope, so that desired maximum display deflection range corresponds to the maximum D-to-A range. At the same time, OCMRUN calculates the output scale factor which will be used later in converting from the digital display error (in cm) to the proper D-to-A signal level (in volts).

OCMRUN also prompts the user for two stick force setpoints to be used in calibrating the stick. A calibrated stick force is provided by the user in both directions, and OCMRUN obtains two corresponding digital values from A-to-D sampling. Using calibrating setpoint values (in pounds) provided by the user, OCMRUN calculates the input scale factor which will be used later in converting from the stick signal level (in volts) to the internal digital value (in pounds). OCMRUN also calculates and displays the maximum allowable stick force in pounds, along with the stick bias due to possible asymmetry in the set-points. The user is then provided the option of recalibrating if any of these values are unacceptable.

A.3. PERFORMANCE ANALYSIS: OCMANL

This section provides a closer look at how the Performance Analyzer analyzes the stored data obtained during a tracking run. The analysis is entirely digital and is implemented by the use of the program OCMANL. The program provides several major functions, ranging from data file reading to spectral analysis, and like OCMRUN, is programmed to provide an interactive dialog with the user. The analysis functions are organized into eight program units which are individually selectable by the user; these units are discussed in more detail in the following subsections.

A.3.1 File Reading

The user will normally begin the data analysis by reading in the appropriate data file from the system disc. OCMANL prompts the user for the data file name, and after reading the header information on the file, prints out the file's name and the run number, date, and time associated with the file's creation. OCMANL then displays to the user the starting point used for generating the scores during real-time control of the tracking task. The user is given the opportunity of changing this start point, since this point determines which portion of the tracking histories will constitute the data base for subsequent analysis. Finally, OCMANL questions the user as to his choice of stick units: either the recorded units of pounds force, or the equivalent plant command units of cm, cm/sec, or cm/sec², the latter being calculated from the recorded units and the stored stick gain.

A.3.2 Listing of Tracking Task Parameters

Since the tracking task parameter values used to define a run are stored with the data of that run, the parameter values are available for inspection by the user. OCMANL can provide a formatted labelled listing of all the parameter values of interest, upon request from the user. This serves as a cross-check of the

actual conditions under which the run was conducted, and thereby serves as a backup to a conventional laboratory notebook or log.

A.3.3 Tracking Scores

On request from the user, OCMANL will read in the time histories of the four loop variables stored on the data file (n^* , s^* , p^* , and e^*), and calculate and display a mean, standard deviation, and RMS value for each variable. These scores are calculated over a time interval equal to the period T_0 of the pseudo-random loop input signal n^* , with scoring beginning at the user specified start point. The stick score is calculated in either pounds force or equivalent display units (cm), depending on the user's earlier choice.

OCMANL also provides the user with the option of calculating and displaying the rate scores for the four loop variables. The rate scores are calculated over the same interval and in the same units as are the position scores just described. To avoid problems associated with numerical differentiation, a frequency domain approach is used, based on the signal's power spectrum, in turn obtained from the frequency spectrum of that signal (see next section).

OCMANL also displays to the user the overall tracking score, based on a weighted sum of the display error variance and stick signal variance (recall equation (A.2.7)).

A.3.4 Signal Spectra

On request from the user, OCMANL will read in the time history of a loop variable, perform a fast Fourier transform on the digitized data contained in the scoring interval, and calculate the signal's associated power spectrum.* Rather than display the

* Assuming this has not been done earlier in response to a user request for a rate score or describing function calculation involving that signal (see sections A.3.3 and A.3.5)

entire spectrum, OCMANL displays a more compact data set, consisting of the correlated power and estimated remnant power at the correlated frequencies. These frequencies are simply those contained in the loop input signal (recall the ω_j of section A.2.1.2). The correlated power is thus the signal's power at these frequencies.

The estimated remnant power at each correlated frequency is obtained by averaging the power in the neighborhood of each correlated frequency, taking care to exclude any correlated power. The size of this neighborhood is set at a fixed fraction of an octave, resulting in a greater number of remnant power measurements being averaged at the higher frequencies. OCMANL displays to the user the number of measurements comprising each average at each frequency.

Using these signal power estimates, OCMANL also estimates the power spectral density (PSD) of both the correlated and remnant components of the signal. This facilitates direct comparisons with human operator model predictions, since models typically utilize remnant sources characterized by PSD's which are continuous with frequency.

To provide the user with an indication of how well-correlated the signal is with the loop input signal, OCMANL calculates and displays the correlated-to-remnant power ratio (C/R), for each frequency in the loop input signal. This C/R ratio is calculated for both the signal power and its power spectral density, the former for assessing degree of correlation, and the latter for direct comparison with typical human operator model predictions. Total power and power ratios are also calculated and displayed; these provide the user with an indication of signal coherence.

A.3.5 Describing Functions

If the user wishes to calculate the describing function relating any one loop variable to any other, OCMANL will prompt the user for the appropriate alphanumeric symbol identifying each of the two variables. One symbol is then associated with the numerator of the desired describing function and the other with the denominator. For each such specified variable, OCMANL reads in its time history, performs a fast Fourier transform on the digitized data contained in the scoring interval and calculates the signal's amplitude and phase as a function of frequency.* The amplitude ratio (in dB) and phase difference (in degrees) are then calculated at each loop input frequency, and displayed to the user in tabular form.

OCMANL provides two other functions when the user requests a describing function calculation. To ensure a smooth progression of phase with frequency, OCMANL checks the calculated phase at each test frequency. If found to be within 360 degrees of the phase calculated at the preceding test frequency, no corrections are made; a larger phase difference, however, results in the addition or subtraction of 360 degrees as necessary to bring the calculated phase value in the "neighborhood" of the preceding phase value.

The second function provided by OCMANL concerns the validity of the calculated gains and phases at each frequency. Since the describing function calculation presumes a negligible remnant contribution to the signal power at the loop input frequencies, a significant remnant contribution can render the gain and phase calculations invalid. OCMANL provides the user with a check on remnant power by utilizing the correlated-to-remnant power ratio (C/R) described earlier in the previous section. If the C/R ratio

* Assuming this has not been done earlier in response to a user's request for a printout of the signal's rate score or power spectrum (see sections A.3.3 and A.3.4).

at a particular frequency is small, indicating a large remnant contribution, the user is alerted to this situation by OCMANL, via a visual flag presented with the tabulated data item.

If the user requests the calculation of the human operator describing function (stick/display). OCMANL provides one further function for the user: a change of sign. Since the basic tracking loop of figure A.1 involves a positive feedback, the human operator must provide a sign reversal to ensure loop stability. To eliminate this sign reversal contained in the digitized stick history, and ensure consistency with conventional human operator measurements made with negative feedback loops, OCMANL adds 180 degrees to the calculated phases, before displaying the results to the user. Again, it should be noted that this occurs only when the user requests the calculation of the human operator describing function; other describing function calculations suffer no such adjustments.

A.3.6 Observation Noise

On request from the user, OCMANL will calculate and display as a function of frequency the human operator's observation noise, referred to both display and display rate. The noise calculations are based on the approach discussed by Levison et al (1969), and involve the stick power spectrum, scores for display and display error rate, and the loop input power referred to the display. The stick power and the scores are calculated as described previously in sections A.3.4 and A.3.3, respectively; the input power is calculated analytically, based on the input signal parameters and the plant dynamics. OCMANL ensure that these calculations are sequenced properly and displays the calculated observation noise at each loop input frequency in an appropriate tabular format.

An additional function provided by OCMANL concerns the validity of the calculated observation noise at each loop input

frequency. Since remnant power estimates may not exist at low frequencies (due to the user's choice of run length), OCMANL checks for their presence. If an estimate is found missing, no noise calculation is made at that frequency and the user is alerted to this situation, via a visual flag presented with the tabulated data item. In addition, OCMANL provides for such flagging when a low stick C/R power ratio is associated with a particular test frequency (recall section A.3.4), since a low ratio may invalidate the associated observation noise estimate.

A.3.7 Amplitude Distribution

A.3.8 Summary Calculations and File Writing

On request, OCMANL will provide the user with a concise summary of the fundamental human operator measurements made possible by the use of the Performance Analyzer. This user option performs the data file reading (see section A.3.1), calculation of the tracking scores (see section A.3.3) for the four loop variables (loop input, stick, plant, and display) and for one of the rate variables (stick rate). In addition, the human operator's describing function is calculated (see section A.3.5), as is his estimated observation noise (see section A.3.6). As described previously, the describing function and noise figures are flagged appropriately to alert the user to marginally valid or invalid data.

OCMANL provides the user with the options of displaying the calculations on the terminal and/or writing the results on a disc file. If the user chooses the latter option, OCMANL prompts the user for an appropriate file name, writes the data on the file, and closes the file to preserve it for later use. This allows the user to condense large volumes of tracking time histories into small files of essential frequency domain information, which can be later processed in an ensemble fashion to obtain statistical descriptions of tracking behavior.

A.4. PERFORMANCE ANALYZER OPERATION

This section provides examples of the Performance Analyzer capabilities just described, and illustrates user interaction during problem definition and tracking analysis. For convenience, the description is divided between the two operating programs, OCMRUN and OCMANL.

A.4.1 Tracking Task Implementation: OCMRUN

OCMRUN provides the user with the capability of defining the tracking task parameters, controlling the tracking task itself, and calibrating the interface modules. The following subsections illustrate these functions in more detail.

A.4.1.1 Definition of the Tracking Task Parameters

The listing given on the following pages illustrates how the user can define the desired tracking task by responding to appropriate program prompts. User responses are circled and labelled.

The user initiates program execution (A), and indicates that the parameters will be entered from the terminal rather than read from a parameter file (B). The user is then prompted for the sample period (C) and run time (D) and the program lists the run length and input signal period, both in seconds and in number of sample points, as a check to the user. The input signal period, in terms of the number of sample points, is chosen as the largest power of two which is less than the run length, in sample points; in this case, the input signal period is 4096. The program then checks with the user if this is satisfactory, and the user responds affirmatively (E). If the choice had not been satisfactory, the user would have been provided the opportunity of reentering a different sample period and/or run length.

☒ A
R OCMRUN

INITIALIZING PARAMETERS FROM A FILE? ☒ B

*****TIME BASE PARAMETERS*****

SAMPLE PERIOD IN MILLISEC: ☒ C 40

RUN TIME IN SECONDS: ☒ D 185

RUN LENGTH= 185.00 SECONDS AND 4626 POINTS
INPT SIGNAL PERIOD= 163.84 SECONDS WITH 4096 POINTS

OK? ☒ E

SCORING START TIME= 10.60 SECONDS AT POINT 266

OK? ☒ F

WANT TIME BASE PARAMETERS LISTED? ☒ G

SAMPLE PERIOD(SECONDS) = 4.000E-02
NUMBER OF POINTS IN RUN= 4626
RUN DURATION(SECONDS) = 1.850E+02

*****INPUT SIGNAL PARAMETERS*****

USING AN EXTERNAL FORCING FUNCTION? ☒ H

WHAT KIND(T OR D)? ☒ I D

PSD FUNCTION TYPE(1 OR 2): ☒ J 1

POLE LOCATION: ☒ K 0.5

RMS LEVEL: ☒ L 1.0

WANT THE NOMINAL SET OF FREQUENCIES? ☒ M

WANT THE FREQUENCIES LISTED? ☒ N

COMP	HARM	WACT	WDES
1	7	0.27	0.25
2	13	0.50	0.50
3	29	1.11	1.00
4	37	1.42	1.41
5	53	2.03	2.00
6	73	2.80	2.83
7	103	3.95	4.00
8	149	5.71	5.66
9	211	8.09	8.00
10	293	11.24	11.30
11	419	16.07	16.00
12	587	22.51	22.60
13	839	32.18	32.00

OK? ☒ O

WANT THE NOMINAL SET OF PHASES:Y—P

WANT THE PHASES LISTED:Y—Q

COMP	PMULT	PHASE
1	2019	177.45
2	3865	339.70
3	919	80.77
4	3494	307.09
5	408	35.86
6	3765	330.91
7	2534	222.71
8	1794	157.68
9	247	21.71
10	1711	150.38
11	3949	347.08
12	103	9.05
13	1933	169.89

WANT THE INPUT SIGNAL PARAMS LISTED:Y—R

TASK IS DISTURBANCE NULLING

NUMBER OF POINTS IN INPUT SIGNAL= 4096
INPUT SIGNAL DURATION(SECONDS) = 1.638E+02
BASE FREQUENCY(RAD/S) = 3.835E-02

PSD FUNCTION IS FIRST ORDER

POLE LOCATION(RAD/SEC)= 5.000E-01
RMS INPUT LEVEL = 1.000E+00

SPECTRAL COMPOSITION OF INPUT SIGNAL

COMP	HARM	FREQ	AMP	PHASE
1	7	0.27	0.90	177.45
2	13	0.50	0.67	339.70
3	29	1.11	0.52	80.77
4	37	1.42	0.34	307.09
5	53	2.03	0.32	35.86
6	73	2.80	0.27	330.91
7	103	3.95	0.24	222.71
8	149	5.71	0.20	157.68
9	211	8.09	0.16	21.71
10	293	11.24	0.14	150.38
11	419	16.07	0.12	347.08
12	587	22.51	0.10	9.05
13	839	32.18	0.08	169.89

*****PLANT PARAMETERS*****

ENTER PLANT TYPE(0 THRU 6): 4 S
 GAIN: 2 T
 POLE: -2 U
 TIME DELAY IN MILLISEC: 25 V
 ACTUAL DELAY WILL BE 20 MILLISEC. OK? Y W
 STICK GAIN IN CM/LB: 5 X
 WANT PLANT PARAMETERS LISTED? Y Y
 PLANT TYPE = 4
 GAIN = 2.000E+00
 POLE(RAD/S) = -2.000E+00
 TIME DELAY = 2.000E-02
 STICK GAIN = 5.000E+00

*****SCORING PARAMETERS*****

STICK WEIGHTING: 0 Z
 WANT SCORING PARAMETERS LISTED? Y AA
 STICK WEIGHTING = 0.000E-01
 SCORING STARTS AT POINT 266
 AND STOPS AT POINT 4361

*****CALIBRATION PARAMETERS*****

FIRST CALIBRATION VALUE(LB): -1 BB
 SECOND CALIBRATION VALUE(LB): 1 CC
 WANT CALIBRATION PARAMETERS LISTED? Y DD
 FIRST CALIBRATION LEVEL = -1.000E+00
 SECOND CALIBRATION LEVEL = 1.000E+00

WANT ALL PARAMETERS LISTED OUT:Y EE

*****TIME BASE PARAMETERS*****

SAMPLE PERIOD(SECONDS) = 4.000E-02
NUMBER OF POINTS IN RUN= 4626
RUN DURATION(SECONDS) = 1.850E+02

*****INPUT SIGNAL PARAMETERS*****

TASK IS DISTURBANCE NULLING

NUMBER OF POINTS IN INPUT SIGNAL= 4096
INPUT SIGNAL DURATION(SECONDS) = 1.638E+02
BASE FREQUENCY(RAD/S) = 3.835E-02

PSD FUNCTION IS FIRST ORDER

POLE LOCATION(RAD/SEC)= 5.000E-01
RMS INPUT LEVEL = 1.000E+00

SPECTRAL COMPOSITION OF INPUT SIGNAL

COMP	HARM	FREQ	AMP	PHASE
1	7	0.27	0.90	177.45
2	13	0.50	0.67	339.70
3	29	1.11	0.52	80.77
4	37	1.42	0.34	307.09
5	53	2.03	0.32	35.86
6	73	2.80	0.27	330.91
7	103	3.95	0.24	222.71
8	149	5.71	0.20	157.68
9	211	8.09	0.16	21.71
10	293	11.24	0.14	150.38
11	419	16.07	0.12	347.08
12	587	22.51	0.10	9.05
13	839	32.18	0.08	169.89

*****PLANT PARAMETERS*****

PLANT TYPE = 4
GAIN = 2.000E+00
POLE(RAD/S)= -2.000E+00
TIME DELAY = 2.000E-02

STICK GAIN = 5.000E+00

*****SCORING PARAMETERS*****

STICK WEIGHTING= 0.000E-01
SCORING STARTS AT POINT 266
AND STOPS AT POINT 4361

*****CALIBRATION PARAMETERS*****

FIRST CALIBRATION LEVEL = -1.000E+00
SECOND CALIBRATION LEVEL = 1.000E+00

ANY CHANGES? ☒ N FF
CREATING A PARAMETER FILE? ☒ Y GG
ENTER FILE NAME FOR OUTPUT: TEMP.PAR HH
DOING A RUN NOW? ☒ N II
REINITIALIZING PARAMETERS JJ
INITIALIZING PARAMETERS FROM A FILE? ☒ N

REINITIALIZING PARAMETERS

INITIALIZING PARAMETERS FROM A FILE? ☒ Y JJ

ENTER FILE NAME FOR INPUT: TEMP.PAR KK

WANT ALL PARAMETERS LISTED OUT? ☒ N LL

ANY CHANGES? ☒ Y MM

WHICH PART? (0 THRU 5) ☒ 3 NN

*****PLANT PARAMETERS*****

ENTER PLANT TYPE (0 THRU 6) ☒ 6 OO

GAIN: ☒ 100 PP

ZETA: ☒ .707 QQ

WN: ☒ 10 RR

TIME DELAY IN MILLISEC: ☒ 0 SS

STICK GAIN IN CM/LB: ☒ 5 TT

WANT PLANT PARAMETERS LISTED? ☒ Y UU

PLANT TYPE = 6

GAIN = 1.000E+02

ZETA = 7.070E-01

WN = 1.000E+01

TIME DELAY = 0.000E-01

STICK GAIN = 5.000E+00

MORE CHANGES? ☒ N VV

WANT ALL PARAMETERS LISTED OUT? ☒ N WW

CREATING A PARAMETER FILE? ☒ Y XX YY

ENTER FILE NAME FOR OUTPUT: TEMP1.PAR

DOING A RUN NOW? ☒ N ZZ

REINITIALIZING PARAMETERS

The program then lists the time at which scoring will begin, here chosen so as to "center" the scoring interval of 163.84 seconds within the run interval of 185 seconds. The program then checks with the user if this is satisfactory and the user responds affirmatively (F). If the scoring start time had not been satisfactory, the user would have been provided the opportunity of entering a different start time. Finally, the program lists the time base parameters in response to the user's request (G).

The user is then prompted for information concerning the input signal, after requesting that one be used in the tracking task (H). The user then specifies a disturbance input (rather than a target input) (I), the order and pole location of the power spectral density function to be approximated (J,K), and finally the desired RMS value of the input signal (L). The user then indicates that he wishes to use the nominal set of pre-defined input signal frequencies (M), and then requests a listing of them (N). Had the user not wished to use the nominal frequency set, the program would have provided him the opportunity of defining his own set of frequencies. In either case, the affirmative answer to the listing request (N) results in a listing as shown: the frequency component is given first (COMP), followed by the harmonic multiplier (HARM), the actual input frequency in radians/sec (WACT), and the desired frequency (WDES). The desired frequencies (WDES) are those specified by the user and, in this case, are those comprising the nominal frequency set having half-octave jumps. The actual frequencies (WACT) differ from the desired frequencies since the actual frequencies are chosen to be harmonics of a base frequency and the harmonics (HARM), in turn, are chosen to be all prime numbers.

After listing the frequencies, the program then checks with the user if this is satisfactory and the user responds affirmatively (O). If this frequency set had not been

satisfactory, the user would have been provided the opportunity of changing either the entire set of desired frequencies or specific components of it. The user would have also been given the choice of relaxing the constraint of prime harmonics in favor of simple integer harmonics.

The user then indicates that he wishes to use the nominal set of phases associated with the input signal sinusoids (P), and requests a listing of them (Q). The listing shown gives the component number (COMP), the integer phase multiplier (PMULT) and the phase in degrees (PHASE). For each component, the phase multiplier is chosen to be a random number between zero and the number of points in the input signal (here, 4096); and the phase itself is calculated correspondingly between zero and 360 degrees. The resulting string of random phases is based on a random number generator "seed" of unity; had the user responded negatively to the question concerning the use of the nominal phase set (P), the program would have provided him with the opportunity of choosing a different "seed" value to be used to generate a different string of random phases.

By responding affirmatively to an input signal parameter listing request (R), the user is provided with a summary of the signal parameters as shown. In addition to the parameters just described, the program lists the amplitudes (AMP) associated with each component sinusoid, calculated so as to approximate the specified first-order power spectral density function and RMS level.

The user is then prompted for the type of plant dynamics to be incorporated in the tracking task. Here the user responds (S) with a 4, indicating a first-order plant; had he responded with a zero, a listing of the plant codes would have been provided. The user then specifies the plant gain (T) and pole location (U); the

negative value corresponds to an unstable pole. The user also specifies a 25 millisecond dead-time to be included in the plant dynamics (V) but the program restricts this to be an integral multiple of half the sample period (in this example, 20 msec). The program then checks with the user if this choice is satisfactory and the user responds affirmatively (W). Had this not been satisfactory, the user would have been provided the opportunity of reentering a different value for the time delay.

The user then specifies the stick gain value (X), which is used to convert the stick force in pounds to centimeters of display units. A single or double integrator in the plant dynamics would have resulted in a prompt for a corresponding velocity or acceleration conversion factor. The affirmative answer to the listing request (Y) results in a summary of the chosen plant parameter values.

The user is then prompted for the stick weighting factor to be used in calculating the overall tracking score. The zero response by the user (Z) implies that the tracking score is to be calculated on the basis of display displacement alone. The affirmative response to the listing request (AA) displays the stick weighting and the scoring start and stop points, the last two parameters having been defined earlier with the time base parameter selection.

The user is then prompted for the two values to be used in calibrating the stick force. The user indicates that one pound force levels will be used (BB,CC); the negative sign of the first value indicates a left stick deflection and the positive sign of the second value indicates a right stick deflection. The affirmative response to the listing request (DD) results in a listing of these two values.

At this point, the parameter specifications are complete and the user is provided the opportunity of listing the entire

parameter set defining the tracking task. His affirmative answer (EE) results in the tracking task parameter summary shown. At the end of this listing, he is provided the opportunity of changing any of the parameter values currently specified. Here, he responds negatively (FF), but had he responded affirmatively, the program would have provided appropriate prompts to effect the desired parameter value changes.

The user is then questioned as to the creation of a parameter file. The affirmative response (GG) results in a prompt for a file name, which the user then provides (HH). After a check on the legality of the file name, the program opens a disk file with that name, writes all of the tracking task parameter values into the file, and then closes the file. This ensures that the parameter values will be saved for future use, thus obviating the need for a repetition of the parameter specification procedure just described.

With the parameter values specified and saved at this point, the user is provided the opportunity of conducting a tracking run. Had the user responded affirmatively at this point (II), final initialization of the run parameters would have been conducted (see next section). However, the negative response (II) results in a reinitialization message, followed by a prompt as to the source of the new parameter set (JJ). At this point, the program has looped back to the initial question asked of the user (B), and the parameter definition process can be repeated.

If the user wishes to create multiple parameter files defining different tracking tasks (e.g., different plant dynamics), he has two choices: a parameter-by-parameter specification as just outlined, executed for each desired parameter file; or a change of the desired parameters from one set to another, creating a new file with each new set. The former situation is illustrated in the previous example, where the user enters a second pass of individual

specification of all the tracking task parameters, by answering negatively to the last program prompt (JJ).

The alternative approach to multiple parameter file creation is illustrated in the listing below, which begins with the user requesting that the parameter set be read in from a previously created file (JJ). He is then prompted for the parameter file name, and after giving it (KK), is asked if he wishes a listing of the complete parameter set. His negative response (LL) results in a prompt for a change request and his affirmative answer here (MM) results in a request for a specification of the parameter subset to be changed. Here, the user responds (NN) with a 3, indicating a change in the plant parameter set; had he responded with a zero, a listing of the parameter set codes would have been provided.

At this point the user can specify a new set of plant parameters, differing from the ones given in the previous example. Here, he specifies that the dynamics be second-order (OO), and specifies the gain (PP), damping ratio (QQ), and natural frequency (RR). No time delay is desired so the user responds with a zero (SS). After specifying the stick gain (TT), the user has the plant parameters listed (UU).

Since the user wishes to change only the plant dynamics, he indicates that no further changes are to be made (VV), and that a complete parameter set listing is unnecessary (WW). However, since the user does wish this new parameter set to be saved, he responds affirmatively to the parameter file query (XX), and provides a new file name for parameter storage (YY). A negative answer to the run initialization question (ZZ) results in a program loop back to parameter reinitialization (JJ).

With the procedure just described, the user can rapidly create several parameter files for different tracking situations by changing only a few parameters at a time.

A.4.1.2 Run Identification and File Labelling

The listing given on the following page illustrates how the user can initiate a run once the tracking task parameters have been defined.

The user initiates program execution (A), and indicates that the parameters are to be read from a previously-created parameter file (B). He is then prompted for the parameter file name and after giving it (C). is asked if he wishes a listing of the complete parameter set. His negative response (D) results in a prompt for a change request to which he also responds negatively (E).

Since the user indicates that no parameter file is to be created (F), the program assumes that the user wishes to conduct a tracking run with the current parameter set. Before continuing, however, the program first checks for the presence of valid stick and display input/output scale factors, factors calculated on the basis of a previously-conducted calibration (see section A.4.1.4). In this example, a calibration had been conducted earlier and the results stored in the specified input file TEMP.DAT; thus, the program questions the user as to whether or not he wishes to use this old set of scale factors. The user's response is affirmative (G), thus bypassing a calibration. If the user's response had been negative, or if the input file had not contained a valid set of scale factors, the user would have been forced to conduct a calibration to generate a valid set.

The program then prints out the run number and current date. In this case the run number is unity because this is the first run following program execution (A); repeated runs conducted by the program result in an automatic incrementing of the run number. In either case, the user is given the opportunity of changing the run number; here, he chooses not to (H).

A
INITIALIZING PARAMETERS FROM A FILE: B
ENTER FILE NAME FOR INPUT: C
WANT ALL PARAMETERS LISTED OUT?: D
ANY CHANGES?: E
CREATING A PARAMETER FILE?: F
WANT CALIB VALUES FROM CURRENT INPUT FILE?: G

RUN NUMBER: 1 DATE: 02-JUL-78

CHANGING THE RUN NUMBER?: H

OF LINES IN TITLE: I

J

K

ENTER FILE NAME FOR OUTPUT: L

TYPE S TO START: M

The user is then prompted for the number of lines of comment he wishes to enter. His non-zero response (I) results in an exclamation mark prompt character for each line of input; the user input (J,K) is then stored with the other parameters defining the tracking task. Had the user specified zero lines of comment, no prompts would have been provided and no comments expected by the program.

The user is then prompted for the file name to be used for storage of the tracking task parameters and the tracking data. The user response (L) is then checked for legality and if valid, a disc file of that name is opened and used to store the tracking parameters. The file remains open and ready to receive the tracking data as it is generated.

Finally, the user is prompted for a start signal (M) which initiates control of the tracking task. Under normal circumstances, control does not return to the user until the end of the specified run length, although certain conditions can result in early run termination (see below).

A.4.1.3 Run Termination and Multiple Runs

The listing on the following page illustrates program output at the end of a run and demonstrates how the user can initiate additional runs with a minimum of terminal entries.

The user starts the run by responding with the start character (A). The tracking run is then conducted under control of the program until the designated run time has elapsed. At this point the tracking data is saved on the user-specified disc file (in this case, A1.TMV) and summary scoring information is presented on the terminal as shown. Mean, standard deviation, and RMS values are given for the input signal (INPT), stick deflection (STCK), plant (PLNT), and display displacement (DISP). In addition, the percentage of overloads (OLPCT) occurring for the stick and display

TYPE S TO START: ☒ S — A

FILE:A1.TMV RUN NUMBER: 1 DATE:29-MAR-78 TIME:10:24:40

VARBL	MEAN	S.D.	RMS	OLPCT	OLPNT
INPT	-0.00	0.50	0.50		
STCK	0.01	0.24	0.24	0.00	0
PLNT	-0.06	0.57	0.57		
DISP	-0.06	0.57	0.57	0.00	0

COST= 0.57

DOING ANOTHER RUN? ☒ Y — B

ANY CHANGES? ☒ N — C

RUN NUMBER: 2 DATE:29-MAR-78

CHANGING THE RUN NUMBER? ☒ N — D

OF LINES IN TITLE: ☐ — E

ENTER FILE NAME FOR OUTPUT: A2.TMV — F

TYPE S TO START: ☒ S — G

FILE:A2.TMV RUN NUMBER: 2 DATE:29-MAR-78 TIME:10:29: 1

VARBL	MEAN	S.D.	RMS	OLPCT	OLPNT
INPT	-0.00	0.50	0.50		
STCK	0.00	0.22	0.22	0.00	0
PLNT	-0.01	0.54	0.54		
DISP	-0.01	0.54	0.54	0.00	0

COST= 0.54

DOING ANOTHER RUN? ☒ Y — H

are given, along with the points at which these initially occurred during the run (OLPNT); in this example, no overloads were present. Finally, the overall tracking score (COST) is given based on the stick and display scores and the stick weighting factor (which is zero in this case).

The user is then questioned as to whether or not he wishes to conduct another tracking run. A negative response here would have terminated program execution. The affirmative response (B), however, results in a change request prompt. Had the user requested a change, he would have been provided the opportunity of changing the entire parameter set (by reading in a new parameter file) or of changing only a few parameters of interest. The user's negative response (C), however, results in an incrementing of the run number, followed by a series of program prompts and user responses (D,E,F,G) which initiate another tracking run. In this example, the user elects to conduct a third tracking run (H), once the tracking scores from the second have been displayed.

Early termination of a tracking run can occur if : a) the subject loses control of the task; b) an A-to-D conversion error occurs; or c) a timing error occurs. Should one of these situations occur, an appropriate error message is displayed on the terminal at the of occurrence, the run is halted, and the tracking scores are displayed in the manner just illustrated. The user is then provided the opportunity of conducting another run, if desired.

A.4.1.4 Calibration

The listing given on the following page illustrates how the user can calibrate the stick and display and generate a valid set of input/output scale factors.

☐ R OCMRUN **A**

INITIALIZING PARAMETERS FROM A FILE: ☐ Y **B**

ENTER FILE NAME FOR INPUT: TEMP.PAR **C**

WANT ALL PARAMETERS LISTED OUT? ☐ N **D**

ANY CHANGES? ☐ N **E**

CREATING A PARAMETER FILE: ☐ N **F**

CALIBRATION REQUIRED

ENTER MAX SCOPE DEFLECTION IN CM: ☐ 5 **G**

SET SCOPE ZERO, THEN HIT CR ☐ **H**

SET BAR TO MAX LEFT CM, THEN HIT CR ☐ **I**

SET BAR TO MAX RIGHT CM, THEN HIT CR ☐ **J**

OK?: ☐ Y **K**

SET STICK, THEN HIT CR ☐ **L**

SET STICK, THEN HIT CR ☐ **M**

MAX STICK= 1.24

ZERO STICK= 0.07

MIN STICK= -1.10

STICK BIAS (% F.S.) = 2.95

OK?: ☐ Y **N**

RUN NUMBER: 1 DATE: 03-JUL-78

CHANGING THE RUN NUMBER?: ☐ N

OF LINES IN TITLE:

The user initiates program execution (A), and indicates that the parameters are to be read from a previously-created parameter file (B). He is then prompted for the parameter file name and after giving it (C), declines to list out the parameters (D), make changes (E), or create a new parameter file(F). At this point, the program checks for the presence of a valid set of input/output scale factors and, finding none, indicates to the user that a calibration is required.

The user is then prompted for the maximum deflection of the display scope expressed in centimeters. After the user response (G), he is prompted to zero the display bar present on the scope, using the scope centering controls. Once he has completed this, he enters a carriage return (H), and is then prompted to adjust the full scale (left) scope deflection to the specified maximum (in this case, 5 cm). A second carriage return (I) results in a similar prompt for adjustment of the right maximum, and the third carriage return (J) results in a prompt by the program checking for satisfactory scope adjustment. The user's affirmative response (K) indicates a satisfactory adjustment. Had the user's response been negative, the scope adjustment procedure would have been repeated, thus allowing the user to readjust the scope's centering and gain controls.

Once the display calibration is complete, the user can then proceed to calibrate the stick. The user is prompted to set the stick at the first calibration level specified by the calibration parameter set (recall section A.4.1.1) In this case, the parameter set calls for a calibration level of -1, corresponding to a one pound force applied to the stick in the leftward direction. The user is expected to apply this force to the stick, enter a carriage return (L), and hold this force for approximately 5 seconds. During this time the program samples the stick voltage and calculates an average value over the sampling interval, a value

which is used later to generate a stick force-to-voltage scale factor. The user is then prompted to apply the second calibration force level to the stick and a similar sampling procedure is initiated with another carriage return (M).

With the two force-voltage points thus obtained, the program calculates the force-to-voltage scale factor. Using this and the maximum range of the A-to-D converter, the program also calculates the corresponding maximum and minimum stick forces; the values shown on the listing indicate these saturation levels for the stick force input. The program also calculates the equivalent stick force bias (ZERO STICK), which is the force level corresponding to zero stick voltage. This bias is then expressed in terms of full-scale stick range to indicate to the user the degree of left-right asymmetry in the stick. Finally, the program checks if the user is satisfied with this calibration. The user's affirmative response (N) indicates that such is the case. Had the user's response been negative, the stick calibration procedure would have been repeated.

Before proceeding with the tracking run initialization, the newly created input/output scale factors are stored with the tracking task parameter set. Thus, the scale factors are saved with the parameters when a data file is created, making it possible for the user to conduct later runs without the need for a new calibration.

A.4.2 Performance Analysis: OCMANL

OCMANL provides the user with the capability of flexible analysis of the stored tracking data, including score calculations, spectral analysis, and describing function computations. The following subsections illustrate these functions in more detail.

A.4.2.1 File Reading

The listing given on the following page illustrates how the user begins the data analysis by reading the appropriate disc file.

The user initiates program execution (A) and indicates that he is unfamiliar with the executive structure of the program by entering a zero in response to the part query (B). This results in a listing of the parts of the program, followed by another part query. This time, the user's response (C) is 1, indicating that he wishes to read a data file. This results in a prompt for the file name, which the user enters (D).

The program then reads the beginning of the specified file and outputs a header line identifying the file with its name, the run number associated with its creation, and the data and time the run was conducted. The point defining the beginning of the scoring interval is then noted to the user, and he is provided the opportunity of changing it if he so desires; here the user's response (E) is negative, indicating that the start point is satisfactory. The user is then questioned as to whether the stick is to be expressed in the recorded units of pounds or in equivalent plant command units of cm, cm/sec, or cm/sec²; here, the user indicates the latter (F).

With these preliminaries completed, the user is then able to proceed to any other program part as desired; the following sections describe the possible options.

A.4.2.2 Parameter Listing

The listing given on the following page illustrates how the user can request (A) a complete printout of the tracking task parameters associated with the data being analyzed. The printout includes information on the time base, input signal, plant, and scoring and calibration parameters. This information effectively

R OCMANL A

WHICH PART?(0-8) 0 B

PART 1: FILE READ
2: HEADER LIST
3: SCORES
4: SPECTRUM
5: DESC FCN
6: OBS NOISE
7: AMP DIST
8: SUMMARY

WHICH PART?(0-8) 1 C

ENTER FILE NAME FOR INPUT: B5.SAH D

FILE: B5.SAH RUN NUMBER: 5 DATE: 18-APR-78 TIME: 3:10:21

NOMINAL B

SCORING STARTS AT POINT 501 WANT TO CHANGE? N E

STICK MEASURED IN LB OR IN CM? C F

WHICH PART?(0-8) 2 -A

*****TIME BASE PARAMETERS*****

SAMPLE PERIOD(SECONDS) = 4.000E-02
NUMBER OF POINTS IN RUN= 4626
RUN DURATION(SECONDS) = 1.850E+02

*****INPUT SIGNAL PARAMETERS*****

TASK IS DISTURBANCE NULLING

NUMBER OF POINTS IN INPUT SIGNAL= 4096
INPUT SIGNAL DURATION(SECONDS) = 1.638E+02
BASE FREQUENCY(RAD/S) = 3.835E-02

PSD FUNCTION IS FIRST ORDER

POLE LOCATION(RAD/SEC)= 5.000E-01
RMS INPUT LEVEL = 1.000E+00

SPECTRAL COMPOSITION OF INPUT SIGNAL

COMP	HARM	FREQ	AMP	PHASE
1	7	0.27	0.90	130.61
2	13	0.50	0.67	281.16
3	29	1.11	0.52	151.44
4	37	1.42	0.34	177.98
5	53	2.03	0.32	64.95
6	73	2.80	0.27	227.46
7	103	3.95	0.24	60.12
8	149	5.71	0.20	113.29
9	211	8.09	0.16	138.96
10	293	11.24	0.14	173.67
11	419	16.07	0.12	151.26
12	587	22.51	0.10	64.69
13	839	32.18	0.08	106.44

*****PLANT PARAMETERS*****

PLANT TYPE = 4
GAIN = 2.000E+00
POLE(RAD/S)= -2.000E+00
TIME DELAY = 0.000E-01

STICK GAIN = 5.000E+00

*****SCORING PARAMETERS*****

STICK WEIGHTING= 0.000E-01
SCORING STARTS AT POINT 501
AND STOPS AT POINT 4596

*****CALIBRATION PARAMETERS*****

FIRST CALIBRATION LEVEL = -1.000E+00
SECOND CALIBRATION LEVEL = 1.000E+00

augments the laboratory notebook and can be used to precisely identify the experimental conditions under which the tracking data was collected.

A.4.2.3 Tracking Scores

The listing given on the following page illustrates how the user can request (A) a printout of the tracking scores. The program prompts the user as to whether or not he wishes the scores calculated for the rates of the tracking variables; here he responds affirmatively (B). The program then sequentially reads in the stored time history for each variable and calculates its mean, standard deviation, and RMS value over the scoring interval. In addition, since the rate scores are requested, the signal's power spectrum is computed; this is used in a frequency domain calculation of the signal's rate statistics.

With all four tracking signals so processed, the program lists the pertinent scores as shown. In addition, the overall tracking score (COST) is given, based on the stick and display scores, and the stick weighting factor (which is zero in this case).

A.4.2.4 Signal Spectra

The listing just described also illustrates how the user can request (C) a printout of a signal's power spectrum. His null response (D) to the signal query results in a letter code listing for each signal, followed by another signal query. The user's response at this point (E) results in a printout of the file header information, followed by the power spectrum for the stick.

Since the spectrum is calculated at the frequencies contained in the loop input (see parameter listing of section A.4.2.2), the first two columns give the component index (COMP) and frequency (FREQ). The next two columns give the correlated (COR) and remnant

WHICH PART?(0-8):3-A
WANT RATE SCORES?Y-B

FILE:B5.SAH RUN NUMBER: 5 DATE:18-APR-78 TIME: 3:10:21

VARBL	MEAN	S.D.	RMS
INFT	0.00	1.00	1.00
STCK	-0.02	1.59	1.59
PLNT	0.02	0.44	0.44
DISP	0.02	0.44	0.44
INFTDOT	0.00	3.48	3.48
STCKDOT	0.00	7.96	7.96
PLNTDOT	-0.00	1.85	1.85
DISPDOT	-0.00	1.85	1.85

COST= 0.44

WHICH PART?(0-8):4-C

SPECTRUM FOR:D

SIGNAL CODE IS: I FOR INPUT
S STICK
P PLANT
D DISPLAY
C PLANT COMMAND

TRY AGAIN:S-E

FILE:B5.SAH RUN NUMBER: 5 DATE:18-APR-78 TIME: 3:10:21

SPECTRUM FOR STCK

COMP	FREQ	PWR/WINDOW			PWR/RFS			NREM
		COR	REM	C/R	COR	REM	C/R	
1	0.27	-2.58	-43.74	41.16	1.33	-29.58	30.90	2
2	0.50	-4.53	-38.56	34.03	0.07	-24.40	24.47	2
3	1.11	-5.19	-36.21	31.02	-3.20	-22.05	18.85	5
4	1.42	-8.06	-33.68	25.62	-4.27	-19.51	15.24	6
5	2.03	-7.55	-35.04	27.49	-5.99	-20.88	14.89	9
6	2.80	-8.12	-34.13	26.02	-7.79	-19.97	12.18	13
7	3.95	-7.51	-28.80	21.29	-8.99	-14.64	5.65	18
8	5.71	-8.57	-29.34	20.77	-11.73	-15.18	3.45	25
9	8.09	-10.51	-28.04	17.52	-14.92	-13.87	-1.04	37
10	11.24	-13.15	-31.53	18.38	-19.00	-17.36	-1.63	51
11	16.07	-19.01	-36.70	17.69	-26.51	-22.54	-3.98	73
12	22.51	-30.01	-44.97	14.96	-38.93	-30.81	-8.12	102
13	32.18	-35.53	-47.34	11.81	-46.15	-33.18	-12.97	146

TOTAL PWR= 2.53

COR PWR = 2.16 COR/TOT PWR= 0.85
REM PWR = 0.37 REM/TOT PWR= 0.15

ANOTHER SIGNAL SPECTRUM:N-F

(REM) power. the former being simply the signal power at the indicated frequency, and the latter obtained by averaging the signal power over the neighboring measurement frequencies. The power is expressed in decibels (dB), and, in this case, reflects stick power per measurement window, expressed in the units specified by the user during the file read procedure (recall section A.4.2.1). The next column gives the signal's correlated-to-remnant power ratio (C/R), to provide the user with an indication of how well-correlated the signal is with the loop input.

Since these power measures reflect the width of the measurement window, that is, the frequency resolution of the digitized spectrum, the program also estimates the signal's power spectral density. The next two columns (labelled COR and REM) give the corresponding power spectral densities in terms of power/(radian/second), with the next to last column (C/R) giving the associated C/R ratio. The column (NREM) displays the number of neighboring measurement frequencies utilized in estimating the remnant power at each correlated frequency.

Following this spectrum printout, are total power measurement figures, for both the correlated and remnant portions of the signal, expressed not in dB but in units associated with the signal (in this case, cm^2). Also, given are the correlated and remnant power ratios, useful in indicating signal coherence.

The program then questions the user as to whether or not another signal spectrum is desired. Here, the user response is negative (F); had it been affirmative, the user would have been prompted for the appropriate signal code, and the above process repeated.

A.4.2.5 Describing Functions

The listing given on the following page illustrates how the user can request (A) a describing function printout relating any one loop variable to any other. The program prompts the user for the symbol of the signal to be associated with the describing function numerator (B), and denominator (C). In this example, the user requests a computation of the display-to-stick describing function.

The program responds with the file header information followed by a describing function identifier (DFCN), followed by the computed gain and phase at each loop input signal frequency. As before, the frequency is in radians/second; gain and phase are in dB and degrees, respectively.

The program then questions the user as to whether or not another describing function is desired. Here, the response is negative (D); had it been affirmative, the user would have been prompted for the appropriate numerator and denominator signal codes, and the above process repeated.

A.4.2.6 Observation Noise

The listing just described also illustrates how the user can request (E) a printout of the computed observation noise associated with the subject's tracking performance.

The program responds with the file header information, followed by a data identifier, followed by the observation noise power computed at each frequency contained in the loop input. As before the frequency is in radians/second, and the power is in dB. The column labelled POSN gives the noise related to the display displacement, and the column labelled RATE gives the noise related to display rate.

WHICH PART?(0-8):5-A

DFCN NUM: S-B

DFCN DENOM: D-C

FILE:B5.SAH

RUN NUMBER: 5

DATE:18-APR-78

TIME: 3:10:21

DFCN=(STCK)/(DISP)

COMP	FREQ	GAIN	PHASE
1	0.27	16.71	-36.23
2	0.50	13.53	-31.57
3	1.11	10.84	-28.85
4	1.42	10.03	-30.58
5	2.03	9.40	-32.87
6	2.80	9.35	-34.99
7	3.95	8.92	-40.96
8	5.71	9.51	-49.04
9	8.09	10.24	-62.98
10	11.24	12.18	-87.93
11	16.07	18.33	-125.62
12	22.51	20.38	-266.02
13	32.18	13.18	-392.58

ANOTHER DESCRIBING FUNCTION?:N-D

WHICH PART?(0-8):6-E

FILE:B5.SAH

RUN NUMBER: 5

DATE:18-APR-78

TIME: 3:10:21

OBSERVATION NOISE

COMP	FREQ	POSN	RATE
1	0.27	-23.94	-47.74
2	0.50	-19.59	-38.01
3	1.11	-19.63	-31.08
4	1.42	-18.44	-27.78
5	2.03	-22.27	-28.48
6	2.80	-23.85	-27.29
7	3.95	-22.43	-22.88
8	5.71	-26.12	-23.36
9	8.09	-27.42	-21.63
10	11.24	-32.40	-23.76
11	16.07	-36.19	-24.45
12	22.51	-37.87	-23.20
13	32.18	-39.21	-21.44

A.4.2.7 Amplitude Distribution

A.4.2.8 Summary Calculations and File Writing

The listing given on the following page illustrates how the user can request (A) a printout summarizing the fundamental human operator measurements made possible by the Performance Analyzer. The user is first prompted as to whether or not a new input file is to be read in. The user's negative response (B) is interpreted by the program as a request that summary calculations be conducted with the currently open file. Had the user responded affirmatively, a new file would have been read in and processed.

After prompting, the user indicates that the summary data is to be displayed on the terminal (C), and to be stored on a disc file (D). This results in a prompt for the file name to be used for summary data storage, and the user responds with the file name (E). The program then lists the file header information identifying the file containing the tracking histories, and then lists the tracking scores for the four loop variables. Also given are the scores for the stick rate and the overall tracking score. These scores are followed by the pertinent frequency domain information, consisting of the subject's calculated gain and phase (stick/display) and his observation noise, referred to display position and rate. The first blank column is available to flag low C/R ratios in either the stick or display spectra, and the last column is available to flag possibly invalid observation noise calculations. Additional details concerning the score, describing function, and observation noise calculations are to be found in sections A.4.2.3, A.4.2.5, and A.4.2.6, respectively.

Following this summary printout, the program writes the corresponding information on the output file designated earlier by the user (TEMP.DAT). This allows the user to save the summary calculations for possible later analysis and/or ensemble averaging.

WHICH PART?(0-8): 8 — A
 NEW INPUT FILE?: N — B
 OUTPUT ON TT?: Y — C
 OUTPUT ON DK?: Y — D
 ENTER FILE NAME FOR OUTPUT: TEMP.DAT — E

FILE: B5.SAH RUN NUMBER: 5 DATE: 18-APR-78 TIME: 3:10:21

VARBL	MEAN	S.D.	RMS
INPT	0.00	1.00	1.00
STCK	-0.02	1.59	1.59
PLNT	0.02	0.44	0.44
DISP	0.02	0.44	0.44
STCKDOT	0.00	7.96	7.96
COST=	0.44		

COMP	FREQ	GAIN	PHASE	POSN N	RATE N
1	0.27	16.71	-36.23	-23.94	-47.74
2	0.50	13.53	-31.57	-19.59	-38.01
3	1.11	10.84	-28.85	-19.63	-31.08
4	1.42	10.03	-30.58	-18.44	-27.78
5	2.03	9.40	-32.87	-22.27	-28.48
6	2.80	9.35	-34.99	-23.85	-27.29
7	3.95	8.92	-40.96	-22.43	-22.88
8	5.71	9.51	-49.04	-26.12	-23.36
9	8.09	10.24	-62.98	-27.42	-21.63
10	11.24	12.18	-87.93	-32.40	-23.76
11	16.07	18.33	-125.62	-36.19	-24.45
12	22.51	20.38	-266.02	-37.87	-23.20
13	32.18	13.18	-392.58	-39.21	-21.44

A.5. INTERFACE MODULES AND REAL-TIME HARDWARE

This section provides a brief description of the input and output interface modules indicated earlier in figure A.2 of section A.2. Also given here are brief summaries of the performance specifications of the digital computer real-time hardware used to implement the Performance Analyzer.

A.5.1 Input Interface

The input interface consists of a force stick in cascade with a noise-suppressing low-pass filter.

The force stick used is a Model 435 Hand Control manufactured by Measurement Systems, Inc. of Norwalk, Conn. When driven by an AC source, the stick provides a DC voltage linearly proportional to the force applied to the handle. Currently, the stick is driven by an 18.4 volt (RMS) source at 1500 Hz. With a modified extra-length handle, the stick provides approximately 0.83 volts per pound force deflection.

The low-pass filter is a second-order non-unity gain Butterworth, having a break frequency of 12.5 Hz and a damping ratio of 0.707. The break frequency was chosen to equal half the 25 Hz sampling rate ($T_s=40$ msec) used in the tracking experiments conducted with the Performance Analyzer. The DC filter gain was set at 4.85 volt/volt, to provide an overall force-to-voltage gain of 4 volt/pound.

A.5.2 Output Interface

The output interface consists of a Type 503 rack-mounted cathode ray oscilloscope manufactured by Tektronix, Inc. of Beaverton, Oregon. The vertical channel is adjusted to 20 volt/cm, and is driven by the 18.4 volt RMS source used to drive the stick. The horizontal channel is adjusted to one volt/cm, and is driven by the D-to-A channel used to interface with the Performance Analyzer

software. This combination of vertical and horizontal inputs results in a vertical bar display, having a height of 2.6 cm, and a horizontal displacement proportional to the D-to-A output voltage.

A.5.3 Real-Time Hardware

The real-time hardware used to implement the Performance Analyzer consists of a real-time clock and A-to-D and D-to-A converters, all manufactured by Digital Equipment Corp. of Maynard, Mass.

The clock is a DEC KW11-K dual programmable real-time clock, and is used in a repeated interval mode for timing information by the Performance Analyzer. A variety of clock functions are called for by the Analyzer software, including starting and stopping the clock, setting its base rate, initializing a "stop watch" counter, and reading the counter's contents. These functions are currently performed by a set of clock handler routines comprising one of the systems's resident utility libraries.

The A-to-D converter is a DEC AD11-K analog-to-digital converter, which is a 12-bit 16-channel converter currently configured for bipolar 5 volt inputs. The 22 microsecond conversion time is an insignificant fraction of typical sample times used during Performance Analyzer operation ($T_S=40$ msec), and the 12-bit resolution provides for a quantization error on the order of one millivolt, a level well below expected signal transmission noise levels. The A-to-D handler utilized by the Performance Analyzer provides a check for conversion errors, and maintains control of the system software during a conversion.

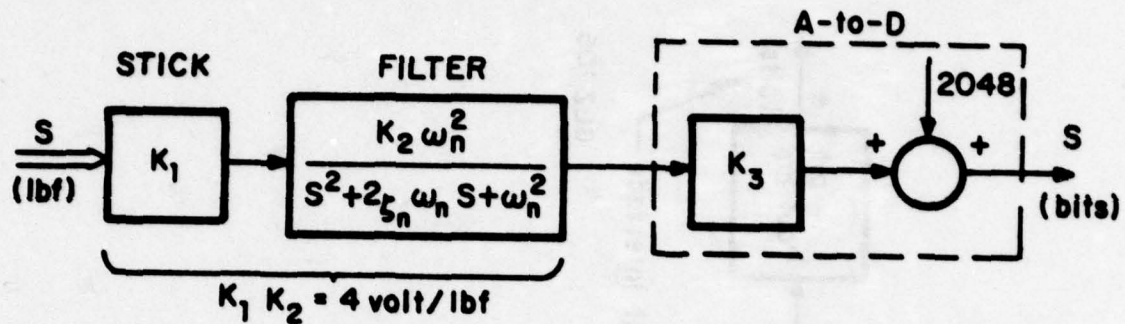
The D-to-A converter is a DEC AA11-K digital-to-analog converter, which is a 12-bit 4-channel converter currently configured for bipolar 5 volt outputs. The conversion time is on the order of 5 microseconds, again insignificant with respect to

typical sample times used; quantization errors are the same as those of the A-to-D converter.

A.5.4 Interface Module Diagrams

Figure A.3 summarizes the input/output interfaces just described, and illustrates the interconnection between the A-to-D converter, D-to-A converter, stick and display. For completeness, figure A.4 illustrates in block diagram form the signal processing provided by the Performance Analyzer software.

Figure A.3a: Input Interface



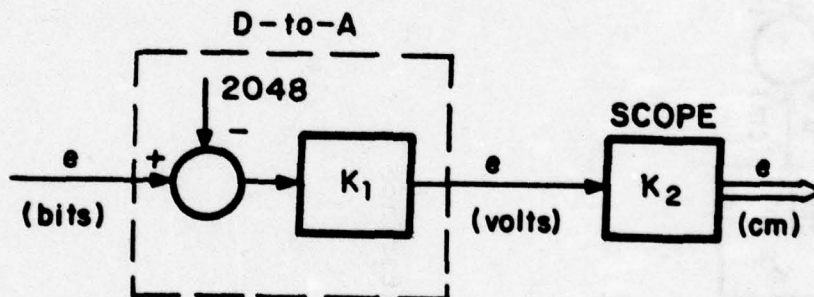
$$K_1 = 0.825 \text{ volt/lbf}$$

$$K_2 = 4.85 \text{ volt/volt}$$

$$K_3 = 409.6 \text{ bit/volt}$$

$$(\omega_n, \zeta_n) = (78.53, 0.707)$$

Figure A.3b: Output Interface



$$K_1 = 1 \text{ volt/409.6 bits}$$

$$K_2 = 1 \text{ cm/volt}$$

GLZ 104

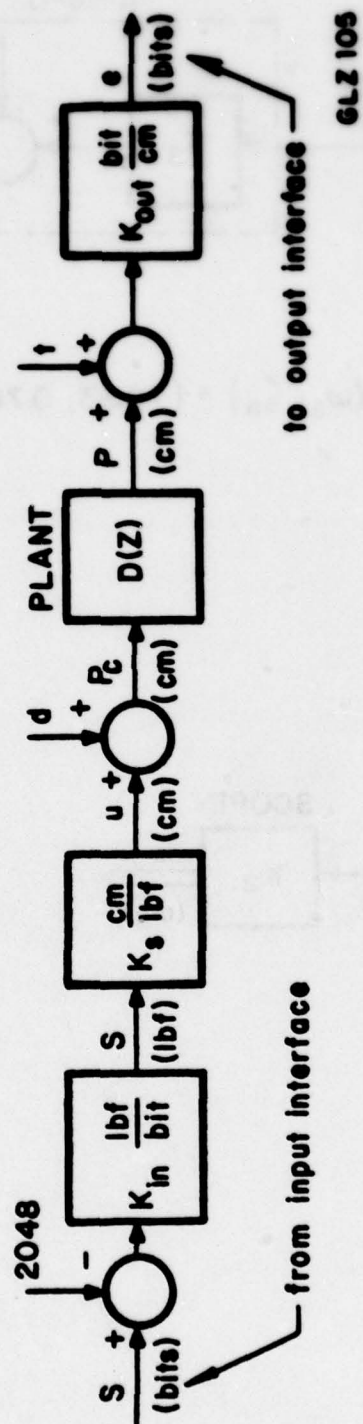


Figure A.4: Software Interface

Appendix B: Task Dynamics

A series of input-output measurements were made on the Performance Analyzer to validate the proper implementation of the desired task dynamics. Measurements were made in "autopilot mode", which consisted of connecting the display signal line directly to the input of the Butterworth filter used for conditioning the stick signal (see figures A.3 and A.4 of appendix A), the stick signal having been disconnected for these measurements. In this way the human operator was eliminated from the task, and loop stabilization was provided by the display-to-filter feedback.

An earlier calibration was used to ensure that one volt of display signal resulted in one centimeter of display displacement. In addition, the calibration resulted in one volt of stick signal being interpreted as 1.21 pounds force. Since the "autopilot" used in these measurements had unity voltage gain, its gain, as seen by the Performance Analyzer was 1.212 lbf/cm. To provide negative feedback and avoid saturation, the stick gain K_s (see figure A.4 of appendix A) was chosen to be -3 cm/lbf, opposite in sign and of smaller magnitude than the 5 cm/lbf value used in the human operator runs. The equivalent autopilot gain was thus -3.64 cm/cm, or 11.23 dB, if the sign is discounted.

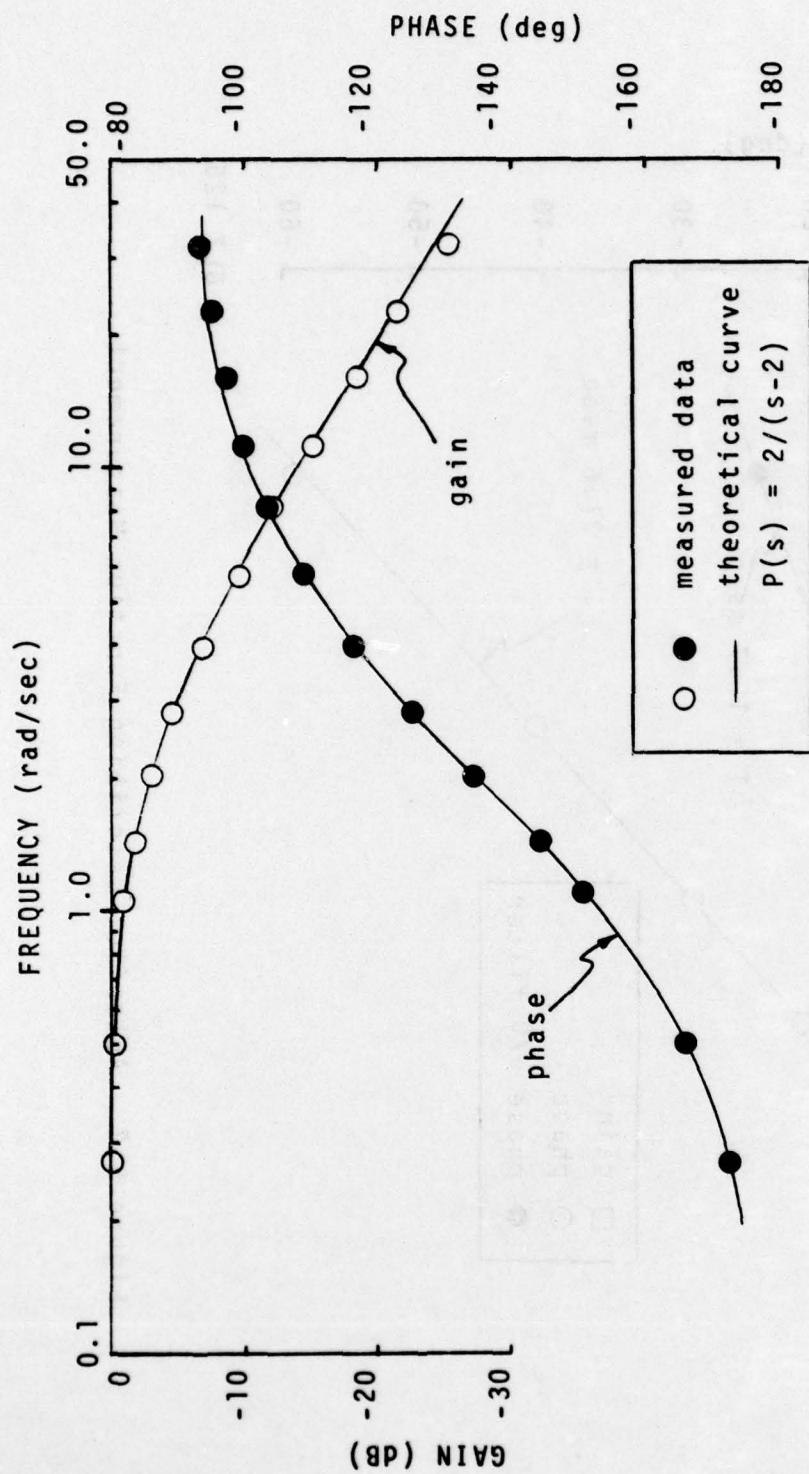
A tracking run was conducted with the autopilot, using the same plant dynamics and loop input disturbance function as were used in the human operator tracking runs. In addition, the same 40 msec sample time was used, to provide a control for sample-and-hold effects. After the run, the Performance Analyzer was used to calculate the describing function relating plant command p_c to plant output p , as a check on the unstable plant dynamics specified in the tracking task.

Figure B.1 shows the measurements obtained, along with the theoretical curves associated with the specified $2/(s-2)$ dynamics. Except for the highest measurement frequency where the gain drops 1.5 dB below that desired, the measured gain and phase follow the continuous curves quite closely, and thus validate the internal plant dynamics implemented on the Performance Analyzer.

Reference to figure A.4 of appendix A shows, however, that this measurement is across the digital filter $D(z)$ used to implement the plant dynamics. Thus, it is internal to the Performance Analyzer and takes no account of the overall input-output delays introduced by the computation times and sampling holds characterizing the digital system. These effects can be measured quite simply, however, by using the Performance Analyzer to calculate the autopilot describing function, relating effective stick output to display input. If no distortion is introduced by the digital system, then one would expect the autopilot measurement to simply reflect the autopilot gain in cascade with the Butterworth filter dynamics, since the filter was used to condition the autopilot signal.

Figure B.2 shows the gain and phase measured for the autopilot, plotted linearly against frequency. The gain measurements are quite close to the expected 11.23 dB, with less than 0.2 dB drop at the highest frequency of 32 rad/sec. Since the Butterworth filter, with its 78 rad/sec break frequency, contributes approximately 0.1 dB drop at 32 rad/sec, one can conclude that the Performance Analyzer contributes effectively no amplitude distortion.

Phase distortion is introduced, however, as is clear from the increasing lag with frequency seen on the figure. The measurements made on the zero-phase autopilot are indicated by the



GLZ 124

Figure B.1: Performance Analyzer Plant Dynamics

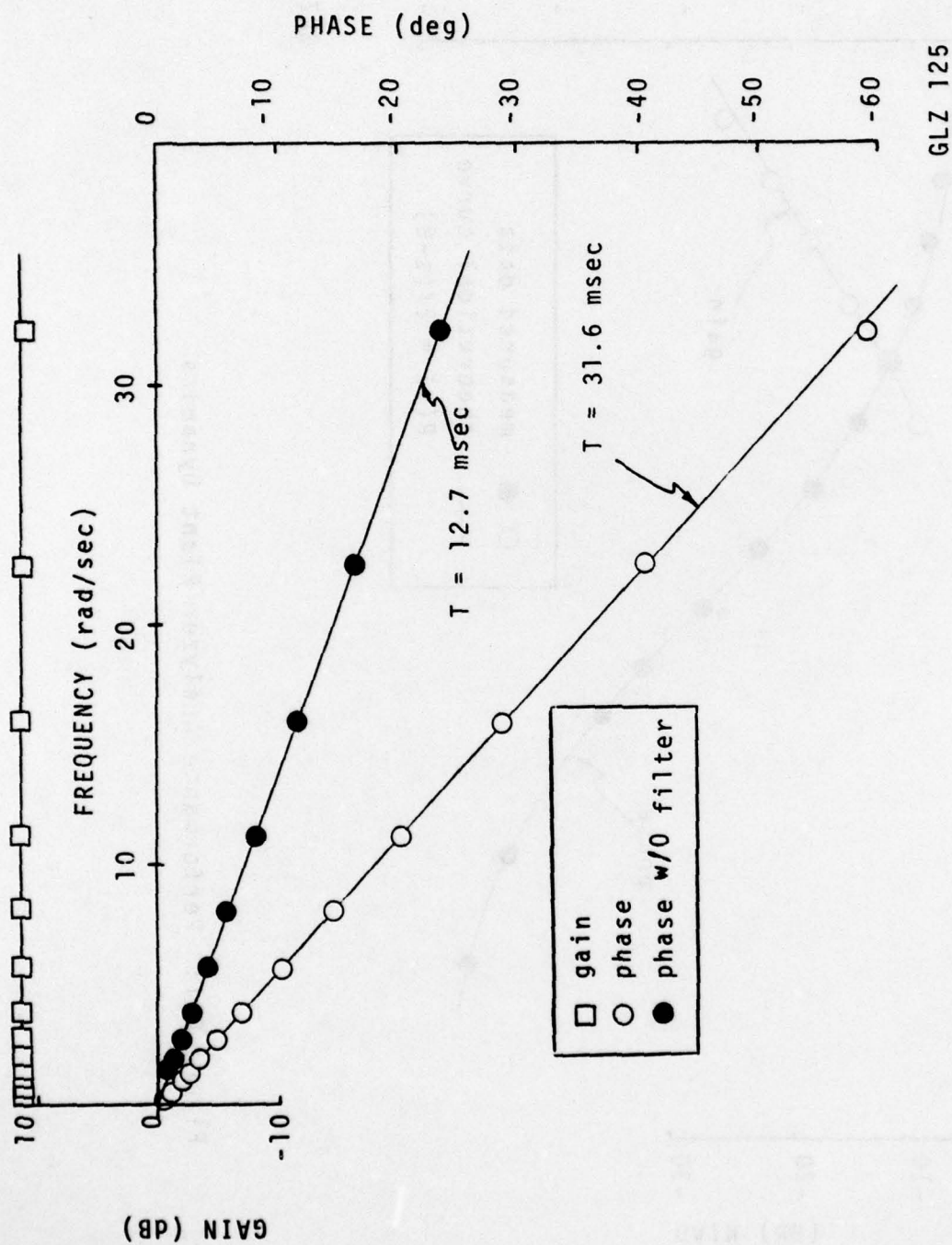


Figure B.2: Autopilot Describing Function Measurement

open circles, and can be well-modelled by a simple dead-time. The straight line fitting the data indicates an effective dead-time of approximately 32 msec, a delay which is due to both the Butterworth filter dynamics and the digital implementation of the Performance Analyzer. This, then, is a delay which the human operator sees while tracking the display, in addition to the dynamic lags introduced by the plant transfer function of figure B.1. Human operator measurements made with the Performance Analyzer must thus be compensated by the addition of a 32 msec lead, to arrive at the true operator describing function. As might be expected, this 32 msec figure is a function of sample rate and stick filter break frequency, and thus is only appropriate for the single configuration described here.

The phase shift due to the stick filter above can be computed as a function of frequency, based on the parameter values given in figure A.3 of appendix A. If this phase shift is then added to the measured phase of figure B.2, the phase values indicated by the closed circles result. The straight-line fit through this data set indicates a dead-time of approximately 13 msec, and can be attributed to the Performance Analyzer's digital processing delays, when operating with a sample period of 40 msec.

APPENDIX C: TABULATED EXPERIMENTAL RESULTS

This appendix contains tabulated data to supplement the discussion given in Chapter 5. Tables C.1 and C.2 give across-subject means and standard deviations of tracking scores obtained during the initial and intermediate training phases of the experiment, respectively. The latter table also gives a breakdown with tracking condition.

Table C.3 gives across-subject means and standard deviations of performance scores obtained during the control phase of the experiment, for each condition tested. Significance levels are also given for differences between conditions, based on individual subject paired differences; levels greater than 0.05 are considered not significant (NS). Similar information for the frequency response measures are given in Tables C.4 (amplitude ratio), C.5 (phase shift), and C.6 (remnant ratio).

The mean phase shifts of Table C.5 include a 32 msec lead to account for delays introduced by the Performance Analyzer. In addition, the mean phase shifts associated with the time delay condition include an additional 40 msec lag to simulate an operator delay, so that these phase means include a net 8 msec lag.

TABLE C.1: TRACKING SCORE VS. RUN NUMBER (initial training phase)

Score (cm)			Score (cm)		
Run	Mean	Standard Deviation	Run	Mean	Standard Deviation
1	1.54	.658	25	.60	.103
2	1.29	.515	26	.57	.081
3	1.12	.526	27	.52	.080
4	1.14	.692	28	.53	.089
5	.94	.317	29	.53	.086
6	.96	.434	30	.55	.082
7	.81	.311	31	.54	.104
8	.80	.220	32	.52	.063
9	.75	.174	33	.52	.068
10	.64	.136	34	.57	.126
11	.74	.183	35	.56	.094
12	.71	.174	36	.53	.060
13	.71	.226	37	.54	.043
14	.62	.137	38	.51	.080
15	.64	.234	39	.49	.088
16	.63	.149	40	.46	.056
17	.66	.224	41	.46	.068
18	.65	.147	42	.46	.064
19	.67	.194	43	.46	.076
20	.62	.129	44	.50	.091
21	.65	.152	45	.47	.059
22	.56	.107	46	.47	.059
23	.62	.117	47	.49	.058
24	.57	.109	48	.49	.080

TABLE C.2: TRACKING SCORE VS. RUN NUMBER AND CONDITION
(intermediate training phase)

Run	nominal		diffused		delayed	
	mean	standard deviation	mean	standard deviation	mean	standard deviation
1	.48	.081	.63	.045	.67	.063
2	.48	.054	.62	.046	.68	.060
3	.46	.066	.63	.044	.66	.084
4	.45	.051	.56	.052	.64	.117
5	.47	.067	.58	.037	.66	.076
6	.48	.064	.58	.066	.62	.062
7	.48	.064	.56	.097	.62	.062
8	.46	.087	.57	.084	.66	.065
9	.48	.049	.54	.080	.73	.125
10	.47	.048	.56	.073	.63	.071
11	.50	.076	.56	.074	.64	.078
12	.49	.068	.56	.093	.62	.070

TABLE C.3: PERFORMANCE SCORES

score	nominal		diffused		delayed		significance levels	
	mean	std. dev.	mean	std. dev.	mean	std. dev.	nom-dif	nom-del
σ_e (cm)	0.47	0.066	0.59	0.069	0.62	0.078	.001	.001
σ_u (cm)	1.64	0.065	1.80	0.094	1.89	0.099	.001	.001
$\sigma_{\hat{u}}$ (cm/s)	8.96	2.00	9.60	2.37	10.10	2.12	NS	.001
								NS

TABLE C.4: DESCRIBING FUNCTION AMPLITUDE RATIOS (dB)

frequency (rad/sec)	nominal		diffused		delayed		significance levels	
	mean	std.dev.	mean	std.dev.	mean	std.dev.	nom-dif.	nom-del dif-del
0.27	17.2	1.9	15.3	2.4	15.2	2.3	.01	.001 NS
0.50	13.8	1.7	12.4	1.9	11.7	1.3	.01	.001 NS
1.11	11.0	1.3	9.8	1.3	9.6	1.0	.01	.001 NS
1.42	10.7	1.1	9.3	0.8	9.6	1.1	.01	.001 NS
2.03	9.7	0.9	8.6	0.9	8.6	0.6	.01	.001 NS
2.80	9.3	1.0	8.2	0.6	8.3	0.7	.02	.01 NS
3.95	9.0	0.9	7.9	0.6	8.2	0.8	.001	.001 .02
5.71	9.2	0.9	8.6	0.6	8.8	0.6	.02	.05 NS
8.09	10.0	0.7	9.7	0.6	10.1	0.4	NS	NS .05
11.24	12.0	0.6	12.2	0.4	12.7	0.7	NS	.01 NS
16.07	18.3	1.0	20.1	2.4	20.9	2.2	.05	.01 NS
22.51	19.4	3.3	16.4	3.7	18.4	3.7	.001	.05 .01
32.18	11.8	3.8	9.9	2.9	11.3	3.3	NS	NS

TABLE C.5: DESCRIBING FUNCTION PHASE SHIFTS (deg.)

frequency (rad/sec)	nominal*		diffused*		delayed**		Significance Levels		
	mean	std. dev.	mean	std. dev.	mean	std. dev.	nom-dif	nom-del	dif-del
0.27	-38	11	-39	11	-35	9	NS	NS	.05
0.50	-39	8	-39	8	-35	5	NS	.05	NS
1.11	-33	6	-32	6	-31	5	NS	.01	NS
1.42	-33	5	-31	7	-31	4	NS	.01	NS
2.03	-32	4	-32	6	-32	4	NS	.01	NS
2.80	-33	3	-33	4	-34	2	NS	.05	NS
3.95	-35	2	-36	3	-38	2	NS	.02	.01
5.71	-40	3	-42	4	-47	3	NS	NS	.01
8.09	-50	3	-56	4	-62	7	.001	NS	.05
11.24	-65	6	-76	7	-84	9	.001	.02	.02
16.07	-106	25	-132	29	-143	23	.01	.05	NS
22.51	-244	19	-276	24	-305	13	.01	.01	NS
32.18	-334	25	-368	26	-417	30	NS	.001	NS

* includes 32 msec lead

** includes 8 msec lag

TABLE C.6: NORMALIZED REMNANT RATIOS (dB)

frequency (rad/sec)	nominal		diffused		delayed		significance levels		
	mean	std. dev.	mean	std. dev.	mean	std. dev.	nom	dif	nom - dif
0.27	-42.7	2.6	-41.0	2.6	-41.5	1.5	.05	NS	NS
0.50	-37.2	4.2	-36.9	2.1	-36.8	1.4	NS	NS	NS
1.11	-30.7	1.4	-29.8	2.6	-31.0	1.3	NS	NS	NS
1.42	-29.5	2.7	-28.8	2.3	-29.2	0.9	NS	NS	NS
2.03	-27.1	1.0	-25.8	1.0	-26.8	1.0	.05	NS	.05
2.80	-25.1	1.3	-24.4	1.1	-25.6	0.7	.02	NS	.02
3.95	-24.0	1.6	-22.9	1.1	-24.4	0.8	.05	NS	.05
5.71	-22.9	0.9	-22.3	0.7	-22.8	0.9	NS	NS	NS
8.09	-22.1	1.1	-21.6	0.7	-23.1	0.4	NS	.05	.01
11.24	-22.2	0.9	-21.9	0.5	-22.9	1.5	NS	NS	NS
16.07	-22.3	0.8	-21.7	1.0	-23.1	1.1	.05	.05	.01
22.51	-21.9	1.2	-20.7	1.3	-22.6	2.3	.01	NS	.05
32.18	-19.6	2.0	-17.8	1.7	-20.3	2.0	NS	NS	.02

REFERENCES

1. Baron, S., D. L. Kleinman, and W. H. Levison, "An Optimal Control Model of Human Response - Part II: Prediction of Human Performance in a Complex Task," Automatica, 6: 371-383, 1970.
2. Baron, S. and W. H. Levison, "Analysis and Modelling Human Performance in AAA Tracking," BBN Report No. 2557, Bolt Beranek and Newman Inc., Cambridge, Mass., March 1974.
3. Gai, E. G., and R. E. Curry, "A Model of the Human Observer in Failure Detection Tasks." IEEE Transactions on Systems, Man, and Cybernetics, SMC-6: 85-94, 1976.
4. Jex, H. R., J. D. McDonnell, and A. V. Phatak, "Critical Tracking Task for Man-Machine Research Related to the Operator's Delay Time," NASA CR-616, 1966.
5. Jex, H. R., J. D. McDonnell, and A. V. Phatak, "A Critical Tracking Task for Manual Control Research," IEEE Transactions on Human Factors Engineering, HFE-7: 138-145, 1966.
6. Kleinman, D. L. and S. Baron, "Analytic Evaluation of Display Requirements for Approach to Landing," NASA CR-1952, November 1971.
7. Kleinman, D. L., S. Baron, and W. H. Levison, "An Optimal Control Model of Human Response - Part I: Theory and Validation," Automatica, 6: 357-369, 1970.
8. Kleinman, D. L., S. Baron, and W. H. Levison, "A Control Theoretic Approach to Manned-Vehicle Systems Analysis," IEEE Transactions on Automatic Control, AC-16: 824-831, 1971.
9. Kleinman, D. L. and W. R. Killingsworth, "A Predictive Pilot Model for STOL Aircraft Landing," NASA CR-2374, March 1974.
10. Levison, W. H., "Biomechanical Response and Manual Tracking Performance in Sinusoidal, Sum-of-Sines, and Random Vibration Environments," AMRL-TR-75-94, Aerospace Medical Research Laboratory, Wright-Patterson Air Force Base, Ohio, April 1976. (AD A026286)

11. Levison, W. H., "Biomechanical and Performance Response of Man in Six Different Directional Axis Vibration Environments", BBN Report No. 3343, Bolt Beranek and Newman Inc., Cambridge, Mass., September 1976.
12. Levison, W. H., S. Baron, and A. M. Junker, "Modeling the Effects of Environmental Factors on Human Control and Information Processing," AMRL-TR-76-74, Aerospace Medical Research Laboratory, Wright-Patterson Air Force Base, Ohio, August 1976. (AD A030585)
13. Levison, W. H., S. Baron, and D. L. Kleinman, "A Model for Human Controller Remnant," IEEE Transactions on Man-Machine Systems, MMS-10: 101-108, December 1969.
14. Levison, W. H., J. I. Elkind, and J. L. Ward, "Studies of Multi-Variable Manual Control Systems: A Model for Task Interference," NASA CR-1746, May 1971.
15. Levison, W. H. and P. D. Houck, "Guide for the Design of Control Sticks in Vibration Environments," AMRL-TR-74-127, Aerospace Medical Research Laboratory, Wright-Patterson Air Force Base, Ohio, February 1975. (AD A008533)
16. Levison, W. H. and A. M. Junker, "A Model for the Pilot's Use of Motion Cues in Roll-Axis Tracking tasks," AMRL-TR-77-40, Wright-Patterson Air Force Base, Ohio, June 1977. (AD A043690)
17. Levison, W. H. and R. B. Tanner, "A Control-Theory Model for Human Decision Making," NASA CR-1953, December 1971.
18. Replogle, C. R., et al., "Human Operator Performance in Hypoxic Stress," Aerospace Medical Research Laboratory, Wright-Patterson Air Force Base, Ohio, November 1970.
19. Sadoff, M. and C. B. Dolkas, "Acceleration Stress Effects on Pilot Performance and Dynamic Response," IEEE Transactions on Human Factors Engineering, HFE-8: 138-145, June 1967.